

Test Report No. 609971-01



**TESTING AND EVALUATION OF FLARED MGS SYSTEM AT
MASH TEST LEVEL 3 CONDITIONS**

Sponsored by
Washington State Department of Transportation (WsDOT)

TEXAS A&M TRANSPORTATION INSTITUTE PROVING GROUND

Roadside Safety & Physical Security
Texas A&M University System RELLIS Campus
Building 7091
1254 Avenue A
Bryan, TX 77807

1. Report No. 609971-01		2. Government Accession No.		3. Recipient's Catalog No.	
4. Title and Subtitle TESTING AND EVALUATION OF FLARED MGS SYSTEM AT <i>MASH</i> TEST LEVEL 3 CONDITIONS				5. Report Date March 2023	
				6. Performing Organization Code	
7. Author(s) Chiara Silvestri Dobrovolny, Sun Hee Park, Bill Griffith, and Darrell L. Kuhn				8. Performing Organization Report No. Report 609971-01	
9. Performing Organization Name and Address Texas A&M Transportation Institute Proving Ground 3135 TAMU College Station, Texas 77843-3135				10. Work Unit No. (TRAIS)	
				11. Contract or Grant No. Project T4541	
12. Sponsoring Agency Name and Address Washington State Department of Transportation Research Office MS 47372 Transportation Building Olympia, WA 98504-7372				13. Type of Report and Period Covered Technical Report: November 2022–January 2023	
				14. Sponsoring Agency Code	
15. Supplementary Notes Project Title: Testing and Evaluation of Flared MGS System at <i>MASH</i> Test Level 3 Conditions Name of Contacting Representative: Mary McRae					
16. Abstract <p>The purpose of the tests reported herein was to assess the performance of the Midwest Guardrail System (MGS) with critical flare according to the safety-performance evaluation guidelines included in the American Association of State Highway and Transportation Officials <i>Manual for Assessing Safety Hardware (MASH)</i>, Second Edition (1). The crash tests were performed in accordance with <i>MASH</i> Test Level 3 (TL-3), which requires two crash tests:</p> <ol style="list-style-type: none"> 1. <i>MASH</i> Test 3-10: An 1100C vehicle weighing 2,420 lb impacting the guardrail while traveling at 62 mi/h and 25 degrees. 2. <i>MASH</i> Test 3-11: A 2270P vehicle weighing 5,000 lb impacting the guardrail while traveling at 62 mi/h and 25 degrees. <p>This report provides details on the MGS guardrail with critical flare, the crash tests and results, and the performance assessment of the MGS guardrail with flare for <i>MASH</i> TL-3 guardrail evaluation criteria.</p> <p>The MGS guardrail with critical flare tested at the considered flare conditions did not meet the performance criteria for <i>MASH</i> TL-3 guardrails.</p> <p>After the full-scale crash tests were complete, an effort was initiated through finite element modeling and simulations to investigate the crashworthiness of the MGS at smaller flare rates and to consider prioritized MGS retrofit options, still for high-speed impact conditions.</p>					
17. Key Words Guardrail, MGS, Flare, Impact Severity, Longitudinal Barrier, <i>MASH</i> , Crash Testing, Finite Element Simulations, Test Level 3, High Speed			18. Distribution Statement No restrictions. This document is available to the public through NTIS: National Technical Information Service Alexandria, Virginia 22312 http://www.ntis.gov		
19. Security Classif. (of this report) Unclassified		20. Security Classif. (of this page) Unclassified		21. No. of Pages 170	22. Price

**TESTING AND EVALUATION OF FLARED MGS SYSTEM AT
MASH TEST LEVEL 3 CONDITIONS**

by

Chiara Silvestri Dobrovolny, Ph.D.
Research Scientist
Texas A&M Transportation Institute

Sun Hee Park, Ph.D.
Associate Transportation Researcher
Texas A&M Transportation Institute

Bill Griffith
Research Specialist
Texas A&M Transportation Institute

and

Darrell L. Kuhn, P.E.
Research Specialist
Texas A&M Transportation Institute

Report 609971-01

Contract No.: T4541

Project Title: Testing and Evaluation of the MGS System
with Critical Flare at MASH Test Level 3 Conditions

Sponsored by the
Washington State Department of Transportation

March 2023

TEXAS A&M TRANSPORTATION INSTITUTE
College Station, Texas 77843-3135

DISCLAIMER

The contents of this report reflect the views of the authors, who are solely responsible for the facts and accuracy of the data and the opinions, findings, and conclusions presented herein. The contents do not necessarily reflect the official views or policies of the Washington State Department of Transportation (WsDOT), the Roadside Safety Pooled Fund, The Texas A&M University System, or the Texas A&M Transportation Institute (TTI). This report does not constitute a standard, specification, or regulation. In addition, the above-listed agencies/companies assume no liability for its contents or use thereof. The names of specific products or manufacturers listed herein do not imply endorsement of those products or manufacturers.

The results reported herein apply only to the article tested. The full-scale crash tests were performed according to TTI Proving Ground quality procedures and American Association of State Highway and Transportation Officials *Manual for Assessing Safety Hardware*, Second Edition, guidelines and standards.

The Proving Ground Laboratory within TTI's Roadside Safety and Physical Security Division ("TTI Lab") strives for accuracy and completeness in its crash test reports. On rare occasions, unintentional or inadvertent clerical errors, technical errors, omissions, oversights, or misunderstandings (collectively referred to as "errors") may occur and may not be identified for corrective action prior to the final report being published and issued. If, and when, the TTI Lab discovers an error in a published and issued final report, the TTI Lab will promptly disclose such error to WsDOT and the Roadside Safety Pooled Fund, and all parties shall endeavor in good faith to resolve this situation. The TTI Lab will be responsible for correcting the error that occurred in the report, which may be in the form of errata, amendment, replacement sections, or up to and including full reissuance of the report. The cost of correcting an error in the report shall be borne by the TTI Lab. Any such errors or inadvertent delays that occur in connection with the performance of the related testing contract will not constitute a breach of the testing contract.

THE TTI LAB WILL NOT BE LIABLE FOR ANY INDIRECT, CONSEQUENTIAL, PUNITIVE, OR OTHER DAMAGES SUFFERED BY WSDOT, THE ROADSIDE SAFETY POOLED FUND, OR ANY OTHER PERSON OR ENTITY, WHETHER SUCH LIABILITY IS BASED, OR CLAIMED TO BE BASED, UPON ANY NEGLIGENT ACT, OMISSION, ERROR, CORRECTION OF ERROR, DELAY, OR BREACH OF AN OBLIGATION BY THE TTI LAB.

ACKNOWLEDGMENTS

This research project was performed under a pooled fund program between the following states and agencies. The authors acknowledge and appreciate their guidance and assistance.

Roadside Safety Research Pooled Fund Committee Revised January 2023

ALABAMA

Stanley (Stan) C. Biddick, P.E.
Assistant State Design Engineer
Design Bureau, Final Design Division
Alabama Dept. of Transportation
1409 Coliseum Boulevard, T-205
Montgomery, AL 36110
(334) 242-6833
biddicks@dot.state.al.us

ALASKA

Mary McRae, P.E.
Statewide Standard Specifications
Alaska Department of Transportation &
Public Facilities
3132 Channel Drive
P.O. Box 112500
Juneau, AK 99811-2500
(907) 465-1222
mary.mcrae@alaska.gov

CALIFORNIA

Bob Meline, P.E.
Caltrans
Office of Materials and Infrastructure
Division of Research and Innovation
5900 Folsom Blvd
Sacramento, CA 95819
(916) 227-7031
Bob.Meline@dot.ca.gov

John Jewell, P.E.
Senior Crash Testing Engineer
Office of Safety Innovation & Cooperative
Research
(916) 227-5824
John.Jewell@dot.ca.gov

COLORADO

Joshua Keith, P.E.
Standards & Specifications Engineer
Project Development Branch

Colorado Dept. of Transportation
4201 E Arkansas Ave, 4th Floor
Denver, CO 80222
(303) 757-9021
Josh.Keith@state.co.us

CONNECTICUT

David Kilpatrick
State of Connecticut Dept. of
Transportation
2800 Berlin Turnpike
Newington, CT 06131-7546
(806) 594-3288
David.Kilpatrick@ct.gov

DELAWARE

Jeffery Van Horn, P.E.
Civil Engineering Program Manager
Transportation Solutions – Traffic
Operations
Office: (302) 659-4606; Cell:(302) 922-7279
Jeffery.VanHorn@delaware.gov

Craig Blowers

Craig.Blowers@delaware.gov

FLORIDA

Derwood C. Sheppard, Jr., P.E.
Standard Plans Publication Engineer
Florida Dept. of Transportation
Roadway Design Office
605 Suwannee Street, MS-32
Tallahassee, FL 32399-0450
(850) 414-4334
Derwood.Sheppard@dot.state.fl.us

IDAHO

Marc Danley, P.E.
Technical Engineer
(208) 334-8558
Marc.danley@itd.idaho.gov

ILLINOIS

Martha A. Brown, P.E.

Safety Design Bureau Chief
Bureau of Safety Programs and Engineering
Illinois Depart. of Transportation
2300 Dirksen Parkway, Room 005
Springfield, IL 62764
(217) 785-3034

Martha.A.Brown@illinois.gov

Edgar Galofre

Safety Design Engineer
(217) 558-9089

edgar.glofre@illinois.gov

IOWA

Daniel Harness

Office of Design – Methods
Iowa Department of Transportation
Daniel.Harness@iowadot.us

Zac Abrams

Traffic and Safety Project Engineer
Iowa Department of Transportation
(515) 239-1567

Zachary.Abrams@iowadot.us

LOUISIANA

Chris Guidry

Bridge Manager
Louisiana Transportation Center
Bridge & Structural Design Section
P.O. Box 94245
Baton Rouge, LA 79084-9245
(225) 379-1933

Chris.Guidry@la.gov

Kurt Brauner, P.E.

Bridge Engineer Manager
Louisiana Transportation Center
1201 Capital Road, Suite 605G
Baton Rouge, LA 70802
(225) 379-1933

Kurt.Brauner@la.gov

MARYLAND

Matamba Kabengele

Traffic Engineer
Office of Traffic and Safety
Maryland State Highway Administration
MKabengele@mdot.maryland.gov

MASSACHUSETTS

Alex Bardow

Director of Bridges and Structure
Massachusetts Depart. of Transportation
10 Park Plaza, Room 6430
Boston, MA 02116
(517) 335-9430

Alexander.Bardow@state.ma.us

James Danila

State Traffic Engineer
(857) 368-9640

James.Danila@state.ma.us

MICHIGAN

Carlos Torres, P.E.

Crash Barrier Engineer
Geometric Design Unit, Design Division
Michigan Depart. of Transportation
P. O. Box 30050
Lansing, MI 48909
(517) 335-2852

TorresC@michigan.gov

MINNESOTA

Khamsai Yang

Design Standards Engineer
Office of Project Management and
Technical Support
(651) 366-4622

Khamsai.Yang@state.mn.us

MISSOURI

Sarah Kleinschmit, P.E.

Policy and Innovations Engineer,
Missouri Department of Transportation
P.O. Box 270
Jefferson City, MO 65102
(573) 751-7412

sarah.kleinschmit@modot.mo.gov

Kaitlyn Bower

kaitlyn.bower@modot.mo.gov

NEW MEXICO

Brad Julian

Traffic Technical Support Engineer
(505) 827-3263
Brad.Julian@state.nm.us

OHIO

Don P. Fisher, P.E.

Ohio Depart. of Transportation
1980 West Broad Street
Mail Stop 1230
Columbus, OH 43223
(614) 387-6214
Don.fisher@dot.ohio.gov

OREGON

Christopher Henson

Senior Roadside Design Engineer
Oregon Depart. of Transportation
Technical Service Branch
4040 Fairview Industrial Drive, SE
Salem, OR 97302-1142
(503) 986-3561
Christopher.S.Henson@odot.state.or.us

PENNSYLVANIA

Evan Pursel

Senior Civil Engineer
epursel@pa.gov

Nina Ertel

nertel@pa.gov

TEXAS

Chris Lindsey

Transportation Engineer
Design Division
Texas Department of Transportation
125 East 11th Street
Austin, TX 78701-2483
(512) 416-2750
Christopher.Lindsey@txdot.gov

Taya Retterer P.E.

TXDOT Bridge Standards Engineer
(512) 416-2719
Taya.Retterer@txdot.gov

UTAH

Shawn Debenham

Traffic and Safety Division
Utah Depart. of Transportation
4501 South 2700 West
PO Box 143200
Salt Lake City UT 84114-3200
(801) 965-4590
sdebenham@utah.gov

WASHINGTON

John Donahue

Design Policy and Analysis Manager
Washington State Dept. of Transportation
Development Division
P.O. Box 47329
Olympia, WA 98504-7246
(360) 704-6381
donahjo@wsdot.wa.gov

Mustafa Mohamedali

Assistant Research Project Manager
P.O. Box 47372
Olympia, WA 98504-7372
(360) 704-6307
mohamem@wsdot.wa.gov

Tim Moeckel

Policy Support Engineer
Washington State Department of
Transportation
moecket@wsdot.wa.gov

WEST VIRGINIA

Donna J. Hardy, P.E.

Safety Programs Engineer
West Virginia Depart. of
Transportation – Traffic Engineering
Building 5, Room A-550
1900 Kanawha Blvd E.
Charleston, WV 25305-0430
(304) 558-9576
Donna.J.Hardy@wv.gov

Ted Whitmore

Traffic Services Engineer
(304) 558-9468
Ted.J.Whitmore@wv.gov

WISCONSIN

Erik Emerson, P.E.

Standards Development Engineer –
Roadside Design
Wisconsin Department of Transportation
Bureau of Project Development
4802 Sheboygan Avenue, Room 651
P. O. Box 7916
Madison, WI 53707-7916
(608) 266-2842
Erik.Emerson@wi.gov

CANADA – ONTARIO

Kenneth Shannon, P. Eng.

Senior Engineer, Highway Design (A)
Ontario Ministry of Transportation
301 St. Paul Street
St. Catharines, ON L2R 7R4
CANADA
(904) 704-3106
Kenneth.Shannon@ontario.ca

FEDERAL HIGHWAY ADMINISTRATION (FHWA)

Website: safety.fhwa.dot.gov

Richard B. (Dick) Albin, P.E.

Safety Engineer
FHWA Resource Center Safety & Design
Technical Services Team
711 S. Capital
Olympia, WA 98501
(303) 550-8804
Dick.Albin@dot.gov

Eduardo Arispe

Research Highway Safety Specialist
U.S. Department of Transportation
Federal Highway Administration
Turner-Fairbank Highway Research Center
Mail Code: HRDS-10
6300 Georgetown Pike
McLean, VA 22101
(202) 493-3291
Eduardo.arispe@dot.gov

Christine Black

Highway Safety Engineer

Central Federal Lands Highway Division
12300 West Dakota Ave.
Lakewood, CO 80228
(720) 963-3662

Christine.black@dot.gov

Isbel Ramos-Reyes

Lead Safety and Transportation Operations
Engineer
(703) 948-1442
isbel.ramos-reyes@dot.gov

Matt Hinshaw, M.S., P.E.

Highway Safety Engineer
Central Federal Lands Highway Division
(360)619-7677
matthew.hinshaw@dot.gov

TEXAS A&M TRANSPORTATION INSTITUTE (TTI)

Website: tti.tamu.edu
www.roadsidepooledfund.org

D. Lance Bullard, Jr., P.E.

Senior Research Engineer
Roadside Safety & Physical Security Div.
Texas A&M Transportation Institute
3135 TAMU
College Station, TX 77843-3135
(979) 317-2855
L-Bullard@tti.tamu.edu

Roger P. Bligh, Ph.D., P.E.

Senior Research Engineer
(979) 317-2703
R-Bligh@tti.tamu.edu

REPORT REVIEWED BY:

DocuSigned by:
Glenn Schroeder
E692F9CB5047487...

Glenn Schroeder, Research Specialist
Drafting & Reporting

DocuSigned by:
Ken Reeves
60D556935596468...

Ken Reeves, Research Specialist
Electronics Instrumentation

DocuSigned by:
Adam Mayer
F7A06F754E02430...

Adam Mayer, Research Specialist
Construction

DocuSigned by:
Richard Badillo
0F51DA60AB144F9...

Richard Badillo, Research Specialist
Photographic Instrumentation

DocuSigned by:
Scott Dobrovolny
1C613885787C44C...

Scott Dobrovolny, Research Specialist
Mechanical Instrumentation

DocuSigned by:
William J. L. Schroeder
25F29E1BAD624E8...

William J. L. Schroeder, Research
Engineering Associate
Research Evaluation and Reporting

DocuSigned by:
Bill Griffith
44A122CB271845B...

Bill L. Griffith, Research Specialist
Deputy Quality Manager

DocuSigned by:
Darrell L. Kuhn
D4CC23E85D5B4E7...

Darrell L. Kuhn, P.E., Research Specialist
Quality Manager

DocuSigned by:
Matt Robinson
EAA22BFA5BFD417...

Matthew N. Robinson, Research Specialist
Test Facility Manager & Technical Manager

DocuSigned by:
Chiara Silvestri Dobrovolny
36EDAD98EFE94EC...

Chiara Silvestri Dobrovolny, Ph.D
Research Scientist

TABLE OF CONTENTS

	Page
List of Figures	xv
List of Tables	xviii
Chapter 1. Background and Objective	1
1.1. Background	1
1.2. Objective	2
Chapter 2. System Details	3
2.1. Test Article and Installation Details	3
2.2. Design Modifications during Tests	3
2.3. Material Specifications	13
2.4. Soil Conditions	13
Chapter 3. Test Requirements and Evaluation Criteria	15
3.1. Crash Test Performed/Matrix	15
3.2. Evaluation Criteria	16
Chapter 4. Test Conditions	17
4.1. Test Facility	17
4.2. Vehicle Tow and Guidance System	17
4.3. Data Acquisition Systems	17
4.3.1. Vehicle Instrumentation and Data Processing	17
4.3.2. Anthropomorphic Dummy Instrumentation	18
4.3.3. Photographic Instrumentation Data Processing	19
Chapter 5. MASH Test 3-10 (Crash Test No. 609971-01-1)	21
5.1. Test Designation and Actual Impact Conditions	21
5.2. Weather Conditions	23
5.3. Test Vehicle	23
5.4. Test Description	25
5.5. Damage to Test Installation	25
5.6. Damage to Test Vehicle	26
5.7. Occupant Risk Factors	30
Chapter 6. MASH Test 3-11 (Crash Test No. 609971-03-1)	33
6.1. Test Designation and Actual Impact Conditions	33
6.2. Weather Conditions	35
6.3. Test Vehicle	35
6.4. Test Description	37
6.5. Damage to Test Installation	37
6.6. Damage to Test Vehicle	39
6.7. Occupant Risk Factors	42
Chapter 7. MASH Test 3-11 (Crash Test No. 609971-03-2)	45
7.1. Test Designation and Actual Impact Conditions	45
7.2. Weather Conditions	47
7.3. Test Vehicle	47
7.4. Test Description	49
7.5. Damage to Test Installation	49
7.6. Damage to Test Vehicle	51

7.7. Occupant Risk Factors	54
Chapter 8. Finite Element Analysis	57
8.1. Finite Element Modeling and Analysis.....	57
8.1.1. Finite Element Model Validation.....	57
8.1.2. Design Options.....	61
8.2. Summary of Finite Element Analysis.....	80
Chapter 9. Summary and Conclusions	85
9.1. Assessment of Test Results.....	85
9.2. Summary of Finite Element Analysis Research	86
9.3. Conclusions.....	87
References	89
Appendix A. Details of MGS Guardrail with Flare.....	91
A.1. 6099971-01-1 Drawings	91
A.2. 6099971-03-1 Drawings	102
A.3. 6099971-03-2 Drawings	109
Appendix B. Supporting Certification Documents.....	117
Appendix C. MASH Test 3-10 (Crash Test No. 609971-01-1).....	129
C.1. Vehicle Properties and Information	129
C.2. Sequential Photographs.....	131
C.3. Vehicle Angular Displacements	134
C.4. Vehicle Accelerations	135
Appendix D. MASH Test 3-11 (Crash Test No. 609971-03-1).....	137
D.1. Vehicle Properties and Information	137
D.2. Sequential Photographs.....	140
D.3. Vehicle Angular Displacements	143
D.4. Vehicle Accelerations	144
Appendix E. MASH Test 3-11 (Crash Test No. 609971-03-2).....	146
E.1. Vehicle Properties and Information	146
E.2. Sequential Photographs.....	149
E.3. Vehicle Angular Displacements	151
E.4. Vehicle Accelerations	152

LIST OF FIGURES

	Page
Figure 2.1. Details of MGS Guardrail with 7:1 Flare.....	4
Figure 2.2. MGS Guardrail with 7:1 Flare prior to Testing.....	5
Figure 2.3. Upstream Terminal of the MGS Guardrail with 7:1 Flare prior to Testing.	5
Figure 2.4. MGS Guardrail with 7:1 Flare at Impact prior to Testing.....	6
Figure 2.5. In-line View of the MGS Guardrail with 7:1 Flare prior to Testing.	6
Figure 2.6. Details of MGS Guardrail with 11:1 Flare.....	7
Figure 2.7. MGS Guardrail with 11:1 Flare prior to Testing.....	8
Figure 2.8. Upstream Terminal of the MGS Guardrail with 11:1 Flare prior to Testing.	8
Figure 2.9. MGS Guardrail with 11:1 Flare at Impact prior to Testing.....	9
Figure 2.10. In-line View of the MGS Guardrail with 11:1 Flare prior to Testing.	9
Figure 2.11. Details of MGS Guardrail with Reduced-Length 11:1 Flare.	10
Figure 2.12. MGS Guardrail with Shortened 11:1 Flare prior to Testing.....	11
Figure 2.13. Upstream Terminal of the MGS Guardrail with Shortened 11:1 Flare prior to Testing.....	11
Figure 2.14. MGS Guardrail with Shortened 11:1 Flare at Impact prior to Testing.....	12
Figure 2.15. Downstream View of MGS Guardrail with Shortened 11:1 Flare prior to Testing.....	12
Figure 3.1. Target CIP for Test 609971-01-1 on MGS Guardrail with 7:1 Flare.....	15
Figure 3.2. Target CIP for Test 609971-03-1 on MGS Guardrail with 11:1 Flare.....	15
Figure 3.3. Target CIP for Test 609971-03-2 on MGS Guardrail with Shortened 11:1 Flare.....	15
Figure 5.1. MGS Guardrail with Flare/Test Vehicle Geometrics for Test 609971-01-1.....	22
Figure 5.2. MGS Guardrail with Flare/Test Vehicle Impact Location for Test 609971-01-1.....	22
Figure 5.3. Impact Side of Test Vehicle before Test 609971-01-1.	23
Figure 5.4. Opposite Impact Side of Test Vehicle before Test 609971-01-1.	24
Figure 5.5. MGS Guardrail with Flare after Test at Impact Location for Test 609971-01-1.	26
Figure 5.6. MGS Guardrail with Flare after Impact for Test 609971-01-1.	26
Figure 5.7. Impact Side of Test Vehicle after Test 609971-01-1.	27
Figure 5.8. Front View of the Test Vehicle after Test 609971-01-1.	27
Figure 5.9. Overall Interior of Test Vehicle after Test 609971-01-1.....	28
Figure 5.10. Interior of Test Vehicle on Impact Side after Test 609971-01-1.	28
Figure 5.11. Summary of Results for <i>MASH</i> Test 3-10 on MGS Guardrail with Flare.....	31
Figure 6.1. MGS Guardrail with Flare/Test Vehicle Geometrics for Test 609971-03-1.....	34
Figure 6.2. MGS Guardrail with Flare/Test Vehicle Impact Location for Test 609971-03-1.....	34
Figure 6.3. Impact Side of Test Vehicle before Test 609971-03-1.	35
Figure 6.4. Opposite Impact Side of Test Vehicle before Test 609971-03-1.	36
Figure 6.5. MGS Guardrail with Flare after Test at Impact Location for Test 609971-03-1.	38
Figure 6.6. MGS Guardrail with Flare after Test 609971-03-1.....	38
Figure 6.7. Impact Side of Test Vehicle after Test 609971-03-1.	39
Figure 6.8. Rear Impact Side of Test Vehicle after Test 609971-03-1.....	39
Figure 6.9. Overall Interior of Test Vehicle after Test 609971-03-1.....	40
Figure 6.10. Interior of Test Vehicle on Impact Side after Test 609971-03-1.	40
Figure 6.11. Summary of Results for <i>MASH</i> Test 3-11 on MGS Guardrail with Flare.....	43
Figure 7.1. MGS Guardrail with Flare/Test Vehicle Geometrics for Test 609971-03-2.....	46

Figure 7.2. MGS Guardrail with Flare/Test Vehicle Impact Location for Test 609971-03-2.....	46
Figure 7.3. Impact Side of Test Vehicle before Test 609971-03-2.	47
Figure 7.4. Opposite Impact Side of Test Vehicle before Test 609971-03-2.	48
Figure 7.5. MGS Guardrail with Flare after Test at Impact Location for Test 609971-03-2.	50
Figure 7.6. MGS Guardrail with Flare after Test 609971-03-2.....	50
Figure 7.7. Impact Side of Test Vehicle after Test 609971-03-2.	51
Figure 7.8. Rear Impact Side of Test Vehicle after Test 609971-03-2.....	51
Figure 7.9. Overall Interior of Test Vehicle after Test 609971-03-2.....	52
Figure 7.10. Interior of Test Vehicle on Impact Side after Test 609971-03-2.	52
Figure 7.11. Summary of Results for <i>MASH</i> Test 3-11 on MGS Guardrail with Flare.....	55
Figure 8.1. RAM Model Used for FE Simulation.	58
Figure 8.2. Simulation Setup under TL-3 Conditions.....	58
Figure 8.3. Sequential Overhead Frames of Pickup Truck under TL-3 Conditions.	59
Figure 8.4. Sequential Frames to Compare FE Simulation (Top) to Crash Testing (Bottom) Immediately Leading to Rail Rupture Event.	59
Figure 8.5. Rail Rupture Experienced in Full-Scale Testing (Top) and Rail Strains Recorded in FE Simulation (Bottom).....	60
Figure 8.6. Sequential Frames Comparing FE Simulation on Flared MGS (Top) to NCHRP 350 Test No. 2214MG-2 (Bottom) (5).	61
Figure 8.7. Impact Conditions for Different MGS Flare Rates (Effective Angles).....	62
Figure 8.8. Details of Half-Post Spacing and Short Blockout.	65
Figure 8.9. Short Blockout Flared MGS Retrofitted with Channel Rubrail.	66
Figure 8.10. CIPs for Pickup Truck Impacting Flared MGS Retrofitted with Channel Rubrail.	67
Figure 8.11. Sequential Frames for Pickup Truck Impact at CIP on 15:1 Flared MGS Retrofitted with Channel Rubrail.....	68
Figure 8.12. Sequential Frames for Pickup Truck Impact at CIP on 18:1 Flared MGS Retrofitted with Channel Rubrail.....	69
Figure 8.13. CIPs for Small Car Impacting Flared MGS with Channel Rubrail.	70
Figure 8.14. Sequential Frames for Small Passenger Car Impact at CIP on 15:1 Flared MGS Retrofitted with Channel Rubrail.....	71
Figure 8.15. Sequential Frames for Small Passenger Car Impact at CIP on 18:1 Flared MGS Retrofitted with Channel Rubrail.....	72
Figure 8.16. FE Pickup Truck Tire Model Behavior.	73
Figure 8.17. Modified Channel Rubrail Location.....	74
Figure 8.18. Modified FE Simulation with 18:1 Flared MGS Retrofitted with Channel Rubrail.....	74
Figure 8.19. Sequential Frames for Pickup Truck Impact at CIP on Modified 18:1 Flared MGS Retrofitted with Channel Rubrail.	75
Figure 8.20. Sequential Frames for Small Car Impact at CIP on Modified 18:1 Flared MGS Retrofitted with Channel Rubrail.....	76
Figure 8.21. Sequential Frames for Pickup Truck Impact at CIP on Modified 15:1 Flared MGS Retrofitted with Channel Rubrail.	78
Figure 8.20. Sequential Frames for Small Car Impact at CIP on Modified 15:1 Flared MGS Retrofitted with Channel Rubrail.....	79
Figure B.1. Test Day Static Soil Strength Documentation for Test No. 609971-01-1.	125

Figure B.2. Test Day Static Soil Strength Documentation for Test No. 609971-03-1.	126
Figure B.3. Test Day Static Soil Strength Documentation for Test No. 609971-03-2.	127
Figure C.1. Vehicle Properties for Test No. 609971-01-1.	129
Figure C.2. Exterior Crush Measurements for Test No. 609971-01-1.	130
Figure C.3. Sequential Photographs for Test No. 609971-01-1 (Overhead Views).	131
Figure C.4. Sequential Photographs for Test No. 609971-01-1 (Frontal Views).	132
Figure C.5. Sequential Photographs for Test No. 609971-01-1 (Rear Views).	133
Figure C.6. Vehicle Angular Displacements for Test No. 609971-01-1.	134
Figure C.7. Vehicle Longitudinal Accelerometer Trace for Test No. 609971-01-1 (Accelerometer Located at Center of Gravity).	135
Figure C.8. Vehicle Lateral Accelerometer Trace for Test No. 609971-01-1 (Accelerometer Located at Center of Gravity).	135
Figure C.9. Vehicle Vertical Accelerometer Trace for Test No. 609971-01-1 (Accelerometer Located at Center of Gravity).	136
Figure D.1. Vehicle Properties for Test No. 609971-03-1.	137
Figure D.2. Exterior Crush Measurements for Test No. 609971-03-1.	138
Figure D.3. Occupant Compartment Measurements for Test No. 609971-03-1.	139
Figure D.4. Sequential Photographs for Test No. 609971-03-1 (Overhead Views).	140
Figure D.5. Sequential Photographs for Test No. 609971-03-1 (Frontal Views).	141
Figure D.6. Sequential Photographs for Test No. 609971-03-1 (Rear Views).	142
Figure D.7. Vehicle Angular Displacements for Test No. 609971-03-1.	143
Figure D.8. Vehicle Longitudinal Accelerometer Trace for Test No. 609971-03-1 (Accelerometer Located at Center of Gravity).	144
Figure D.9. Vehicle Lateral Accelerometer Trace for Test No. 609971-03-1 (Accelerometer Located at Center of Gravity).	144
Figure D.10. Vehicle Vertical Accelerometer Trace for Test No. 609971-03-1 (Accelerometer Located at Center of Gravity).	145
Figure E.1. Vehicle Properties for Test No. 609971-03-2.	146
Figure E.2. Exterior Crush Measurements for Test No. 609971-03-2.	147
Figure E.3. Occupant Compartment Measurements for Test No. 609971-03-2.	148
Figure E.4. Sequential Photographs for Test No. 609971-03-2 (Overhead Views).	149
Figure E.5. Sequential Photographs for Test No. 609971-03-2 (Rear Views).	150
Figure E.6. Vehicle Angular Displacements for Test No. 609971-03-2.	151
Figure E.7. Vehicle Longitudinal Accelerometer Trace for Test No. 609971-03-2 (Accelerometer Located at Center of Gravity).	152
Figure E.8. Vehicle Lateral Accelerometer Trace for Test No. 609971-03-2 (Accelerometer Located at Center of Gravity).	152
Figure E.9. Vehicle Vertical Accelerometer Trace for Test No. 609971-03-2 (Accelerometer Located at Center of Gravity).	153

LIST OF TABLES

	Page
Table 2.1. Soil Strength for Test 609971-01-1.	13
Table 2.2. Soil Strength for Test 609971-03-1.	13
Table 2.3. Soil Strength for Test 609971-03-2.	14
Table 3.1. Test Conditions and Evaluation Criteria Specified for <i>MASH</i> TL-3 Guardrails.	15
Table 3.2. Evaluation Criteria Required for <i>MASH</i> Testing.	16
Table 5.1. Impact Conditions for <i>MASH</i> Test 3-10, Crash Test No. 609971-01-1.	21
Table 5.2. Exit Parameters for <i>MASH</i> Test 3-10, Crash Test No. 609971-01-1.	21
Table 5.3. Weather Conditions for Test 609971-01-1.	23
Table 5.4. Vehicle Measurements for Test 609971-01-1.	24
Table 5.5. Events during Test 609971-01-1.	25
Table 5.6. Damage to MGS Guardrail with Flare for Test 609971-01-1.	25
Table 5.7. Occupant Compartment Deformation for Test 609971-01-1.	29
Table 5.8. Exterior Vehicle Damage for Test 609971-01-1.	29
Table 5.9. Occupant Risk Factors for Test 609971-01-1.	30
Table 6.1. Impact Conditions for <i>MASH</i> Test 3-11, Crash Test No. 609971-03-1.	33
Table 6.2. Exit Parameters for <i>MASH</i> Test 3-11, Crash Test No. 609971-03-1.	33
Table 6.3. Weather Conditions for Test 609971-03-1.	35
Table 6.4. Vehicle Measurements for Test 609971-03-1.	36
Table 6.5. Events during Test 609971-03-1.	37
Table 6.6. Damage to MGS Guardrail with Flare for Test 609971-03-1.	37
Table 6.7. Occupant Compartment Deformation for Test 609971-03-1.	41
Table 6.8. Exterior Vehicle Damage for Test 609971-03-1.	41
Table 6.9. Occupant Risk Factors for Test 609971-03-1.	42
Table 7.1. Impact Conditions for <i>MASH</i> Test 3-11, Crash Test No. 609971-03-2.	45
Table 7.2. Exit Parameters for <i>MASH</i> Test 3-11, Crash Test No. 609971-03-2.	45
Table 7.3. Weather Conditions for Test 609971-03-2.	47
Table 7.4. Vehicle Measurements for Test 609971-03-2.	48
Table 7.5. Events during Test 609971-03-2.	49
Table 7.6. Damage to MGS Guardrail with Flare for Test 609971-03-2.	49
Table 7.7. Occupant Compartment Deformation for Test 609971-03-2.	53
Table 7.8. Exterior Vehicle Damage for Test 609971-03-2.	53
Table 7.9. Occupant Risk Factors for Test 609971-03-2.	54
Table 8.1. Descriptive Comparison for Timestep.	60
Table 8.2. Comparison of the Occupant Risk Factors (Test 609971-03-2 vs. FE Simulation). ...	61
Table 8.3. Simulation Results from FE Models of MGS with Different Flare Rates.	63
Table 8.4. Simulation Results for Flared Half-Post Spacing MGS with Short Blockout.	66
Table 8.5. Simulation Results for Short Blockout Flared MGS with Channel Rubrail.	67
Table 8.6. CIP Investigation for the Pickup Truck (2270P).	67
Table 8.7. CIP Investigation for Small Car (1100C).	70
Table 8.8. Comparison of Simulation Results for 18:1 Flared MGS Retrofitted with Channel Rubrail with 12-inch Center-to-Ground Distance.	77
Table 8.9. Comparison of Simulation Results for 15:1 Flared MGS Retrofitted with Channel Rubrail with 12-inch Center-to-Ground Distance.	80

Table 8.10. Summary of FE Analysis for Pickup Truck.....	82
Table 8.11. Summary of FE Analysis for Small Car.	83
Table 9.1. Summary of <i>MASH</i> Tests on MGS Guardrail with Flare.	86
Table B.1. Test Day Static Soil Strength Documentation for Test No. 609971-01-1.	125
Table B.2. Test Day Static Soil Strength Documentation for Test No. 609971-03-1.	126
Table B.3. Test Day Static Soil Strength Documentation for Test No. 609971-03-2.	127

SI* (MODERN METRIC) CONVERSION FACTORS

APPROXIMATE CONVERSIONS TO SI UNITS

Symbol	When You Know	Multiply By	To Find	Symbol
LENGTH				
in	inches	25.4	millimeters	mm
ft	feet	0.305	meters	m
yd	yards	0.914	meters	m
mi	miles	1.61	kilometers	km
AREA				
in ²	square inches	645.2	square millimeters	mm ²
ft ²	square feet	0.093	square meters	m ²
yd ²	square yards	0.836	square meters	m ²
ac	acres	0.405	hectares	ha
mi ²	square miles	2.59	square kilometers	km ²
VOLUME				
fl oz	fluid ounces	29.57	milliliters	mL
gal	gallons	3.785	liters	L
ft ³	cubic feet	0.028	cubic meters	m ³
yd ³	cubic yards	0.765	cubic meters	m ³
NOTE: volumes greater than 1000L shall be shown in m ³				
MASS				
oz	ounces	28.35	grams	g
lb	pounds	0.454	kilograms	kg
T	short tons (2000 lb)	0.907	megagrams (or metric ton [†])	Mg (or "t")
TEMPERATURE (exact degrees)				
°F	Fahrenheit	5(F-32)/9 or (F-32)/1.8	Celsius	°C
FORCE and PRESSURE or STRESS				
lbf	poundforce	4.45	newtons	N
lbf/in ²	poundforce per square inch	6.89	kilopascals	kPa

APPROXIMATE CONVERSIONS FROM SI UNITS

Symbol	When You Know	Multiply By	To Find	Symbol
LENGTH				
mm	millimeters	0.039	inches	in
m	meters	3.28	feet	ft
m	meters	1.09	yards	yd
km	kilometers	0.621	miles	mi
AREA				
mm ²	square millimeters	0.0016	square inches	in ²
m ²	square meters	10.764	square feet	ft ²
m ²	square meters	1.195	square yards	yd ²
ha	hectares	2.47	acres	ac
km ²	Square kilometers	0.386	square miles	mi ²
VOLUME				
mL	milliliters	0.034	fluid ounces	oz
L	liters	0.264	gallons	gal
m ³	cubic meters	35.314	cubic feet	ft ³
m ³	cubic meters	1.307	cubic yards	yd ³
MASS				
g	grams	0.035	ounces	oz
kg	kilograms	2.202	pounds	lb
Mg (or "t")	megagrams (or "metric ton")	1.103	short tons (2000lb)	T
TEMPERATURE (exact degrees)				
°C	Celsius	1.8C+32	Fahrenheit	°F
FORCE and PRESSURE or STRESS				
N	newtons	0.225	poundforce	lbf
kPa	kilopascals	0.145	poundforce per square inch	lb/in ²

*SI is the symbol for the International System of Units

Chapter 1. BACKGROUND AND OBJECTIVE

1.1. BACKGROUND

The American Associate of State Highway and Transportation Officials (AASHTO) *Manual for Assessing Safety Hardware (MASH)* 2016 edition is the latest in a series of documents that provide guidance on testing and evaluation of roadside safety features (1). The original *MASH* document was published in 2009 and represents a comprehensive update to crash test and evaluation procedures to reflect changes in the vehicle fleet, operating conditions, and roadside safety knowledge and technology. The *MASH* documents supersede the National Cooperative Highway Research Program (NCHRP) Report 350, *Recommended Procedures for the Safety Performance Evaluation of Highway Features*, standards (2).

The Federal Highway Administration (FHWA) issued a January 7, 2016, memo mandating the AASHTO/FHWA Joint Implementation Agreement for *MASH* with compliance dates for installing *MASH* hardware that differ by hardware category. After December 31, 2019, all roadside safety devices must be successfully tested and evaluated according to the *MASH* 2016 standard edition. FHWA will no longer issue eligibility letters for highway safety hardware that has not been successfully crash tested according to the *MASH* 2016 edition evaluation criteria. At a minimum, all barriers on high-speed roadways on the National Highway System are required to meet Test Level 3 (TL-3) requirements.

A flared strong-post W-beam guardrail system allows for the potential to reduce guardrail installation lengths, which in turn would result in decreased guardrail construction and maintenance costs, as well as reduced impact frequency. Stolle et al. (3) conducted a research and test study to investigate the potential to increase flare rates for the Midwest Guardrail System (MGS) according to NCHRP Report 350 criteria. The researchers conducted computer simulations and full-scale crash testing that showed that the MGS could meet NCHRP Report 350 impact criteria when installed at a 5:1 flare rate. Impact severities during testing were found to be greater than intended, yet the MGS passed all NCHRP 350 requirements. The researchers recommended that whenever a guardrail is outside of the shy line for adjacent traffic, and the roadside terrain is sufficiently flat, flare rates should be increased to as high as 5:1 when using the MGS guardrail.

The structural adequacy *MASH* 2016 test for TL-3 conditions consists of a 5,000-lb pickup truck (denoted 2270P) impacting a barrier at 62 mi/h and 25 degrees with respect to the roadway. The severity *MASH* 2016 test consists of a 2,420-lb passenger car (denoted 1100C) impacting the barrier at 62 mi/h and 25 degrees with respect to the roadway.

MASH was developed to incorporate significant changes and additions to procedures for safety-performance evaluation, as well as updates reflecting the changing character of the highway network and the vehicles using it. For example, *MASH* increased the weight of the pickup truck design test vehicle from 4,409 lb to 5,000 lb, changed the body style from a ¾-ton standard cab to a ½-ton four-door, and imposed a minimum height for the vertical center of gravity (CG) of 28 inches. The increase in vehicle mass represents an increase in impact severity of approximately 13 percent for Test 3-11 with the pickup truck design test vehicle with respect to the impact conditions of NCHRP Report 350. The increased impact severity may, therefore,

result in increased impact forces and larger lateral barrier deflections compared to NCHRP Report 350.

The impact conditions for the small car test have also changed. The weight of the small passenger design test vehicle increased from 1,800 lb to 2,420 lb, and impact angle increased from 20 degrees to 25 degrees with respect to the roadway. These changes represent an increase in impact severity of 105 percent for Test 3-10 with the small car design test vehicle compared to the impact conditions of NCHRP Report 350. This increase in impact severity might result in increased vehicle deformation and could possibly aggravate vehicle stability. Specifically, when a flare rate is included in the guardrail design, there is an increment of the effective impact angle between the vehicle and the guardrail, which results in a considerably higher impact severity and requires an increasing level of demand on the structural capacity of a barrier system. For example, under *MASH* conditions, a 5:1 flare rate would increase the impact severity 196 percent for Test 3-10.

MASH also adopted more quantitative and stringent evaluation criteria for occupant compartment deformation than NCHRP Report 350. An increase in impact severity might result in increased vehicle deformation and could possibly result in failure to meet the latest *MASH* evaluation criteria. For example, NCHRP Report 350 established a 6-inch threshold for occupant compartment deformation or intrusion. *MASH*, by comparison, limited the extent of roof crush to no more than 3.9 inches. In addition, *MASH* requires that the vehicle windshield not sustain a deformation greater than 3 inches and have no holes or tears in the safety lining as a result of the test impact. Although these evaluation criteria are applicable to all roadside safety device testing, they are most relevant for sign support design and testing. In addition, little evaluation of sign supports has been performed with larger vehicles such as the pickup. Systems that have been demonstrated to be crashworthy for passenger cars may not be geometrically compatible with pickup trucks.

1.2. OBJECTIVE

The purpose of the tests reported herein was to assess the performance of the MGS when implemented with flare conditions according to the safety-performance evaluation guidelines included in *MASH (I)*. The crash tests were performed in accordance with *MASH TL-3*, which requires two crash tests (as discussed in Chapter 3 of this report).

After the full-scale crash tests were complete, an effort was initiated through finite element modeling and simulations to investigate the crashworthiness of the MGS at smaller flare rates and when considering prioritized MGS retrofit options, still for high-speed impact conditions. In all, three full-scale crash tests were performed, and five finite element analysis scenarios were evaluated.

Chapter 2. SYSTEM DETAILS

2.1. TEST ARTICLE AND INSTALLATION DETAILS

For the first test (609971-01-1), the test installation measured 181 ft 3 inches long, and the distance from the ground surface to the top of the W-beam was 31 inches for the entire length of the rail. There was a Texas Department of Transportation (TxDOT) downstream anchor terminal (DAT) on each end, and the remainder of the installation was a 12-gauge 4-space W-beam guardrail supported by 72-inch-long wide-flange guardrail posts. These posts were spaced at 75 inches and embedded 40 inches deep in drilled holes. Timber blockouts were used as spacers between the guardrail and the posts. The post holes were backfilled with crushed limestone base, which was compacted to *MASH* standards. Rail splices were midway between the posts. A 131-ft 3-inch long section was flared back from the other 50-ft section at a 7:1 flare, such that the end post was 18 ft 4 inches toward the field side relative to the 50-ft section. Figure 2.1 through Figure 2.5 show the general assembly drawing and photographs of the installation.

Appendix A provides further details on the MGS guardrail with flare. Drawings were provided by the Texas A&M Transportation Institute (TTI) Proving Ground, and construction was performed by DMA Construction Inc. and supervised by TTI Proving Ground personnel.

2.2. DESIGN MODIFICATIONS DURING TESTS

For the second test (609971-03-1), a 131-ft 3-inch long section was flared back from the other 50-ft section at an 11:1 flare, such that the end post of the DAT was 11 ft 10½ inches toward the field side relative to the 50-ft section. Figure 2.6 through Figure 2.10 display the general assembly drawing and photographs of the installation.

For the third test (609971-03-2), a 100-ft long 11:1 flare was located between two 50-ft 9½-inch long SoftStop® terminals. The total length of the installation was 201 ft 7 inches. Figure 2.11 through Figure 2.15 contain the general assembly drawing and photographs of the installation.

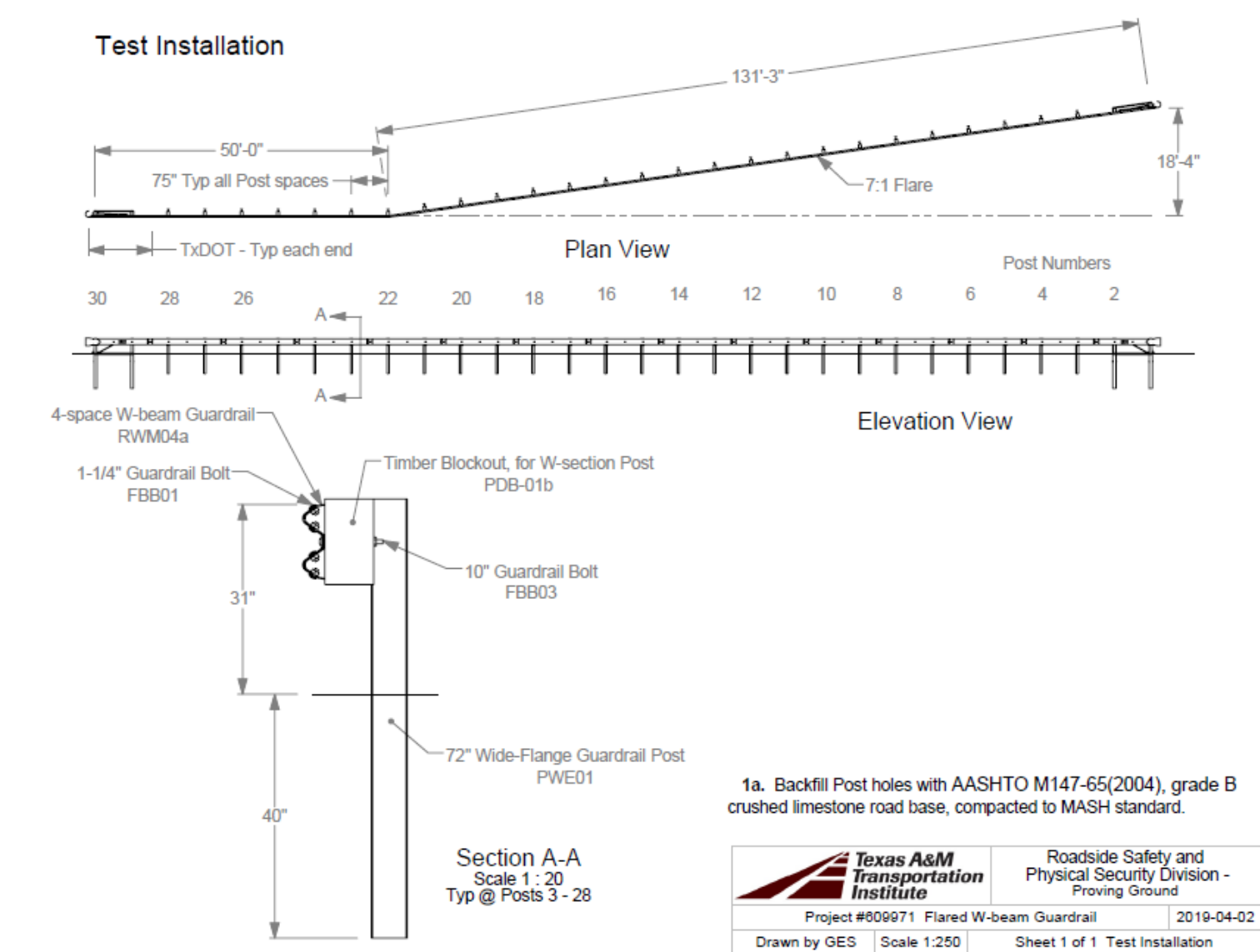


Figure 2.1. Details of MGS Guardrail with 7:1 Flare.



Figure 2.2. MGS Guardrail with 7:1 Flare prior to Testing.

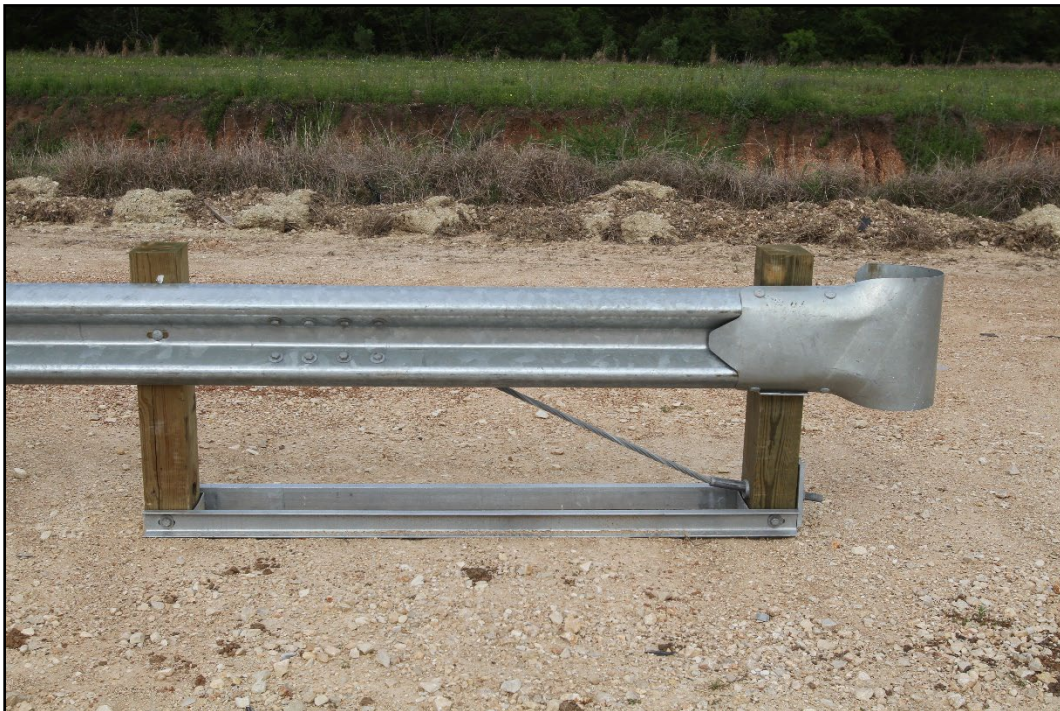


Figure 2.3. Upstream Terminal of the MGS Guardrail with 7:1 Flare prior to Testing.



Figure 2.4. MGS Guardrail with 7:1 Flare at Impact prior to Testing.



Figure 2.5. In-line View of the MGS Guardrail with 7:1 Flare prior to Testing.

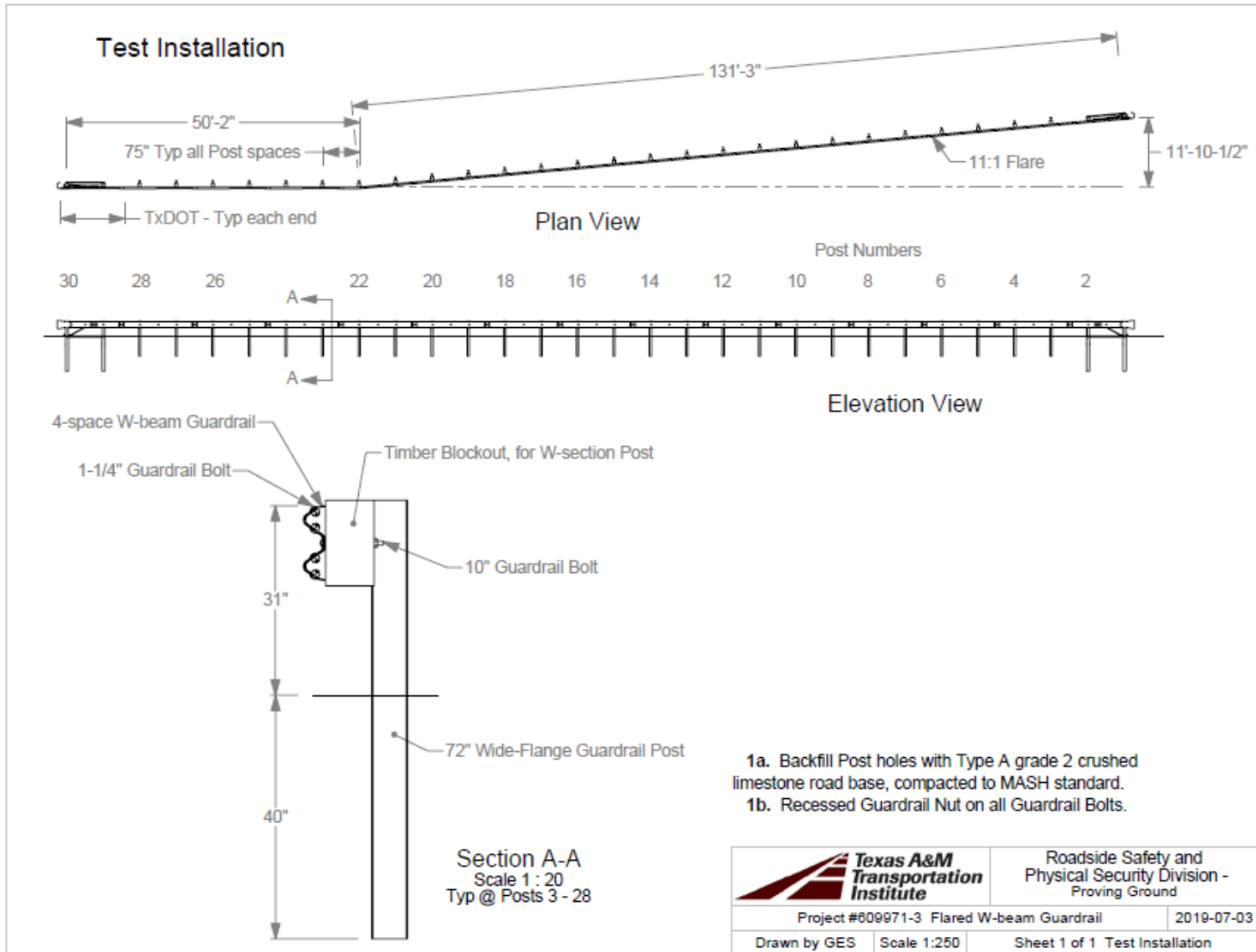


Figure 2.6. Details of MGS Guardrail with 11:1 Flare.



Figure 2.7. MGS Guardrail with 11:1 Flare prior to Testing.



Figure 2.8. Upstream Terminal of the MGS Guardrail with 11:1 Flare prior to Testing.



Figure 2.9. MGS Guardrail with 11:1 Flare at Impact prior to Testing.



Figure 2.10. In-line View of the MGS Guardrail with 11:1 Flare prior to Testing.

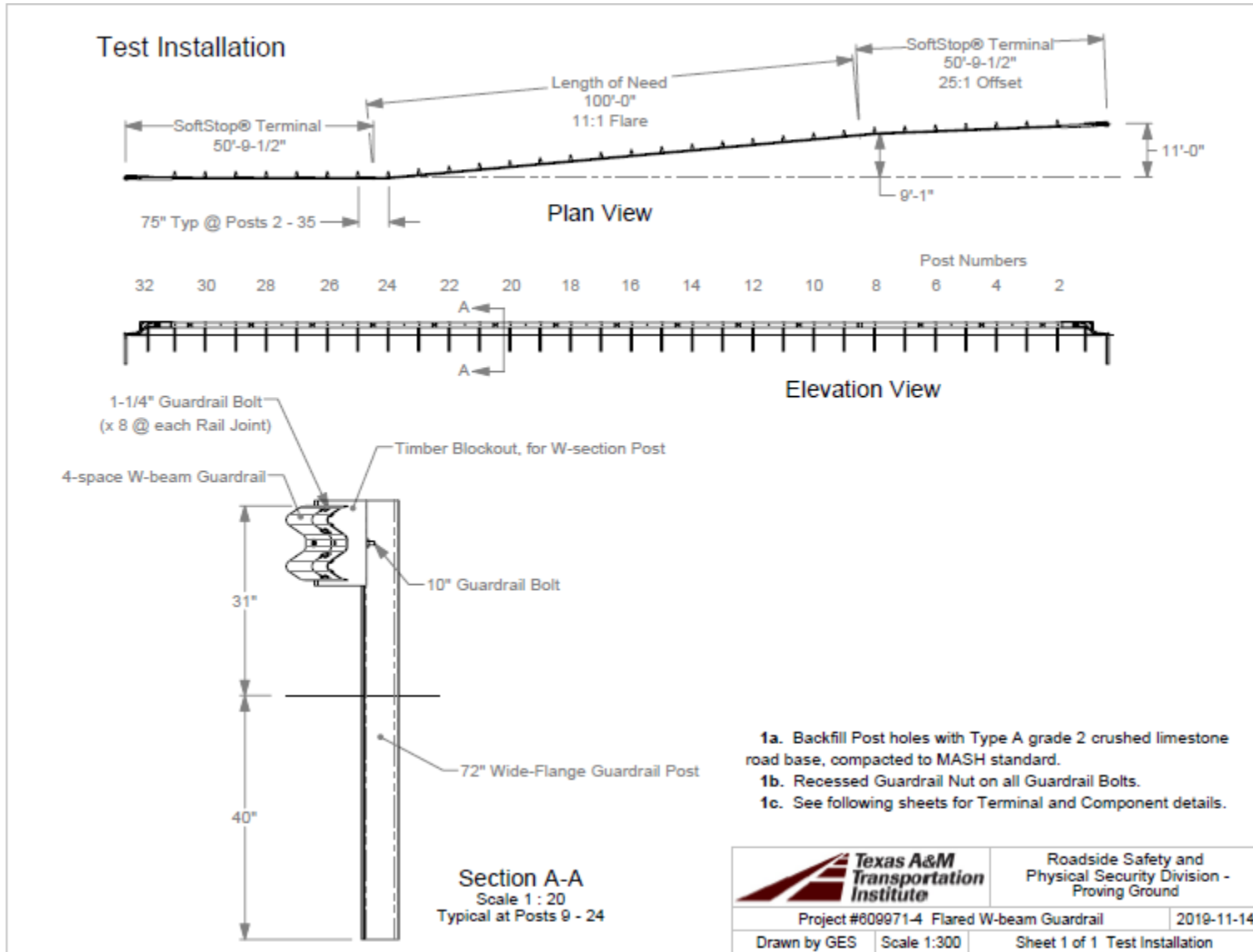


Figure 2.11. Details of MGS Guardrail with Reduced-Length 11:1 Flare.



Figure 2.12. MGS Guardrail with Shortened 11:1 Flare prior to Testing.



Figure 2.13. Upstream Terminal of the MGS Guardrail with Shortened 11:1 Flare prior to Testing.



Figure 2.14. MGS Guardrail with Shortened 11:1 Flare at Impact prior to Testing.



Figure 2.15. Downstream View of MGS Guardrail with Shortened 11:1 Flare prior to Testing.

2.3. MATERIAL SPECIFICATIONS

Appendix B provides material certification documents for the materials used to install/construct the MGS guardrail with flare.

2.4. SOIL CONDITIONS

The test installation was installed in standard soil meeting Grade B crushed limestone of AASHTO standard specification M147-17 “Materials for Aggregate and Soil-Aggregate Subbase, Base, and Surface Courses” for Crash Test 609971-01-1. For Crash Tests 609971-03-1 and 609971-03-2, AASHTO M147-17 Type A Grade 2 Crushed Limestone was used.

In accordance with Appendix B of *MASH*, soil strength was measured the day of each crash test. During installation of the MGS guardrail with flare for full-scale crash testing, two 6-ft-long W6×16 posts were installed in the immediate vicinity of the MGS guardrail with flare using the same fill materials and installation procedures used in the test installation and the standard dynamic test. Table B.1 in Appendix B presents minimum soil strength properties established through the dynamic testing performed in accordance with *MASH* Appendix B.

As determined by the tests summarized in Appendix B, Table B.1, the minimum post loads are shown in Table 2.1 for Test 609971-01-1, Table 2.2 for Test 609971-03-1, and Table 2.3 for Test 609971-03-2.

On the day of Test 609971-01-1, loads on the post at deflections were as follows: the backfill material in which the MGS guardrail with flare was installed met the minimum *MASH* requirements for soil strength.

Table 2.1. Soil Strength for Test 609971-01-1.

Displacement (in.)	Minimum Load (lb)	Actual Load (lb)
5	3,940	10,300
10	5,500	11,300
15	6,540	11,600

On the day of Test 609971-03-1, loads on the post at deflections were as follows: the backfill material in which the MGS guardrail with flare was installed met the minimum *MASH* requirements for soil strength.

Table 2.2. Soil Strength for Test 609971-03-1.

Displacement (in.)	Minimum Load (lb)	Actual Load (lb)
5	3,940	9,122
10	5,500	9,913
15	6,540	10,154

On the day of Test 609971-03-2, loads on the post at deflections were as follows: the backfill material in which the MGS guardrail with flare was installed met the minimum *MASH* requirements for soil strength.

Table 2.3. Soil Strength for Test 609971-03-2.

Displacement (in.)	Minimum Load (lb)	Actual Load (lb)
5	3,940	10,000
10	5,500	10,757
15	6,540	10,656

Chapter 3. TEST REQUIREMENTS AND EVALUATION CRITERIA

3.1. CRASH TEST PERFORMED/MATRIX

Table 3.1 shows the test conditions and evaluation criteria for the *MASH* tests performed on the guardrails. The target critical impact points (CIPs) for each test were determined using the information provided in *MASH* Section 2.2.1 and Section 2.3.2. Figure 3.1, Figure 3.2, and Figure 3.3 show the target CIPs for each *MASH* test on the MGS guardrail with flare.

Table 3.1. Test Conditions and Evaluation Criteria Specified for *MASH* TL-3 Guardrails.

Test Designation	Test Vehicle	Impact Speed	Impact Angle	Evaluation Criteria
3-10	1100C	62 mi/h	25°	A, D, F, H, I
3-11	2270P	62 mi/h	25°	A, D, F, H, I

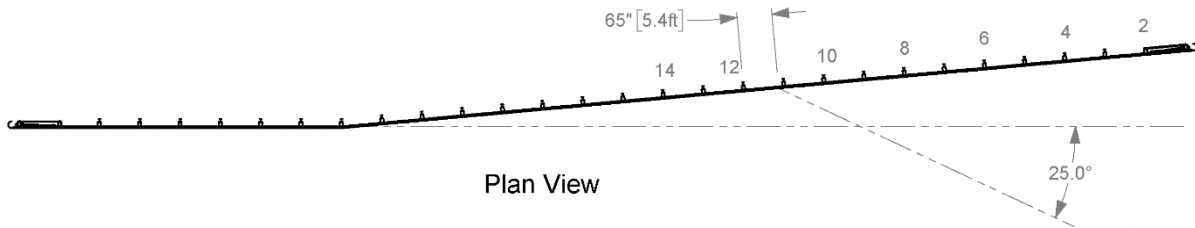


Figure 3.1. Target CIP for Test 609971-01-1 on MGS Guardrail with 7:1 Flare.

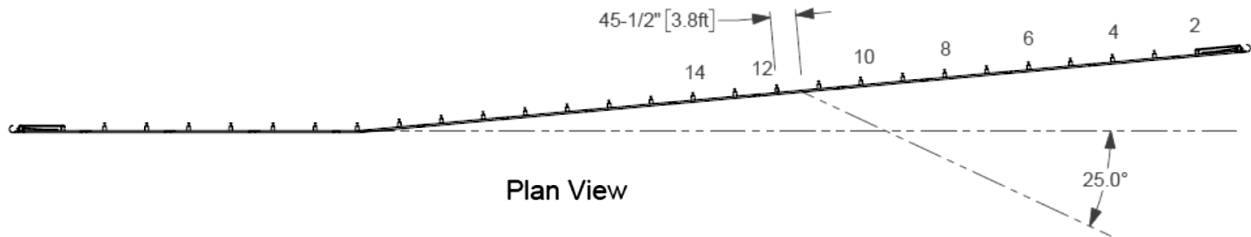


Figure 3.2. Target CIP for Test 609971-03-1 on MGS Guardrail with 11:1 Flare.

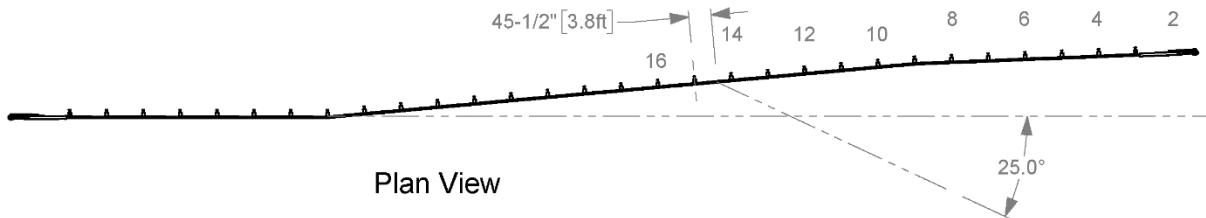


Figure 3.3. Target CIP for Test 609971-03-2 on MGS Guardrail with Shortened 11:1 Flare.

The crash tests and data analysis procedures were in accordance with guidelines presented in *MASH*. Chapter 4 presents brief descriptions of these procedures.

3.2. EVALUATION CRITERIA

The appropriate safety evaluation criteria from Tables 2.2 and 5.1 of *MASH* were used to evaluate the crash tests reported herein. Table 3.2 provides detailed information on the evaluation criteria.

Table 3.2. Evaluation Criteria Required for *MASH* Testing.

Evaluation Factors	Evaluation Criteria	<i>MASH</i> Level 3 Test
A.	Test article should contain and redirect the vehicle or bring the vehicle to a controlled stop; the vehicle should not penetrate, underride, or override the installation although controlled lateral deflection of the test article is acceptable.	10, 11
D.	Detached elements, fragments, or other debris from the test article should not penetrate or show potential for penetrating the occupant compartment, or present undue hazard to other traffic, pedestrians, or personnel in a work zone. Deformations of, or intrusions into, the occupant compartment should not exceed limits set forth in Section 5.2.2 and Appendix E of <i>MASH</i> .	10, 11
F.	The vehicle should remain upright during and after collision. The maximum roll and pitch angles are not to exceed 75 degrees.	10, 11
H.	Occupant impact velocities (OIV) should satisfy the following limits: Preferred value of 30 ft/s, or maximum allowable value of 40 ft/s. Occupant impact velocities (OIV) should satisfy the following limits: Preferred value of 10 ft/s, or maximum allowable value of 16 ft/s.	10, 11
I.	The occupant ridedown accelerations should satisfy the following: Preferred value of 15.0 g, or maximum allowable value of 20.49 g.	10, 11

Chapter 4. TEST CONDITIONS

4.1. TEST FACILITY

The full-scale crash tests reported herein were performed at the TTI Proving Ground, an International Standards Organization (ISO)/International Electrotechnical Commission (IEC) 17025-accredited laboratory with American Association for Laboratory Accreditation (A2LA) Mechanical Testing Certificate 2821.01. The full-scale crash tests were performed according to TTI Proving Ground quality procedures, as well as *MASH* guidelines and standards.

The test facilities of the TTI Proving Ground are located on The Texas A&M University System RELIS Campus, which consists of a 2000-acre complex of research and training facilities situated 10 miles northwest of the flagship campus of Texas A&M University. The site, formerly a United States Army Air Corps base, has large expanses of concrete runways and parking aprons well suited for experimental research and testing in the areas of vehicle performance and handling, vehicle-roadway interaction, highway pavement durability and efficacy, and roadside safety hardware and perimeter protective device evaluation. The sites selected for construction and testing are along the edge of an out-of-service apron/runway. The apron/runway consists of an unreinforced jointed-concrete pavement in 12.5-ft × 15-ft blocks nominally 6 inches deep. The aprons were built in 1942, and the joints have some displacement but are otherwise flat and level.

4.2. VEHICLE TOW AND GUIDANCE SYSTEM

For the testing utilizing the 1100C and 2270P vehicles, each was towed into the test installation using a steel cable guidance and reverse tow system. A steel cable for guiding the test vehicle was tensioned along the path, anchored at each end, and threaded through an attachment to the front wheel of the test vehicle. An additional steel cable was connected to the test vehicle, passed around a pulley near the impact point and through a pulley on the tow vehicle, and then anchored to the ground such that the tow vehicle moved away from the test site. A 2:1 speed ratio between the test and tow vehicle existed with this system. Just prior to impact with the installation, the test vehicle was released and ran unrestrained. The vehicle remained freewheeling (i.e., no steering or braking inputs) until it cleared the immediate area of the test site.

4.3. DATA ACQUISITION SYSTEMS

4.3.1. Vehicle Instrumentation and Data Processing

Each test vehicle was instrumented with a self-contained onboard data acquisition system. The signal conditioning and acquisition system is a multi-channel data acquisition system (DAS) produced by Diversified Technical Systems Inc. The accelerometers, which measure the x, y, and z axis of vehicle acceleration, are strain gauge type with linear millivolt output proportional to acceleration. Angular rate sensors, measuring vehicle roll, pitch, and yaw rates, are ultra-small, solid-state units designed for crash test service. The data acquisition hardware and software conform to the latest SAE J211, Instrumentation for Impact Test. Each of

the channels is capable of providing precision amplification, scaling, and filtering based on transducer specifications and calibrations. During the test, data are recorded from each channel at a rate of 10,000 samples per second with a resolution of one part in 65,536. Once data are recorded, internal batteries back these up inside the unit in case the primary battery cable is severed. Initial contact of the pressure switch on the vehicle bumper provides a time zero mark and initiates the recording process. After each test, the data are downloaded from the DAS unit into a laptop computer at the test site. The Test Risk Assessment Program (TRAP) software then processes the raw data to produce detailed reports of the test results.

Each DAS is returned to the factory annually for complete recalibration and to ensure that all instrumentation used in the vehicle conforms to the specifications outlined by SAE J211. All accelerometers are calibrated annually by means of an ENDEVCO® 2901 precision primary vibration standard. This standard and its support instruments are checked annually and receive a National Institute of Standards Technology (NIST) traceable calibration. The rate transducers used in the data acquisition system receive calibration via a Genisco Rate-of-Turn table. The subsystems of each data channel are also evaluated annually, using instruments with current NIST traceability, and the results are factored into the accuracy of the total data channel per SAE J211. Calibrations and evaluations are also made anytime data are suspect. Acceleration data are measured with an expanded uncertainty of ± 1.7 percent at a confidence factor of 95 percent ($k = 2$).

TRAP uses the DAS-captured data to compute the occupant/compartiment impact velocities, time of occupant/compartiment impact after vehicle impact, and highest 10-millisecond (ms) average ridedown acceleration. TRAP calculates change in vehicle velocity at the end of a given impulse period. In addition, maximum average accelerations over 50-ms intervals in each of the three directions are computed. For reporting purposes, the data from the vehicle-mounted accelerometers are filtered with an SAE Class 180-Hz low-pass digital filter, and acceleration versus time curves for the longitudinal, lateral, and vertical directions are plotted using TRAP.

TRAP uses the data from the yaw, pitch, and roll rate transducers to compute angular displacement in degrees at 0.0001-s intervals, and then plots yaw, pitch, and roll versus time. These displacements are in reference to the vehicle-fixed coordinate system with the initial position and orientation being initial impact. Rate of rotation data is measured with an expanded uncertainty of ± 0.7 percent at a confidence factor of 95 percent ($k = 2$).

4.3.2. Anthropomorphic Dummy Instrumentation

An Alderson Research Laboratories Hybrid II, 50th percentile male anthropomorphic dummy, restrained with lap and shoulder belts, was placed in the front seat on the impact side of impact of the 1100C vehicle. The dummy was not instrumented.

According to *MASH*, use of a dummy in the 2270P vehicle is optional, and no dummy was used in the related tests.

4.3.3. Photographic Instrumentation Data Processing

Photographic coverage of each test included three digital high-speed cameras:

- One located overhead with a field of view perpendicular to the ground and directly over the impact point.
- One placed upstream from the installation at an angle to have a field of view of the interaction of the rear of the vehicle with the installation.
- A third placed with a field of view parallel to and aligned with the installation at the downstream end.

A flashbulb on the impacting vehicle was activated by a pressure-sensitive tape switch to indicate the instant of contact with the MGS guardrail with critical flare. The flashbulb was visible from each camera. The video files from these digital high-speed cameras were analyzed to observe phenomena occurring during the collision and to obtain time-event, displacement, and angular data. A digital camera recorded and documented conditions of each test vehicle and the installation before and after the test.

Chapter 5. *MASH* TEST 3-10 (CRASH TEST NO. 609971-01-1)

5.1. TEST DESIGNATION AND ACTUAL IMPACT CONDITIONS

See Table 5.1 for details on *MASH* impact conditions and Table 5.2 for the exit parameters for Test 609971-01-1. Figure 5.1 and Figure 5.2 depict the target impact setup.

Table 5.1. Impact Conditions for *MASH* Test 3-10, Crash Test No. 609971-01-1.

Test Parameter	Specification	Tolerance	Measured
Impact Speed (mi/h)	62	±2.5	61.8
Impact Angle (deg)	25	±1.5	24.8 (32.8 to the flare)
Vehicle Inertial Weight (lb)	2,420	±55	2,440
Impact Severity (kip-ft)	51	≥51	54.8 (91.4 to the flare)
Impact Location	65 inches upstream of centerline of post 12	±1 ft (12 inches)	63.7 inches upstream of centerline of post 12

Table 5.2. Exit Parameters for *MASH* Test 3-10, Crash Test No. 609971-01-1.

Exit Parameter	Measured
Speed (mi/h)	N/A
Trajectory (deg)	N/A
Heading (deg)	N/A
Brakes applied post impact (s)	Brakes not applied
Vehicle at rest position	93 ft downstream of impact point 25 ft to the field side 95 degrees left
Comments:	Vehicle rolled once and came to rest on its tires Vehicle did not cross exit box ^a Vehicle penetrated through the guardrail

Note: N/A = not applicable.

^a Not less than 32.8 ft downstream from loss of contact for cars and pickups is optimal.



Figure 5.1. MGS Guardrail with Flare/Test Vehicle Geometrics for Test 609971-01-1.



Figure 5.2. MGS Guardrail with Flare/Test Vehicle Impact Location for Test 609971-01-1.

5.2. WEATHER CONDITIONS

Table 5.3 provides the weather conditions for Test 609971-01-1.

Table 5.3. Weather Conditions for Test 609971-01-1.

Date of Test	04-22-2019 AM
Wind Speed (mi/h)	8
Wind Direction (deg)	120
Temperature (°F)	72
Relative Humidity (%)	82
Vehicle Traveling (deg)	195

5.3. TEST VEHICLE

Figure 5.3 and Figure 5.4 show the 2008 Kia Rio used for the crash test. Table 5.4 shows the vehicle measurements. Figure C.1 in Appendix C.1 gives additional dimensions and information on the vehicle.



Figure 5.3. Impact Side of Test Vehicle before Test 609971-01-1.



Figure 5.4. Opposite Impact Side of Test Vehicle before Test 609971-01-1.

Table 5.4. Vehicle Measurements for Test 609971-01-1.

Test Parameter	<i>MASH</i>	Allowed Tolerance	Measured
Dummy (if applicable) ^a (lb)	165	N/A	165
Gross Static ^a (lb)	2,585	±25	2,605
Wheelbase (inches)	98	±5	98.8
Front Overhang (inches)	35	±4	33
Overall Length (inches)	169	±8	165.8
Overall Width (inches)	65	±3	66.4
Hood Height (inches)	28	±4	27
Track Width ^b (inches)	59	±2	57.7
CG aft of Front Axle ^c (inches)	39	±4	35.6
CG above Ground ^{c,d} (inches)	N/A	N/A	N/A

^a If a dummy is used, the gross static vehicle mass should be increased by the mass of the dummy.

^b Average of front and rear axles.

^c For test inertial mass.

^d 2270P vehicle must meet minimum CG height requirement.

5.4. TEST DESCRIPTION

Table 5.5 lists events that occurred during Test 609971-01-1. Figures C.3 through C.5 in Appendix C.2 present sequential photographs during the test.

Table 5.5. Events during Test 609971-01-1.

Time (s)	Events
0.0000	Vehicle contacted the barrier
0.0130	Posts 11 and 12 began to deflect toward field side
0.0360	Vehicle began to redirect
0.0450	Posts 10 and 13 began to rotate toward the impact point
0.0600	Rail disconnected from blockout on post 12
0.0860	Guardrail at Post 12 bolt hole began to rupture
0.1000	Guardrail completely ruptured
0.2860	Entire vehicle was on the field side of the test article

5.5. DAMAGE TO TEST INSTALLATION

The W-beam guardrail ruptured at post 12 and released from post 11 through post 17. The soil was disturbed at posts 1 and 2, post 11 was leaning toward the field side at 2 degrees from vertical, and posts 12 and 13 were leaning toward the field side at 75 degrees from vertical and downstream at 5 degrees from vertical. Post 14 was leaning downstream at 17 degrees from vertical and toward the field side at 2 degrees from vertical. Table 5.6 describes the damage to the MGS guardrail with flare. Figure 5.5 and Figure 5.6 show the damage to the MGS guardrail with flare.

Table 5.6. Damage to MGS Guardrail with Flare for Test 609971-01-1.

Test Parameter	Measured
Permanent Deflection/Location	N/A (vehicle broke through guardrail)
Dynamic Deflection	N/A (vehicle broke through guardrail)
Working Width ^a and Height	N/A (vehicle broke through guardrail)

^a Per *MASH*, “The working width is the maximum dynamic lateral position of any major part of the system or vehicle. These measurements are all relative to the pre-impact traffic face of the test article.” In other words, working width is the total barrier width plus the maximum dynamic intrusion of any portion of the barrier or test vehicle past the field side edge of the barrier.



Figure 5.5. MGS Guardrail with Flare after Test at Impact Location for Test 609971-01-1.



Figure 5.6. MGS Guardrail with Flare after Impact for Test 609971-01-1.

5.6. DAMAGE TO TEST VEHICLE

Figure 5.7 and Figure 5.8 show the damage sustained by the vehicle. Figure 5.9 and Figure 5.10 show the interior of the test vehicle. Table 5.7 and Table 5.8 provide details on the occupant compartment deformation and exterior vehicle damage. Figure C.2 in Appendix C.1 provides exterior crush measurements.



Figure 5.7. Impact Side of Test Vehicle after Test 609971-01-1.



Figure 5.8. Front View of the Test Vehicle after Test 609971-01-1.



Figure 5.9. Overall Interior of Test Vehicle after Test 609971-01-1.



Figure 5.10. Interior of Test Vehicle on Impact Side after Test 609971-01-1.

Table 5.7. Occupant Compartment Deformation for Test 609971-01-1.

Test Parameter	Specification	Measured^a
Roof	≤4.0 inches	N/A
Windshield	≤3.0 inches	N/A
A and B Pillars	≤5.0 overall/≤3.0 inches lateral	N/A
Foot Well/Toe Pan	≤9.0 inches	N/A
Floor Pan/Transmission Tunnel	≤12.0 inches	N/A
Side Front Panel	≤12.0 inches	N/A
Front Door (above Seat)	≤9.0 inches	N/A
Front Door (below Seat)	≤12.0 inches	N/A

^a Due to the test failure from the vehicle rollover, no measurements were taken of the occupant compartment.

Table 5.8. Exterior Vehicle Damage for Test 609971-01-1.

Side Windows	Shattered due to vehicle roll
Maximum Exterior Deformation	9 inches at front bumper
VDS	1RFQ5
CDC	01FRES3
Fuel Tank Damage	None
Description of Damage to Vehicle:	The front bumper, hood, grill, radiator and support, right fender, right tire and rim, right front door and glass, right A pillar, right rear door, right rear tire and rim, and left front fender were damaged. Damage to the windshield was caused by the flexing of the vehicle body during impact, not from contact with the test article.

5.7. OCCUPANT RISK FACTORS

Data from the accelerometers were digitized for evaluation of occupant risk, and the results are shown in Table 5.9. Figure C.6 in Appendix C.3 shows the vehicle angular displacements, and Figures C.7 through C.9 in Appendix C.4 show acceleration versus time traces.

Table 5.9. Occupant Risk Factors for Test 609971-01-1.

Test Parameter	<i>MASH</i>	Measured	Time
OIV, Longitudinal (ft/s)	≤ 40.0 <i>30.0^a</i>	21.8	at 0.1296 s on right side of interior
OIV, Lateral (ft/s)	≤ 40.0 <i>30.0</i>	12.8	at 0.1296 s on right side of interior
Ridedown, Longitudinal (g)	≤ 20.49 <i>15.0</i>	8.3	2.1006–2.1106 s
Ridedown, Lateral (g)	≤ 20.49 <i>15.0</i>	9.4	2.0955–2.1055 s
Theoretical Head Impact Velocity (THIV) (m/s)	N/A	7.0	at 0.1234 s on right side of interior
Acceleration Severity Index (ASI)	N/A	1.0	0.0570–0.1070 s
50-ms Moving Avg. Accelerations (MA) Longitudinal (g)	N/A	8.5	0.0422–0.0922 s
50-ms MA Lateral (g)	N/A	5.6	0.0426–0.0926 s
50-ms MA Vertical (g)	N/A	4.7	0.0770–0.1270 s
Roll (deg)	≤ 75	393	2.9564 s
Pitch (deg)	≤ 75	26	2.2072 s
Yaw (deg)	N/A	91	2.9733 s

^a Values in italics are the preferred *MASH* values.





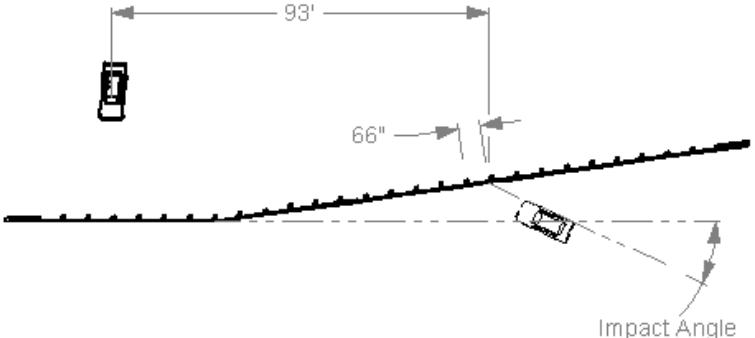
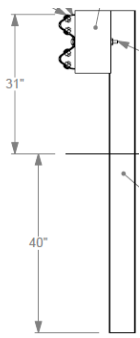
	Test Agency		Texas A&M Transportation Institute (TTI)					
	Test Standard/Test No.		MASH 2016, Test 3-10					
	TTI Project No.		609971-01-1					
	Test Date		2019-04-22					
	TEST ARTICLE							
	Type		Longitudinal Guardrail					
	Name		MGS Guardrail with Flare					
	Length		181 ft 3 inches					
	Key Materials		Steel, wood, crushed concrete					
	Soil Type and Condition		AASHTO M147-17 Grade B Crushed Limestone					
	TEST VEHICLE							
	Type/Designation		1100C					
	Year, Make and Model		2008 Kia Rio					
	Inertial Weight (lb)		2,440					
	Dummy (lb)		165					
	Gross Static (lb)		2,605					
IMPACT CONDITIONS								
Impact Speed (mi/h)		61.8						
Impact Angle (deg)		24.8 (32.8 to the flare)						
Impact Location		63.7 inches upstream of centerline of post 12						
Impact Severity (kip-ft)		54.8 (91.4 to the flare)						
EXIT CONDITIONS								
Exit Speed (mi/h)		N/A						
Trajectory/Heading Angle (deg)		N/A						
Exit Box Criteria		Vehicle did not cross the line						
Stopping Distance		93 ft downstream 25 ft to the field side						
TEST ARTICLE DEFLECTIONS								
Dynamic (inches)		N/A						
Permanent (inches)		N/A						
Working Width/Height (inches)		N/A						
VEHICLE DAMAGE								
VDS		1RFQ5						
CDC		01FRES3						
Max. Ext. Deformation		9 inches at front bumper						
Max Occupant Compartment Deformation		0 inches						
OCCUPANT RISK VALUES								
Long. OIV (ft/s)	21.8	Long. Ridedown (g)	8.3	Max 50-ms Long. (g)	8.5	Max Roll (deg)	393	
Lat. OIV (ft/s)	12.8	Lat. Ridedown (g)	9.4	Max 50-ms Lat. (g)	5.6	Max Pitch (deg)	26	
THIV (m/s)	7.0	ASI	1.0	Max 50-ms Vert. (g)	4.7	Max Yaw (deg)	91	
								

Figure 5.11. Summary of Results for MASH Test 3-10 on MGS Guardrail with Flare.

Chapter 6. *MASH* TEST 3-11 (CRASH TEST NO. 609971-03-1)

6.1. TEST DESIGNATION AND ACTUAL IMPACT CONDITIONS

See Table 6.1 for details on *MASH* impact conditions and Table 6.2 for the exit parameters for Test 609971-03-1. Figure 6.1 and Figure 6.2 depict the target impact setup.

Table 6.1. Impact Conditions for *MASH* Test 3-11, Crash Test No. 609971-03-1.

Test Parameter	Specification	Tolerance	Measured
Impact Speed (mi/h)	62	±2.5	62.6
Impact Angle (deg)	25	±1.5	25.7 (30.9 to the flare)
Vehicle Inertial Weight (lb)	5,000	±110	5,047
Impact Severity (kip-ft)	106	≥106	124.3 (174.4 to the flare)
Impact Location	45.5 inches upstream of the centerline of post 12	±1 ft (12 inches)	44.8 inches upstream of the centerline of post 12

Table 6.2. Exit Parameters for *MASH* Test 3-11, Crash Test No. 609971-03-1.

Exit Parameter	Measured
Speed (mi/h)	N/A
Trajectory (deg)	N/A
Heading (deg)	N/A
Brakes applied post impact (s)	Brakes not applied
Vehicle at rest position	39 ft downstream of impact point 17 ft to the field side 15 degrees left
Comments:	Vehicle rolled onto the passenger side and then back onto the tires Vehicle did not cross exit box ^a Vehicle penetrated through the guardrail

^a Not less than 32.8 ft downstream from loss of contact for cars and pickups is optimal.



Figure 6.1. MGS Guardrail with Flare/Test Vehicle Geometrics for Test 609971-03-1.



Figure 6.2. MGS Guardrail with Flare/Test Vehicle Impact Location for Test 609971-03-1.

6.2. WEATHER CONDITIONS

Table 6.3 provides the weather conditions for Test 609971-03-1.

Table 6.3. Weather Conditions for Test 609971-03-1.

Date of Test	7-22-2019 AM
Wind Speed (mi/h)	2
Wind Direction (deg)	252
Temperature (°F)	87
Relative Humidity (%)	80
Vehicle Traveling (deg)	195

6.3. TEST VEHICLE

Figure 6.3 and Figure 6.4 show the 2013 RAM 1500 used for the crash test. Table 6.4 shows the vehicle measurements. Figure D.1 in Appendix D.1 gives additional dimensions and information on the vehicle.



Figure 6.3. Impact Side of Test Vehicle before Test 609971-03-1.



Figure 6.4. Opposite Impact Side of Test Vehicle before Test 609971-03-1.

Table 6.4. Vehicle Measurements for Test 609971-03-1.

Test Parameter	<i>MASH</i>	Allowed Tolerance	Measured
Dummy (if applicable) ^a (lb)	165	N/A	N/A
Gross Static ^a (lb)	5,000	±110	5,047
Wheelbase (inches)	148	±12	140.5
Front Overhang (inches)	39	±3	40
Overall Length (inches)	237	±13	227.5
Overall Width (inches)	78	±2	78.5
Hood Height (inches)	43	±4	46
Track Width ^b (inches)	67	±1.5	68.3
CG aft of Front Axle ^c (inches)	63	±4	59.6
CG above Ground ^{c,d} (inches)	28	≥28	28.3

^a If a dummy is used, the gross static vehicle mass should be increased by the mass of the dummy.

^b Average of front and rear axles.

^c For test inertial mass.

^d 2270P vehicle must meet minimum CG height requirement.

6.4. TEST DESCRIPTION

Table 6.5 lists events that occurred during Test 609971-03-1. Figures D.4 through D.6 in Appendix D.2 present sequential photographs during the test.

Table 6.5. Events during Test 609971-03-1.

Time (s)	Events
0.0000	Vehicle contacted barrier
0.0170	Post 12 began to lean toward field side
0.0220	Post 11 began to lean toward field side
0.0290	Post 13 began to lean toward field side
0.0340	Vehicle began to redirect
0.0550	Post 14 began to lean toward field side
0.0620	Post 11 began to twist clockwise
0.0860	Rail released from upstream posts
0.2450	Front left tire lifted off ground
0.3180	Rail released from downstream posts
0.3860	Vehicle was parallel with barrier

6.5. DAMAGE TO TEST INSTALLATION

The W-beam guardrail released from all posts. The sleeve at post 1 was deformed and pulled downstream 1.25 inches at ground level. Posts 1 and 2 fractured at the top of the sleeves. Post 11 was pushed back 1.5 inches at grade and rotated 45 degrees clockwise. Posts 12 to 14 were bent to the field side approximately 70 degrees and downstream 45 degrees, and the blockouts were detached. Posts 15 to 17 were leaning downstream from 17 degrees to 72 degrees. The downstream DAT post 30 failed at the top of the sleeve.

Table 6.6 describes the damage to the MGS guardrail with flare. Figure 6.5 and Figure 6.6 show the damage to the MGS guardrail with flare.

Table 6.6. Damage to MGS Guardrail with Flare for Test 609971-03-1.

Test Parameter	Measured
Permanent Deflection/Location	N/A (vehicle broke through guardrail)
Dynamic Deflection	N/A (vehicle broke through guardrail)
Working Width ^a and Height	N/A (vehicle broke through guardrail)

^a Per *MASH*, “The working width is the maximum dynamic lateral position of any major part of the system or vehicle. These measurements are all relative to the pre-impact traffic face of the test article.” In other words, working width is the total barrier width plus the maximum dynamic intrusion of any portion of the barrier or test vehicle past the field side edge of the barrier.



Figure 6.5. MGS Guardrail with Flare after Test at Impact Location for Test 609971-03-1.



Figure 6.6. MGS Guardrail with Flare after Test 609971-03-1.

6.6. DAMAGE TO TEST VEHICLE

Figure 6.7 and Figure 6.8 show the damage sustained by the vehicle. Figure 6.9 and Figure 6.10 show the interior of the test vehicle. Table 6.7 and Table 6.8 provide details on the occupant compartment deformation and exterior vehicle damage. Figures D.2 and D.3 in Appendix D.1 provide exterior crush and occupant compartment measurements.



Figure 6.7. Impact Side of Test Vehicle after Test 609971-03-1.



Figure 6.8. Rear Impact Side of Test Vehicle after Test 609971-03-1.



Figure 6.9. Overall Interior of Test Vehicle after Test 609971-03-1.



Figure 6.10. Interior of Test Vehicle on Impact Side after Test 609971-03-1.

Table 6.7. Occupant Compartment Deformation for Test 609971-03-1.

Test Parameter	Specification	Measured
Roof	≤4.0 inches	0 inches
Windshield	≤3.0 inches	0 inches
A and B Pillars	≤5.0 overall/≤3.0 inches lateral	0 inches
Foot Well/Toe Pan	≤9.0 inches	0 inches
Floor Pan/Transmission Tunnel	≤12.0 inches	0 inches
Side Front Panel	≤12.0 inches	0 inches
Front Door (above Seat)	≤9.0 inches	0 inches
Front Door (below Seat)	≤12.0 inches	0 inches

Table 6.8. Exterior Vehicle Damage for Test 609971-03-1.

Side Windows	No damage
Maximum Exterior Deformation	11 inches in the horizontal plane at the right front corner at bumper height
VDS	1RFQ4
CDC	01FRES3
Fuel Tank Damage	None
Description of Damage to Vehicle:	The front bumper, hood, grill, right front fender, right front tire and rim, right upper and lower A arms and ball joints, right front door, right A post, right C post, right rear cab corner, right rear exterior bed, and rear bumper were damaged.

6.7. OCCUPANT RISK FACTORS

Data from the accelerometers were digitized for evaluation of occupant risk, and the results are shown in Table 6.9. Figure D.7 in Appendix D.3 shows the vehicle angular displacements, and Figures D.8 through D.10 in Appendix D.4 show acceleration versus time traces.

Table 6.9. Occupant Risk Factors for Test 609971-03-1.

Test Parameter	<i>MASH</i>	Measured	Time
OIV, Longitudinal (ft/s)	≤ 40.0 <i>30.0^a</i>	18.5	0.1458 s on left side of interior
OIV, Lateral (ft/s)	≤ 40.0 <i>30.0</i>	13.8	0.1458 s on left side of interior
Ridedown, Longitudinal (g)	≤ 20.49 <i>15.0</i>	11.7	0.2761–0.2861 s
Ridedown, Lateral (g)	≤ 20.49 <i>15.0</i>	5.4	0.1544–0.1644 s
THIV (m/s)	N/A	6.6	0.1385 s on left right of interior
ASI	N/A	0.8	0.0772–0.1272 s
50-ms MA Longitudinal (g)	N/A	-7.9	0.2758–0.3258 s
50-ms MA Lateral (g)	N/A	-5.4	0.0482–0.0982 s
50-ms MA Vertical (g)	N/A	2.3	1.6721–1.7221 s
Roll (deg)	≤ 75	103	2.0000 s
Pitch (deg)	≤ 75	12	1.4035 s
Yaw (deg)	N/A	145	2.0000 s

^a Values in italics are the preferred *MASH* values.





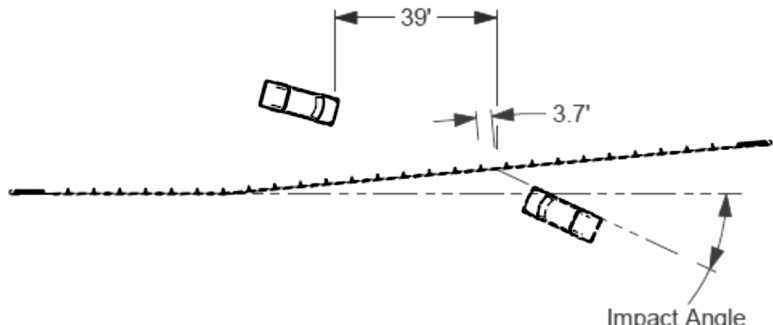
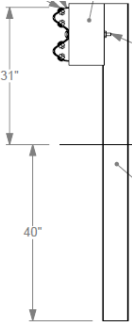
	Test Agency		Texas A&M Transportation Institute (TTI)					
	Test Standard/Test No.		MASH 2016, Test 3-11					
	TTI Project No.		609971-03-1					
	Test Date		7-22-2019					
	TEST ARTICLE		Type	Longitudinal Guardrail				
			Name	MGS Guardrail with Flare				
			Length	181 ft 3 inches				
			Key Materials	Steel, wood, crushed concrete				
	Soil Type and Condition		AASHTO M147-17 Type A Grade 2 Crushed Limestone					
	TEST VEHICLE		Type/Designation	2270P				
			Year, Make and Model	2013 RAM 1500				
			Inertial Weight (lb)	5,047				
			Dummy (lb)	N/A				
			Gross Static (lb)	5,047				
	IMPACT CONDITIONS		Impact Speed (mi/h)	62.6				
			Impact Angle (deg)	25.7 (30.9 to the flare)				
		Impact Location	44.8 inches upstream of the centerline of post 12					
		Impact Severity (kip-ft)	124.3 (174.4 to the flare)					
EXIT CONDITIONS		Exit Speed (mi/h)	N/A					
		Trajectory/Heading Angle (deg)	N/A					
		Exit Box Criteria	Did not cross					
		Stopping Distance	39 ft downstream 17 ft to the field side					
TEST ARTICLE DEFLECTIONS		Dynamic (inches)	N/A					
		Permanent (inches)	N/A					
		Working Width/Height (inches)	N/A					
VEHICLE DAMAGE		VDS	1RFQ4					
		CDC	01FRES2					
		Max. Ext. Deformation	11 inches at the front bumper					
		Max Occupant Compartment Deformation	0 inches					
OCCUPANT RISK VALUES								
Long. OIV (ft/s)	18.5	Long. Ridedown (g)	11.7	Max 50-ms Long. (g)	-7.9	Max Roll (deg)	103	
Lat. OIV (ft/s)	13.8	Lat. Ridedown (g)	5.4	Max 50-ms Lat. (g)	-5.4	Max Pitch (deg)	12	
THIV (m/s)	6.6	ASI	0.8	Max 50-ms Vert. (g)	2.3	Max Yaw (deg)	145	
								

Figure 6.11. Summary of Results for MASH Test 3-11 on MGS Guardrail with Flare.

Chapter 7. *MASH* TEST 3-11 (CRASH TEST NO. 609971-03-2)

7.1. TEST DESIGNATION AND ACTUAL IMPACT CONDITIONS

See Table 7.1 for details on *MASH* impact conditions and Table 7.2 for the exit parameters for Test 609971-03-2. Figure 7.1 and Figure 7.2 depict the target impact setup.

Table 7.1. Impact Conditions for *MASH* Test 3-11, Crash Test No. 609971-03-2.

Test Parameter	Specification	Tolerance	Measured
Impact Speed (mi/h)	62	±2.5	60.3
Impact Angle (deg)	25	±1.5	24.5 (29.7 to the flare)
Vehicle Inertial Weight (lb)	5,000	±110	5,019
Impact Severity (kip-ft)	106	≥106	104.9 (149.8 to the flare)
Impact Location	45.5 inches upstream of the centerline of post 14	±1 ft (12 inches)	41.5 inches upstream of the centerline of post 14

Table 7.2. Exit Parameters for *MASH* Test 3-11, Crash Test No. 609971-03-2.

Exit Parameter	Measured
Speed (mi/h)	N/A
Trajectory (deg)	N/A
Heading (deg)	N/A
Brakes applied post impact (s)	4.1 s
Vehicle at rest position	86 ft downstream of impact point 15 ft to the field side 45 degrees right
Comments:	Vehicle remained upright Vehicle penetrated through the guardrail



Figure 7.1. MGS Guardrail with Flare/Test Vehicle Geometrics for Test 609971-03-2.



Figure 7.2. MGS Guardrail with Flare/Test Vehicle Impact Location for Test 609971-03-2.

7.2. WEATHER CONDITIONS

Table 7.3 provides the weather conditions for Test 609971-03-2.

Table 7.3. Weather Conditions for Test 609971-03-2.

Date of Test	03-18-2020 PM
Wind Speed (mi/h)	10
Wind Direction (deg)	142
Temperature (°F)	80
Relative Humidity (%)	78
Vehicle Traveling (deg)	195

7.3. TEST VEHICLE

Figure 7.3 and Figure 7.4 show the 2014 RAM 1500 used for the crash test. Table 7.4 shows the vehicle measurements. Figure E.1 in Appendix E.1 gives additional dimensions and information on the vehicle.



Figure 7.3. Impact Side of Test Vehicle before Test 609971-03-2.



Figure 7.4. Opposite Impact Side of Test Vehicle before Test 609971-03-2.

Table 7.4. Vehicle Measurements for Test 609971-03-2.

Test Parameter	<i>MASH</i>	Allowed Tolerance	Measured
Dummy (if applicable) ^a (lb)	165	N/A	N/A
Gross Static ^a (lb)	5,000	±110	5,019
Wheelbase (inches)	148	±12	140.5
Front Overhang (inches)	39	±3	40
Overall Length (inches)	237	±13	227.5
Overall Width (inches)	78	±2	78.5
Hood Height (inches)	43	±4	46
Track Width ^b (inches)	67	±1.5	68.3
CG aft of Front Axle ^c (inches)	63	±4	59.5
CG above Ground ^{c,d} (inches)	28	≥28	29

^a If a dummy is used, the gross static vehicle mass should be increased by the mass of the dummy.

^b Average of front and rear axles.

^c For test inertial mass.

^d 2270P vehicle must meet minimum CG height requirement.

7.4. TEST DESCRIPTION

Table 7.5 lists events that occurred during Test 609971-03-2. Figures E.4 and E.5 in Appendix E.2 present sequential photographs during the test.

Table 7.5. Events during Test 609971-03-2.

Time (s)	Events
0.0000	Vehicle contacted barrier
0.0030	Post 13 and 14 began to lean toward field side
0.0310	Post 15 began to lean toward field side
0.0320	Vehicle began to redirect
0.0350	Post 12 began to rotate clockwise
0.2440	Rail next to front right quarter panel of truck began to rupture
0.2630	Rail next to front right quarter panel of truck completely ruptured
0.2680	Vehicle was parallel with barrier

7.5. DAMAGE TO TEST INSTALLATION

The right anchor post pulled downstream 1 inch, and the soil was disturbed at post 1. The rail element released at post 8 until the end of the installation. Post 13 was pushed back 1½ inches at grade. Posts 14–18 were leaning downstream at approximately 60 degrees from vertical, with the blockouts missing. Posts 19–23 were also leaning downstream at approximately 60 degrees from vertical, but the blockouts remained intact. Posts 18–21 showed impact damage on the field-side flange, and post 19 had a tear on the field-side flange as well. The rail and head released from and pushed the anchor posts downstream 7 ft. Post 31 was leaning 10 degrees downstream from vertical. The rail ruptured 20 inches upstream of the joint between posts 16 and 17.

Table 7.6 describes the damage to the MGS guardrail with flare. Figure 7.5 and Figure 7.6 show the damage to the MGS guardrail with flare.

Table 7.6. Damage to MGS Guardrail with Flare for Test 609971-03-2.

Test Parameter	Measured
Permanent Deflection/Location	N/A (vehicle broke through guardrail)
Dynamic Deflection	N/A (vehicle broke through guardrail)
Working Width ^a and Height	N/A (vehicle broke through guardrail)

^a Per *MASH*, “The working width is the maximum dynamic lateral position of any major part of the system or vehicle. These measurements are all relative to the pre-impact traffic face of the test article.” In other words, working width is the total barrier width plus the maximum dynamic intrusion of any portion of the barrier or test vehicle past the field side edge of the barrier.



Figure 7.5. MGS Guardrail with Flare after Test at Impact Location for Test 609971-03-2.



Figure 7.6. MGS Guardrail with Flare after Test 609971-03-2.

7.6. DAMAGE TO TEST VEHICLE

Figure 7.7 and Figure 7.8 show the damage sustained by the vehicle. Figure 7.9 and Figure 7.10 show the interior of the test vehicle. Table 7.7 and Table 7.8 provide details on the occupant compartment deformation and exterior vehicle damage. Figures E.2 and E.3 in Appendix E.1 provide exterior crush and occupant compartment measurements.



Figure 7.7. Impact Side of Test Vehicle after Test 609971-03-2.



Figure 7.8. Rear Impact Side of Test Vehicle after Test 609971-03-2.



Figure 7.9. Overall Interior of Test Vehicle after Test 609971-03-2.



Figure 7.10. Interior of Test Vehicle on Impact Side after Test 609971-03-2.

Table 7.7. Occupant Compartment Deformation for Test 609971-03-2.

Test Parameter	Specification	Measured
Roof	≤4.0 inches	0 inches
Windshield	≤3.0 inches	0 inches
A and B Pillars	≤5.0 overall/≤3.0 inches lateral	0 inches
Foot Well/Toe Pan	≤9.0 inches	0 inches
Floor Pan/Transmission Tunnel	≤12.0 inches	0 inches
Side Front Panel	≤12.0 inches	0 inches
Front Door (above Seat)	≤9.0 inches	0 inches
Front Door (below Seat)	≤12.0 inches	0 inches

Table 7.8. Exterior Vehicle Damage for Test 609971-03-2.

Side Windows	No damage
Maximum Exterior Deformation	10 inches in the horizontal plane at the right front corner at bumper height
VDS	1RFQ4
CDC	01FRES3
Fuel Tank Damage	None
Description of Damage to Vehicle:	The front bumper, hood, grill, radiator and support, right front fender, right front tire and rim, and right front and rear doors were damaged.

7.7. OCCUPANT RISK FACTORS

Data from the accelerometers were digitized for evaluation of occupant risk, and the results are shown in Table 7.9. Figure E.6 in Appendix E.3 shows the vehicle angular displacements, and Figures E.7 through E.9 in Appendix E.4 show acceleration versus time traces.

Table 7.9. Occupant Risk Factors for Test 609971-03-2.

Test Parameter	<i>MASH</i>	Measured	Time
OIV, Longitudinal (ft/s)	≤ 40.0 <i>30.0^a</i>	18.7	0.1555 s on right side of interior
OIV, Lateral (ft/s)	≤ 40.0 <i>30.0</i>	13.9	0.1555 s on right side of interior
Ridedown, Longitudinal (g)	≤ 20.49 <i>15.0</i>	4.8	0.1901–0.2001 s
Ridedown, Lateral (g)	≤ 20.49 <i>15.0</i>	5.0	0.2219–0.2319 s
THIV (m/s)	N/A	6.7	0.1474 s on right side of interior
ASI	N/A	0.6	0.0805–0.1305 s
50-ms MA Longitudinal (g)	N/A	-5.3	0.0640–0.1140 s
50-ms MA Lateral (g)	N/A	-4.1	0.1823–0.2323 s
50-ms MA Vertical (g)	N/A	-1.9	0.4240–0.4740 s
Roll (deg)	≤ 75	9	1.2582 s
Pitch (deg)	≤ 75	6	1.9605 s
Yaw (deg)	N/A	194	2.0000 s

^a Values in italics are the preferred *MASH* values.

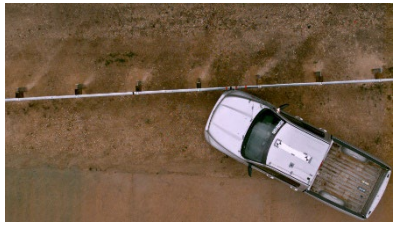
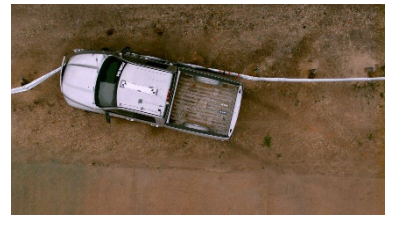


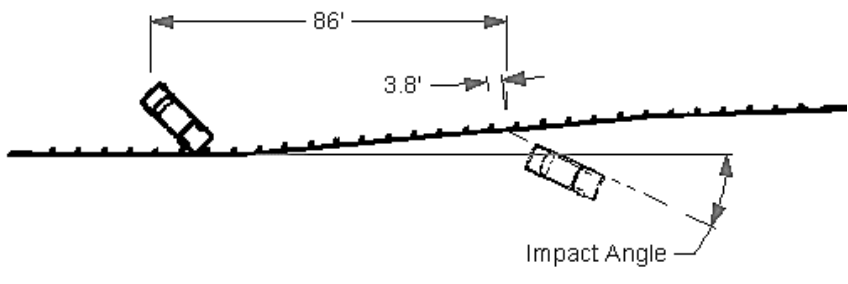
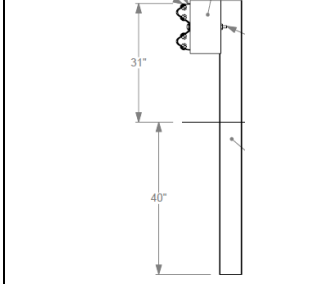
	Test Agency		Texas A&M Transportation Institute (TTI)					
	Test Standard/Test No.		MASH 2016, Test 3-11					
	TTI Project No.		609971-03-2					
	Test Date		03-18-2020					
TEST ARTICLE								
Type		Longitudinal Guardrail						
Name		MGS Guardrail with Flare						
Length		201 ft 7 inches						
Key Materials		Steel, wood, crushed concrete						
	Soil Type and Condition		AASHTO M147-17 Type A Grade 2 Crushed Limestone					
	TEST VEHICLE							
	Type/Designation		2270P					
	Year, Make and Model		2014 RAM 1500					
Inertial Weight (lb)		5019						
Gross Weight (lb)		5019						
	Impact Speed (mi/h)		60.3					
	Impact Angle (deg)		24.5 (29.7 to the flare)					
	Impact Location		41.5 inches upstream of the centerline of post 14					
	Impact Severity (kip-ft)		104.9 (149.8 to the flare)					
EXIT CONDITIONS								
Exit Speed (mi/h)		N/A						
Trajectory/Heading Angle (deg)		N/A						
Exit Box Criteria		Did not cross						
Stopping Distance		86 ft downstream 15 ft to the field side						
	Dynamic (inches)		N/A					
	Permanent (inches)		N/A					
	Working Width/Height (inches)		N/A					
	VEHICLE DAMAGE							
VDS		1RFQ4						
CDC		01FRES3						
Max. Ext. Deformation		10 inches at the front bumper						
Max Occupant Compartment Deformation		0 inches						
OCCUPANT RISK VALUES								
Long. OIV (ft/s)	18.7	Long. Ridedown (g)	4.8	Max 50-ms Long. (g)	-5.3	Max Roll (deg)	9	
Lat. OIV (ft/s)	13.9	Lat. Ridedown (g)	5.0	Max 50-ms Lat. (g)	-4.1	Max Pitch (deg)	6	
THIV (m/s)	6.7	ASI	0.6	Max 50-ms Vert. (g)	-1.9	Max Yaw (deg)	194	
								

Figure 7.11. Summary of Results for MASH Test 3-11 on MGS Guardrail with Flare.

Chapter 8. FINITE ELEMENT ANALYSIS

After the completion of the testing program, and considering the testing results, the research team decided to utilize finite element (FE) computer modeling and simulations to investigate the predictability of the MGS's crashworthiness when implemented at different flare rates and impacted at TL-3 impact conditions.

Researchers investigated two general situations in parallel: (a) the MGS implemented at shallower flare rates than those already failed under the testing program, and (b) the MGS modified/retrofitted and implemented at different flare rates. For both general cases, a predictive analysis was conducted for impacts at *MASH* TL-3 conditions.

In the full-scale testing, MGS rail rupture under the higher impact severity and vehicle interaction during impact was the leading cause for system crashworthiness failure. The biggest challenge when evaluating the FE computer simulation impact results was to develop an alternate method for predicting MGS W-beam rail rupture. While utilization of element erosion was an option, this method was not prioritized due to lack of robustness under multiple predictive modeling and impact condition changes. Conclusions were ultimately made with consideration of the recorded vehicle interaction with the system, lateral deflection of the system during impact, predicted rail stresses/strains, and recorded occupant risk values and vehicle stability. Specifically, the lateral deflection of the system was considered an indication of potential pocketing of the vehicle, which in turn could cause excessive loading on the W-beam railing and ultimate failure.

8.1. FINITE ELEMENT MODELING AND ANALYSIS

This section presents the finite element analysis results. FE models for a vehicle and system were developed and/or modified for a detailed crashworthiness analysis using LS-DYNA to the considered TL-3 impact conditions.

8.1.1. Finite Element Model Validation

To validate the FE model, an FE dynamic impact simulation was conducted and compared to a full-scale crash test (Test No. 609971-03-2). Based on the details of the tests as described in Chapter 7, the FE model was developed and set up with the same conditions as the test. As described previously, the W-beam ruptured during the crash test, but the FE model did not include failure of the W-beam to maintain numerical stability. Therefore, in order to properly compare and validate the FE model, the simulation results were compared with the test only before the rail rupture.

An FE model of a 2018 RAM pickup truck was used to represent a *MASH* 2270P vehicle. Figure 8.1 shows the FE RAM model developed by the Center for Collision Safety and Analysis (CCSA) at George Mason University (4). The model was designed to have suspension failure and tire deflation to represent actual damage on the vehicle.

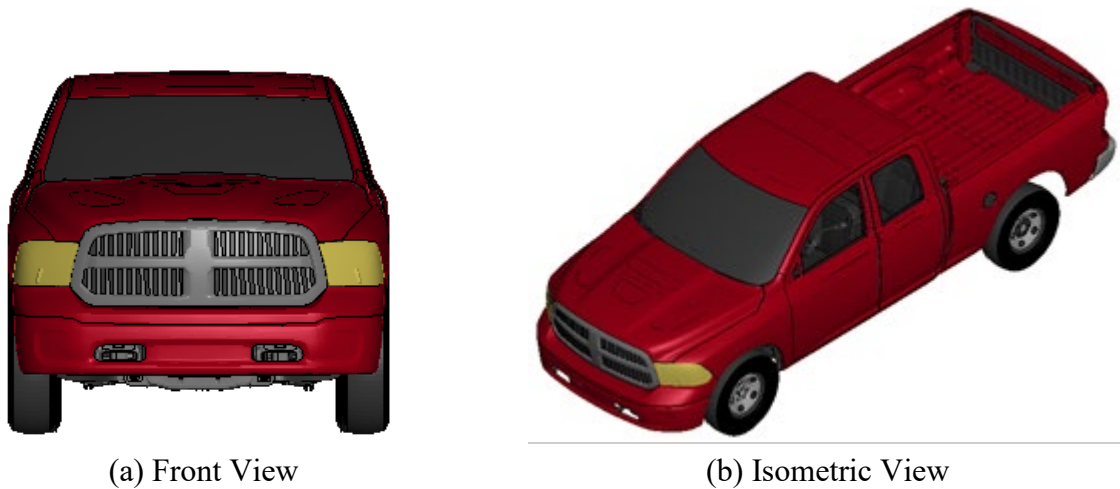


Figure 8.1. RAM Model Used for FE Simulation.

The actual test parameters were used for the FE analysis. The actual impact speed and angle were 60.3 mi/h and 24.5 degrees (to the roadway), resulting in a 29.7-degree orientation angle to the MGS flare, and these values were used to set up the impact simulation. Figure 8.2 shows the impact simulation setup with the 11:1 flared MGS.

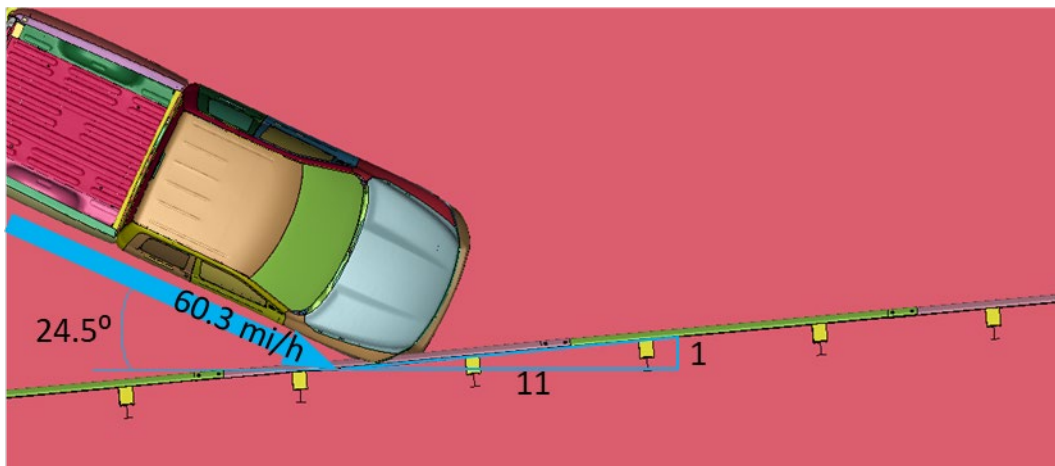
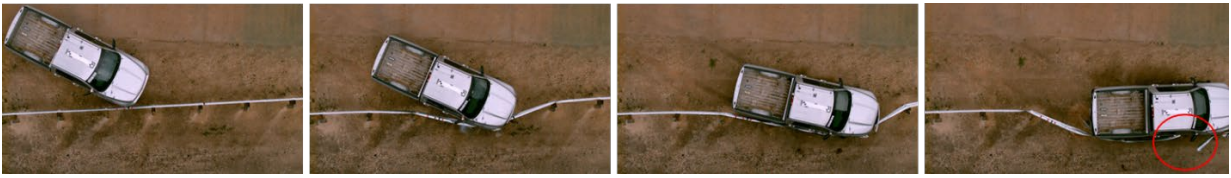
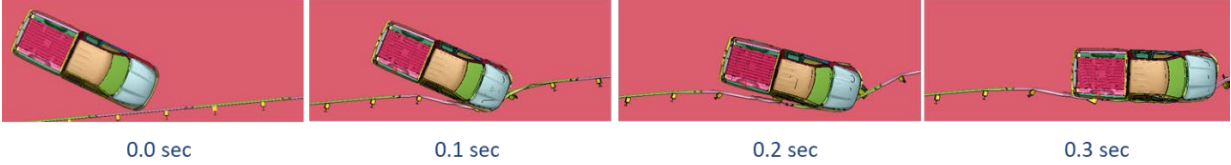


Figure 8.2. Simulation Setup under TL-3 Conditions.

Figure 8.3 shows the sequential photos taken from the full-scale test and simulation to compare vehicular behavior. In the test, the W-beam rail ruptured at 0.2440 s after the vehicle impacted the flared MGS. Figure 8.4 shows the detailed view right before and after the rail rupture. Table 8.1 compares the vehicular behavior by showing the main event and the time of event. Compared to the full-scale test, the FE model shows good agreement before the rail ruptured.



(a) Test



(b) Simulation

Figure 8.3. Sequential Overhead Frames of Pickup Truck under TL-3 Conditions.



(a) Overhead View



(b) Rear View

Figure 8.4. Sequential Frames to Compare FE Simulation (Top) to Crash Testing (Bottom) Immediately Leading to Rail Rupture Event.

Since the FE model was developed without W-beam rail failure, potential rail rupture was investigated based on the rail strain. Figure 8.5 shows the ruptured rail after the test and the rail strain after the impact simulation. Strain larger than 25 percent is shown in red, so the red regions indicate potential rupture locations. In the impact simulation, the maximum strain was

observed at the location similar to where the rail ruptured in the test. This result indicates that although the FE model was not developed with a rail failure mode, the simulation result is promising and may be assumed to be reliable to use for further investigation.

Table 8.1. Descriptive Comparison for Timestep.

Event	Time of Event (s)	
	Test	Simulation
Impacted the rail	0.0000	0.0000
First post deflection started	0.0030	0.0200
Vehicle redirected	0.0320	0.0550
Rail started to separate	0.2440	N/A
Rail separated completely	0.2630	N/A
Vehicle traveled parallel with barrier	0.2680	0.3050

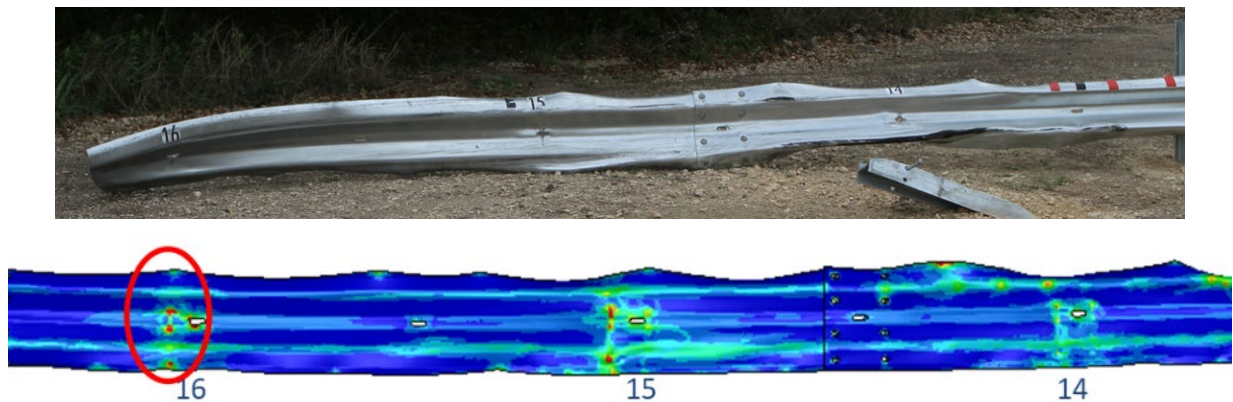


Figure 8.5. Rail Rupture Experienced in Full-Scale Testing (Top) and Rail Strains Recorded in FE Simulation (Bottom).

Table 8.2 lists the occupant risk factors for both the test and the simulation. The table shows that the maximum occupant impact velocity was observed before rail rupture, while the maximum ridedown acceleration was observed right after the rail started rupturing in the test and the rail deflected most for both the test and the simulation.

Table 8.2. Comparison of the Occupant Risk Factors (Test 609971-03-2 vs. FE Simulation).

		Test 609971-03-2	Simulation
Occupant Impact Velocity (ft/s)	X	18.7 (0.1555 s)	7.4 (0.1630 s)
	Y	13.9 (0.1555 s)	4.7 (0.1630 s)
Ridedown Acceleration (g)	X	4.8 (0.19–0.2 s)	8.5 (0.18–0.19 s)
	Y	5.0 (0.22–0.23 s)	9.0 (0.27–0.28 s)
Max. Angle (degrees)	Roll	8.9	4.76
	Pitch	5.6	1.06
	Yaw	194.4	18.13
Maximum Dynamic Lateral Rail Deflection (in.)		52.9 (before rupture)	52.4

To investigate the behavior after 0.2440 s, the simulation result was also compared to NCHRP 350 Test No. 2214MG-2 (5) conducted on the MGS (not flared) (see Figure 8.6). Overall vehicle and system behavior followed the trend shown in the test. The maximum dynamic deflection was 1,114 mm (43.9 inches) and 1,330 mm (52.4 inches), respectively, in the test and the impact simulation. The maximum permanent deflection was 803 mm (31.6 inches) and 955 mm (37.6 inches) in the test and the simulation, respectively. These results were interpreted to indicate that the maximum dynamic rail deflection parameter to consider appropriate for vehicle containment and redirection during the impact event were 52 inches and close to 44 inches.

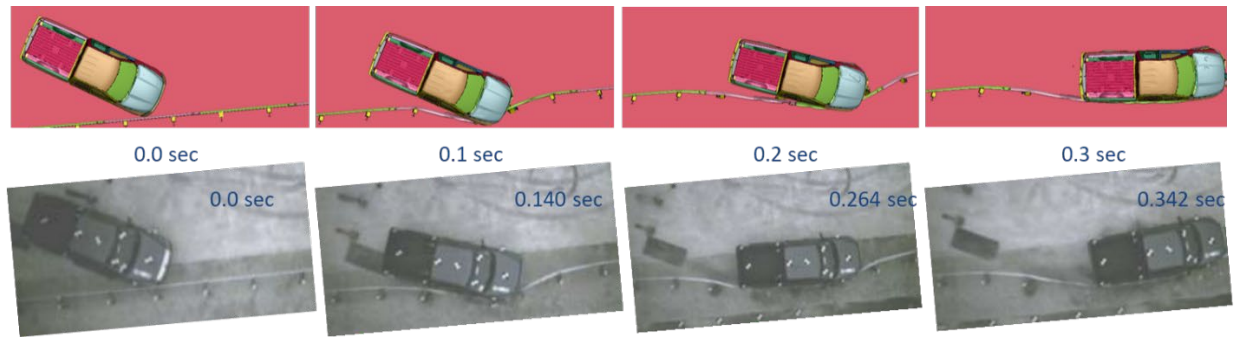


Figure 8.6. Sequential Frames Comparing FE Simulation on Flared MGS (Top) to NCHRP 350 Test No. 2214MG-2 (Bottom) (5).

Based on the comparison, the FE model was considered and calibrated to a level that can provide reliability for further flare rate investigation.

8.1.2. Design Options

This section provides the results recorded from FE simulations predicting impacts against the MGS at various flare rates (shallower than 11:1, as implemented in the crash testing), as well as against proposed retrofit MGS designs.

8.2.1.1. Different Flare Rate Conditions

The following MGS flares shallower than the 11:1 rate were investigated without retrofitting the existing MGS: 15:1, 18:1, and 21:1. Figure 8.7 shows the impact condition setup for a pickup truck (2270P) model at each considered flare rate. The impact angle and speed were set as 25 degrees and 62 mi/h, respectively. With different flare rates, the effective angles were different.

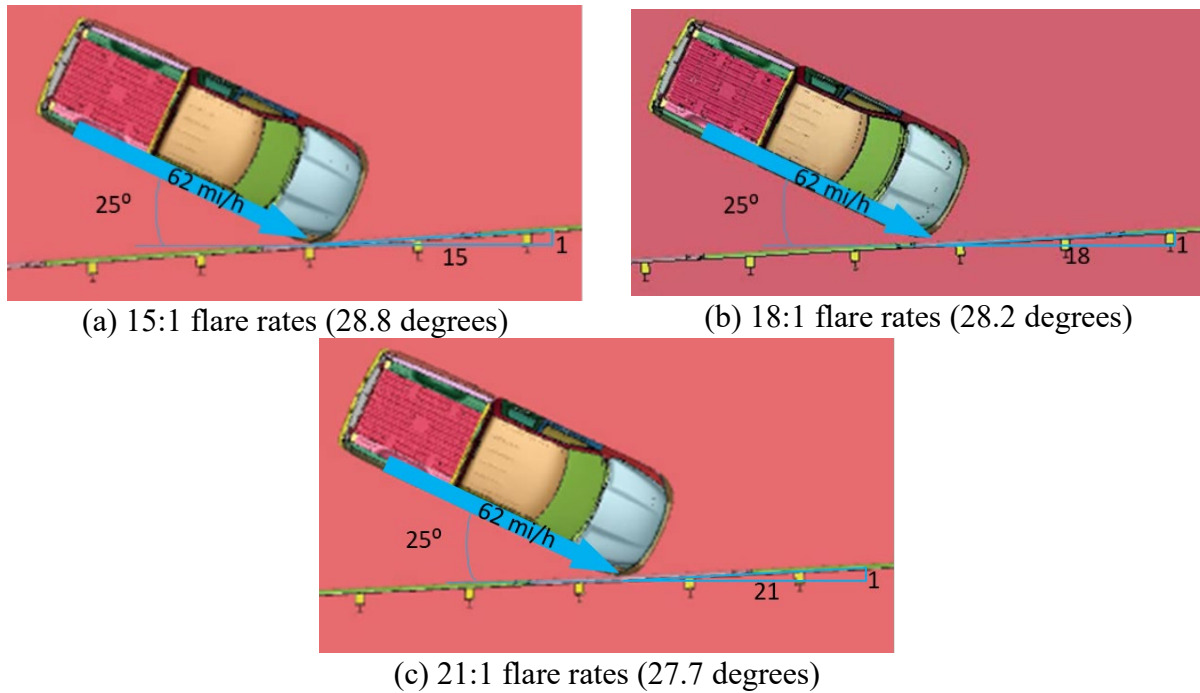








Figure 8.7. Impact Conditions for Different MGS Flare Rates (Effective Angles).

Table 8.3 lists the occupant risk factors and the maximum lateral rail deflection results from the simulated cases compared to the full-scale test results from the 11:1 flare rate case. Specifically, the simulation impact against the MGS at a 15:1 flare rate shows a similar lateral deflection behavior as the one recorded in the 11:1 full-scale test, when the rail rupture occurred (52.8 inches for the 15:1 FE case vs. 52.9 inches in the 11:1 test case). When considering shallower MGS flare rates, the maximum lateral rail deflections observed from FE simulations were reduced to 49.2 inches and 48.4 inches for the 18:1 and 21:1 flare rates, respectively.

Table 8.3. Simulation Results from FE Models of MGS with Different Flare Rates.

Flare Rate (Effective Angle)		11:1 (30.2°)		15:1 (28.8°)	18:1 (28.4°)	21:1 (27.7°)		
Vehicle Model								
		Test	Pickup Truck	Pickup Truck	Pickup Truck	Pickup Truck	Small Car	
Occupant Risk Factors	Occupant Impact Velocity (ft/s)	X	18.7	23.4	23.6	24.0	20.7	42.0
		Y	13.9	15.4	14.8	13.1	14.8	14.4
	Ridedown Acceleration (g)	X	4.8	8.5	13.8	14.3	10.7	21.1
		Y	5.0	9.0	13.8	7.0	9.1	18.0
	Max. Angle (degrees)	Roll	8.9	4.76	8.8	3.1	10.2	19.5
		Pitch	5.6	1.06	9.2	5.9	3.1	5.9
		Yaw	194.4	18.13	56.2	54.1	57.9	85.7
Maximum Dynamic Lateral Rail Deflection (in.)		52.9 (before rail rupture)	52.4	52.8	49.3	48.4	34.6	

The system with a 21:1 flare rate was also investigated with the small passenger car (1100C) FE model. The maximum ridedown acceleration recorded from the simulated case of the small passenger car impacting the MGS at a 21:1 flare rate exceeded the *MASH* limit of 20.49 g. While there have been indications that the available small passenger car FE model might overpredict occupant risk during an impact in other conducted research studies, it is concerning to have such a high value. It is also important to note that suspension failure was not applied for the investigation through this simulation. Application of suspension failure is recommended for further investigation, although a validated suspension failure model is not yet available and such investigation was beyond the scope of this research.

Based on overall simulation results, the MGS behavior did not seem to show much difference in terms of dynamic lateral deflection and vehicle interaction when impacted at different flare rates (between the 11:1 and 21:1 flare rates). It is especially concerning that the lateral deflection was not further contained significantly when shallower flares were considered, at least based on the FE results. This finding could indicate the potential for vehicle pocketing and eventually rail rupture, as happened in the failed crash test.

While validating these results through full-scale testing is suggested to allow researchers to have more data points to work with, particularly given the very limited flared MGS testing conducted under *MASH* conditions, the researchers decided to investigate MGS retrofit options to pair with the flare condition implementation.

8.2.1.2. *Retrofitting Options*

Figure 8.5 in the previous section illustrated a photo of the W-beam rail rupture experienced during the full-scale testing of the 11:1 flared MGS. In the same figure, a frame from the FE simulation shows the W-beam rail strains recorded during the simulated impact event with the same impact conditions. The FE simulation indicated the presence of localized higher strains, which seemed to be located at the bottom edge of the rail. This result could be an indication of increased stress/strain due to blockout contact, although it is not clear whether that could have created the rail rupture during the full-scale test.

Therefore, the first considered retrofit flared MGS option was to include “short” blockouts to prevent rail high concentration stresses and potential tearing due to direct contact/interaction between the blockout and the rail. Use of short blockouts that were 10 inches high and 8 inches deep was successful in previous MGS design/testing, such as in the MGS with half-post spacing (6). Therefore, it was decided to utilize the short blockout and pair it with half-post spacing (37½-inch post spacing) to investigate the crashworthiness of the flared MGS. This combination of system design changes was chosen to limit the lateral deflection of the system during impact and limit rail stress concentrations due to blockout interaction, with the ultimate goal of reducing the probability of vehicle pocketing and rail rupture during the event.

Figure 8.8 presents the details of the short blockout system. The figure shows the post spacing, blockout geometry, and rail connections used for Test No. 610211-6 (6), and the same geometrical characteristics were adopted for the MGS flared system.

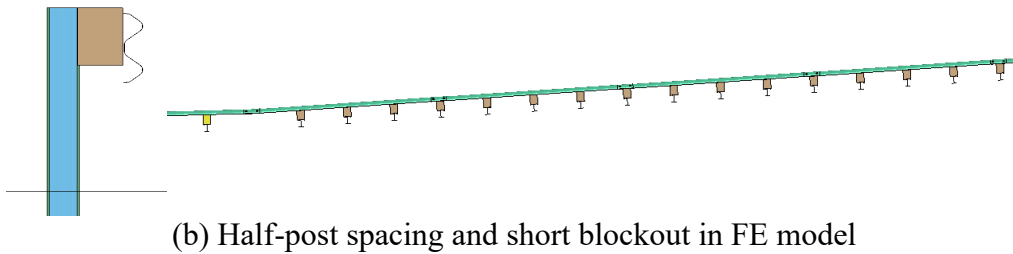
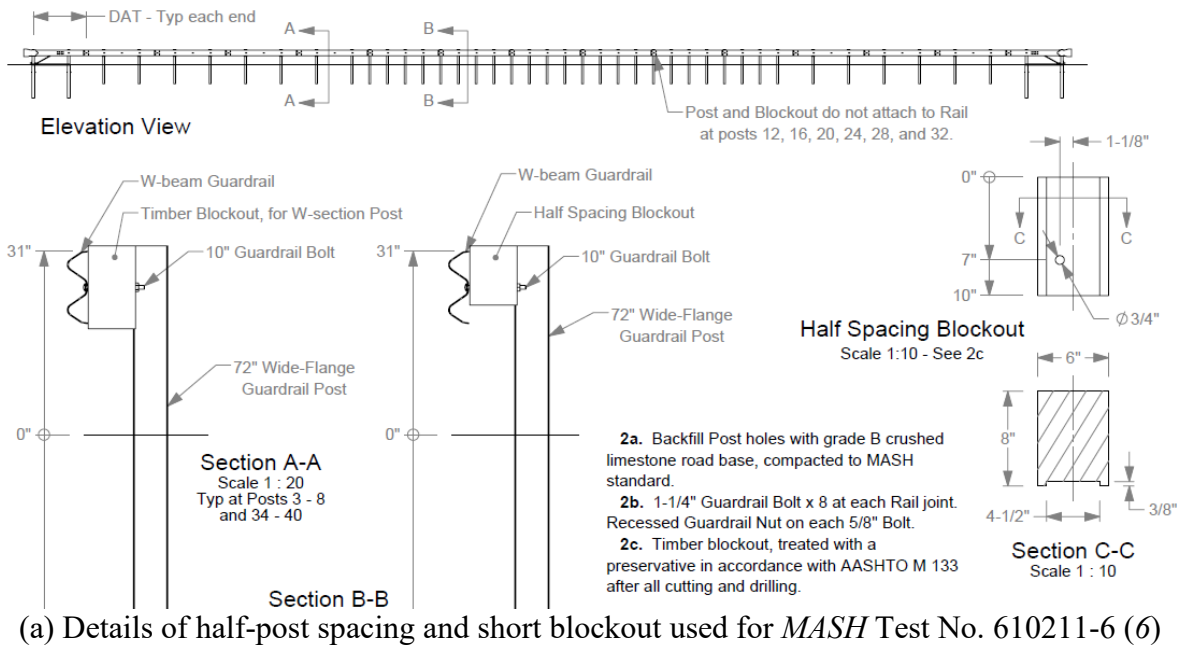


Figure 8.8. Details of Half-Post Spacing and Short Blockout.

Simulations were conducted to predict the retrofit flared MGS behavior under impacts at *MASH* TL-3 conditions. Table 8.4 summarizes the results from the simulations, reporting occupant risk factors and maximum rail deflection for each simulated case. For the half-post spacing system, a flare rate of 11:1 was adopted. As expected, the rail lateral deflection was significantly reduced when compared to the one recorded with the system with regular post spacing. Also as expected, however, occupant risks, maximum occupant impact velocity, and ridedown acceleration were higher than those recorded with the regular post spacing due to the increased system stiffness from the added posts.

The same system design was also investigated with a 15:1 flare rate, showing anticipated improvement in terms of both rail deflection and occupant risks given the shallower flare rate. In the 15:1 flare rate retrofit system with the small passenger car, however, the recorded ridedown acceleration result was higher than the allowable *MASH* limit. Therefore, additional investigation was conducted with a flare rate of 18:1 for the same system. Under passenger car impact, while the occupant risk improved, the ridedown acceleration peaked to 20.3 g, which was still too close to the *MASH* allowed limit of 20.49 g.

Table 8.4. Simulation Results for Flared Half-Post Spacing MGS with Short Blockout.

Flare Rate			11:1 (30.2°)	15:1 (28.8°)		18:1 (28.4°)
Vehicle Model			Pickup Truck	Pickup Truck	Small Car	Small Car
Occupant Risk Factors	Occupant Impact Velocity (ft/s)	X	29.9	22.3	47.2	39.4
		Y	17.7	16.4	18.0	14.1
	Ridedown Acceleration (g)	X	17.1	11.0	23.8	20.3
		Y	12.4	10.3	11.3	16.1
	Max. Angle (degrees)	Roll	15.8	6.8	14.0	10.9
		Pitch	7.4	2.3	6.2	6.1
		Yaw	58.0	40.7	33.6	41.3
Maximum Rail Deflection (in.)			33.5	33.1	23.8	24.2

As a next step to reduce the ridedown acceleration, a rubrail was added to a short blockout (10-inch height) MGS with regular post spacing of 75 inches. A typical C6×8 steel channel was used as a rubrail and installed to have a 12-inch distance from the top of the channel to the ground. Figure 8.9 illustrates the elevation view of the short blockout MGS with a channel rubrail.

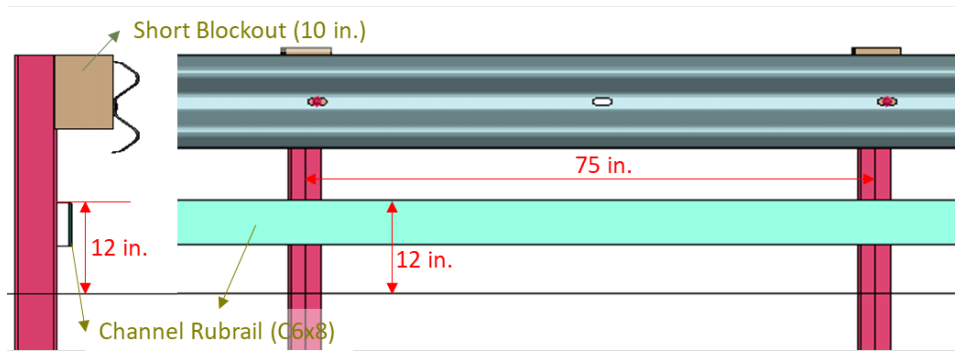


Figure 8.9. Short Blockout Flared MGS Retrofitted with Channel Rubrail.

Based on the previous simulations, the flared MGS at 15:1 and 18:1 flares improved vehicular behavior and structural behavior, as well as reduced the maximum rail deflection compared to the 11:1 flared MGS. Therefore, the flare rates of 15:1 and 18:1 were adopted for the retrofitted MGS. Once the simulation results indicated that a flared MGS retrofitted with a rubrail was able to stably redirect the pickup truck model, small car simulations were performed.

Table 8.5 lists the occupant risk factors and the maximum dynamic W-beam rail deflection. Overall, the flared MGS retrofitted with a channel rubrail was able to improve the structural behavior. The maximum rail deflection was reduced, and occupant risk factors met *MASH* evaluation criteria. However, a clear trend was not found when comparing the systems with 15:1 and 18:1 flares. Therefore, performing parametric simulations to find the most critical flare rates and impact point was needed.

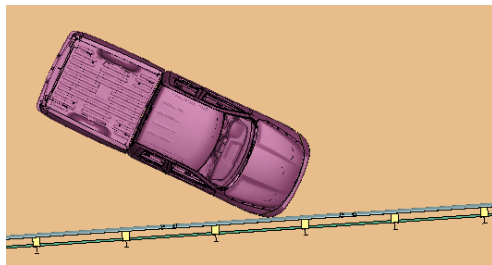
Table 8.5. Simulation Results for Short Blockout Flared MGS with Channel Rubrail.

Flare Rate			15:1 (28.8°)		18:1 (28.4°)		
Vehicle Model			Pickup Truck	Small Car	Pickup Truck	Small Car	
Occupant Risk Factors	Occupant Impact Velocity (ft/s)	X	18.4	38.7	20.3	36.7	
		Y	16.1	22.3	16.1	23.0	
	Ridedown Acceleration (g)	X	10.4	13.1	12.8	12.2	
		Y	11.2	9.8	9.7	11.7	
	Max. Angle (degrees)	Roll	15.8	9.5	4.4	6.2	
		Pitch	11.5	8.5	8.4	4.9	
		Yaw	37.7	48.2	34.7	50.9	
	Maximum Dynamic Lateral Rail Deflection (in.)			45.3	24.6	48.0	25.5

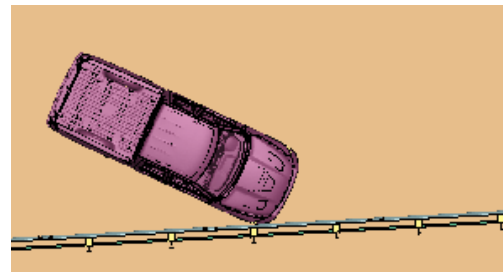
To investigate the CIP, the vehicular and structural behaviors of the system were evaluated after impacting three different points: (a) 2 ft upstream from a post; (b) at the middle of the W-beam (mid-span); and (c) at a post. Table 8.6 lists the occupant risk factors and maximum dynamic rail deflection for the pickup truck impacting at each CIP. For the flared MGS at a 15:1 rate, impacting 2 ft upstream from a post was most critical based on the overall behavior of the system. For the system flared at an 18:1 rate, impacting a post was most critical based on the overall behavior of the system. Figure 8.10 shows the CIP for the flared MGS retrofitted with a channel rubrail. Figure 8.11 and Figure 8.12 show the sequential frames for the most critical impact simulation for the pickup truck on the system at 15:1 and 18:1 flare rates, respectively.

Table 8.6. CIP Investigation for the Pickup Truck (2270P).

Flare Rate			15:1 (28.8°)			18:1 (28.4°)			
CIP			2 ft upstream from post	Mid-span	At post	2 ft upstream from post	At post	Mid-span	
Occupant Risk Factors	Occupant Impact Velocity (ft/s)	X	22.3	18.4	21.3	24.9	20.3	19.4	
		Y	14.4	16.1	15.4	14.8	16.1	14.8	
	Ridedown Acceleration (g)	X	11.7	10.4	10.0	11.9	12.8	11.6	
		Y	10.4	11.2	8.9	7.9	9.7	8.8	
	Max. Angle (degrees)	Roll	17.4	15.8	10.0	6.7	4.4	18.6	
		Pitch	4.5	11.5	10.4	9.6	8.4	11.3	
		Yaw	37.1	37.7	51.8	33.4	34.7	30.6	
	Maximum Lateral Rail Deflection (in.)			49.1	45.3	49.6	44.1	48.0	47.4



(a) CIP for 15:1 flared MGS



(b) CIP for 18:1 flared MGS

Figure 8.10. CIPs for Pickup Truck Impacting Flared MGS Retrofitted with Channel Rubrail.

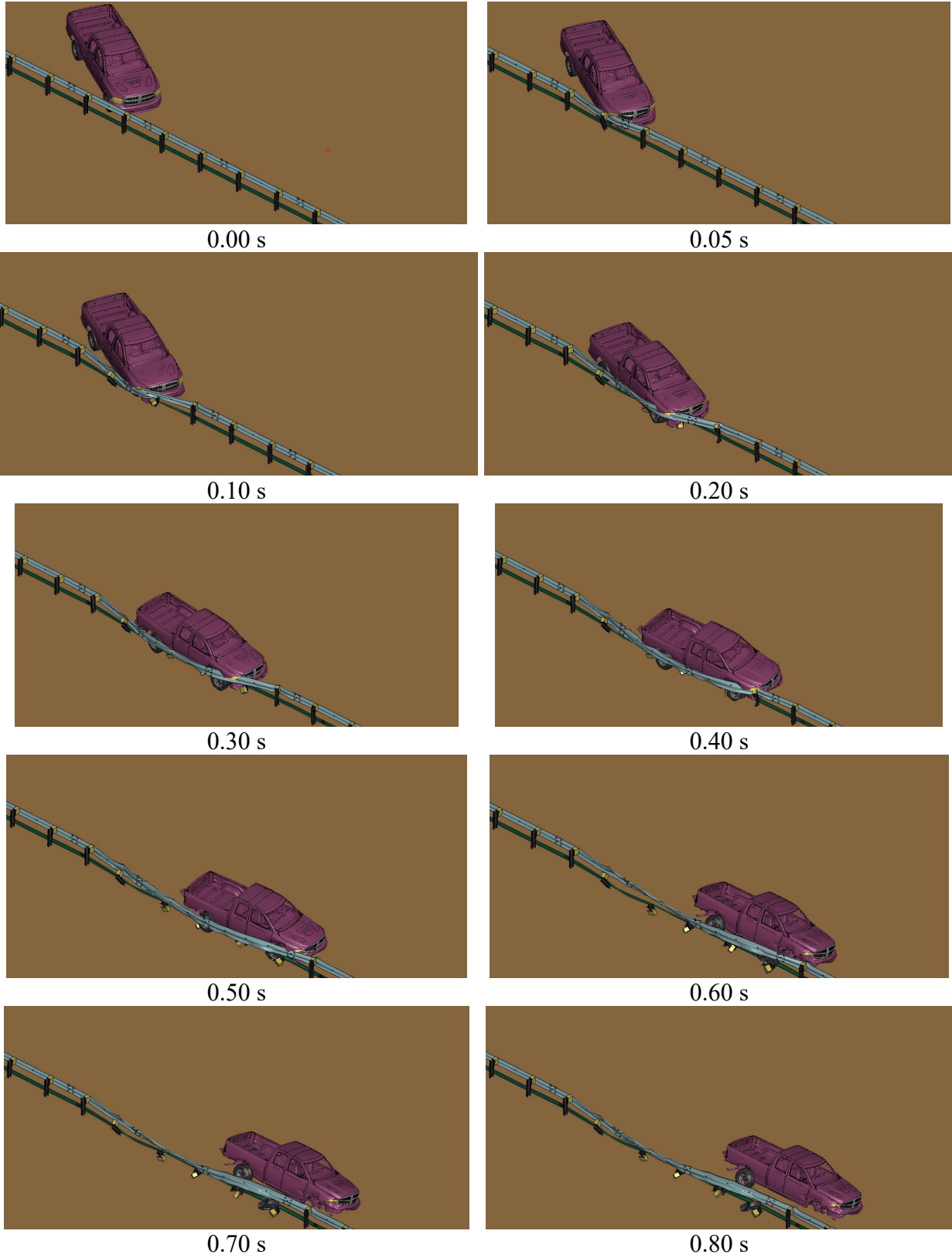


Figure 8.11. Sequential Frames for Pickup Truck Impact at CIP on 15:1 Flared MGS Retrofitted with Channel Rubrail.

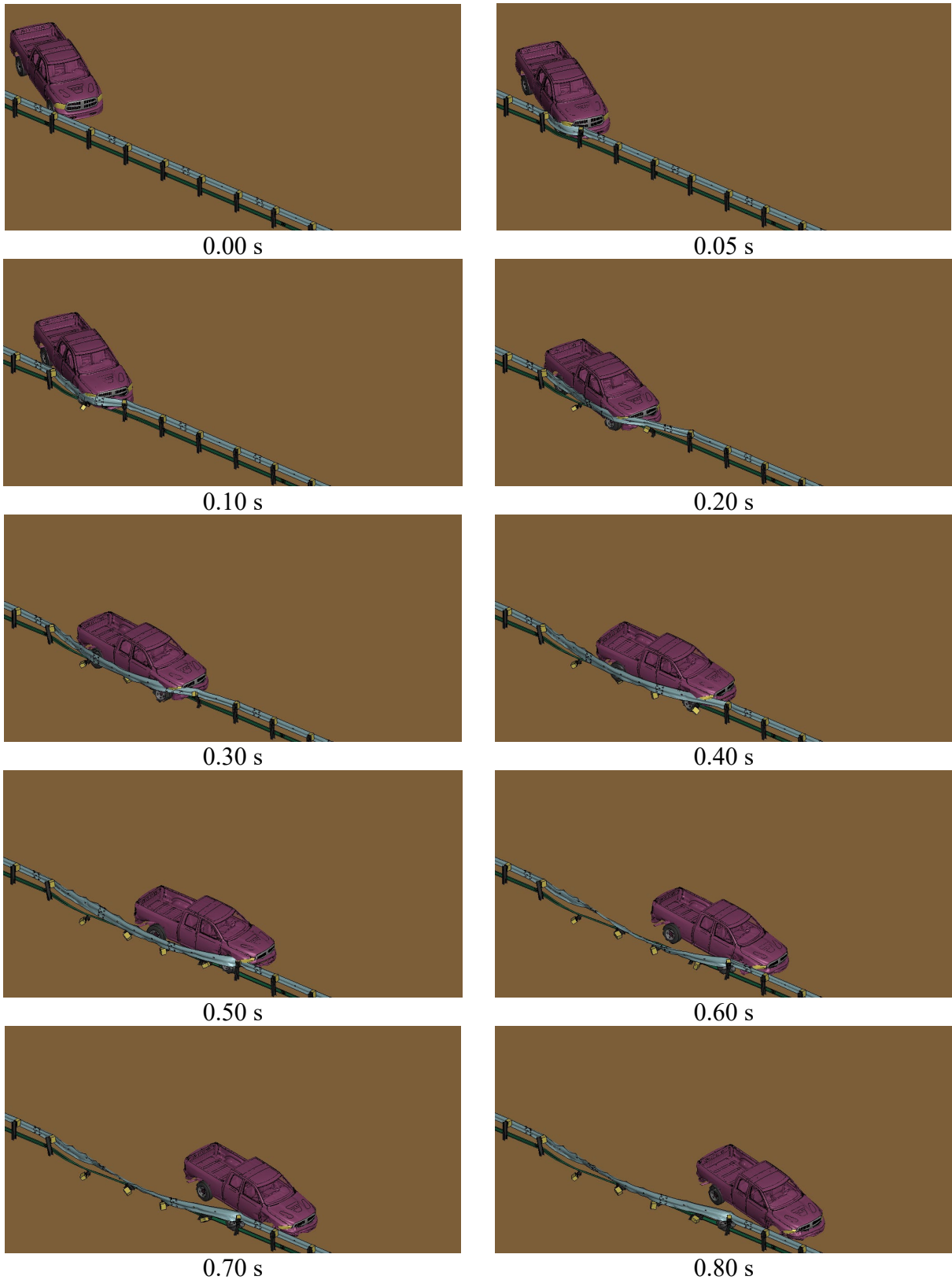
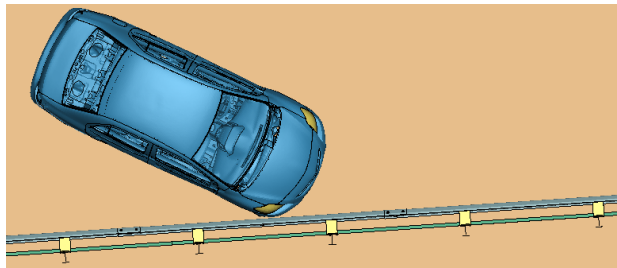


Figure 8.12. Sequential Frames for Pickup Truck Impact at CIP on 18:1 Flared MGS Retrofitted with Channel Rubrail.

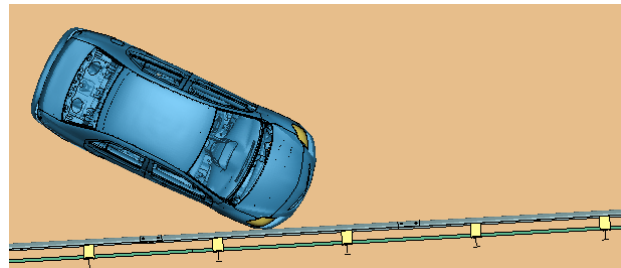
Table 8.7 shows the occupant risk factors and maximum dynamic rail deflection for the small passenger car impacting at each CIP. For the MGS flared at both 15:1 and 18:1 rates, impacting at the middle of the W-beam (mid-span) was found to be the most critical case based on the overall behavior of the system. For the system flared at the 18:1 rate, impacting a post also resulted in high ridedown acceleration but produced less maximum W-beam rail deflection compared to the case impacting at mid-span. Figure 8.13 shows the CIP for the flared MGS retrofitted with a channel rubrail. Figure 8.14 and Figure 8.15 show the sequential frames for the most critical impact simulation for the small passenger car on the flared MGS at the 15:1 and 18:1 rates, respectively.

Table 8.7. CIP Investigation for Small Car (1100C).

Flare Rate			15:1 (28.8°)			18:1 (28.4°)			
CIP			At post	2 ft downstream from post	Mid-span	2 ft upstream from post	At post	Mid-span	
Occupant Risk Factors	Occupant Impact Velocity (ft/s)	X	38.7	26.9	32.8	36.7	24.6	31.5	
		Y	22.3	27.6	25.9	23.0	24.0	25.6	
	Ridedown Acceleration (g)	X	13.1	12.4	19.6	12.2	19.5	19.6	
		Y	9.8	12.2	7.2	11.7	12.3	7.3	
	Max. Angle (degrees)	Roll	9.5	11.5	8.3	6.2	8.9	8.1	
		Pitch	8.5	5.1	5.6	4.9	7.6	5.5	
		Yaw	48.2	53.4	50.1	50.9	49.3	50.1	
	Maximum Rail Deflection (in.)			24.6	25.6	25.6	25.5	21.6	26.8



(a) CIP for 15:1 flared MGS



(b) CIP for 18:1 flared MGS

Figure 8.13. CIPs for Small Car Impacting Flared MGS with Channel Rubrail.

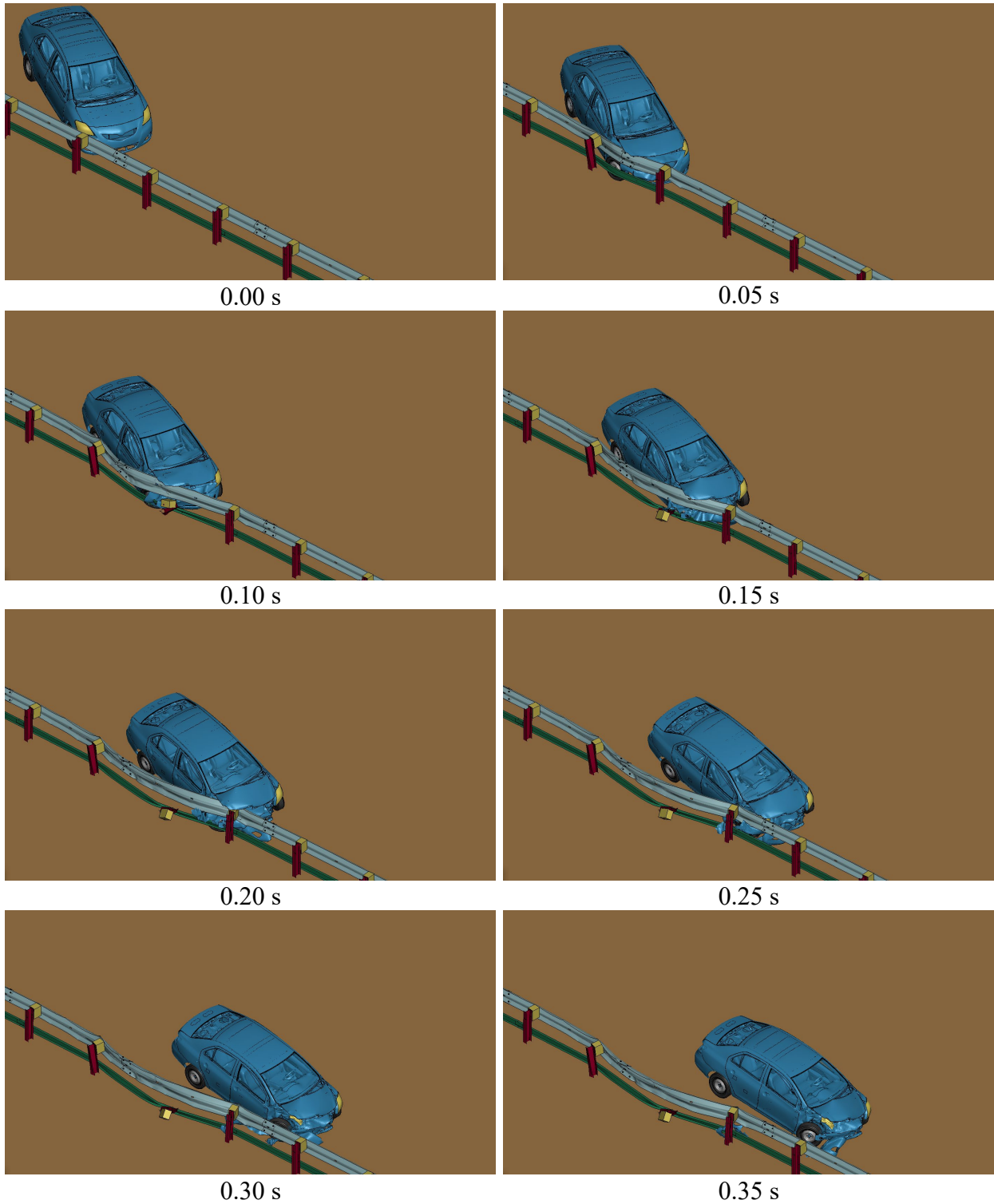


Figure 8.14. Sequential Frames for Small Passenger Car Impact at CIP on 15:1 Flared MGS Retrofitted with Channel Rubrail.

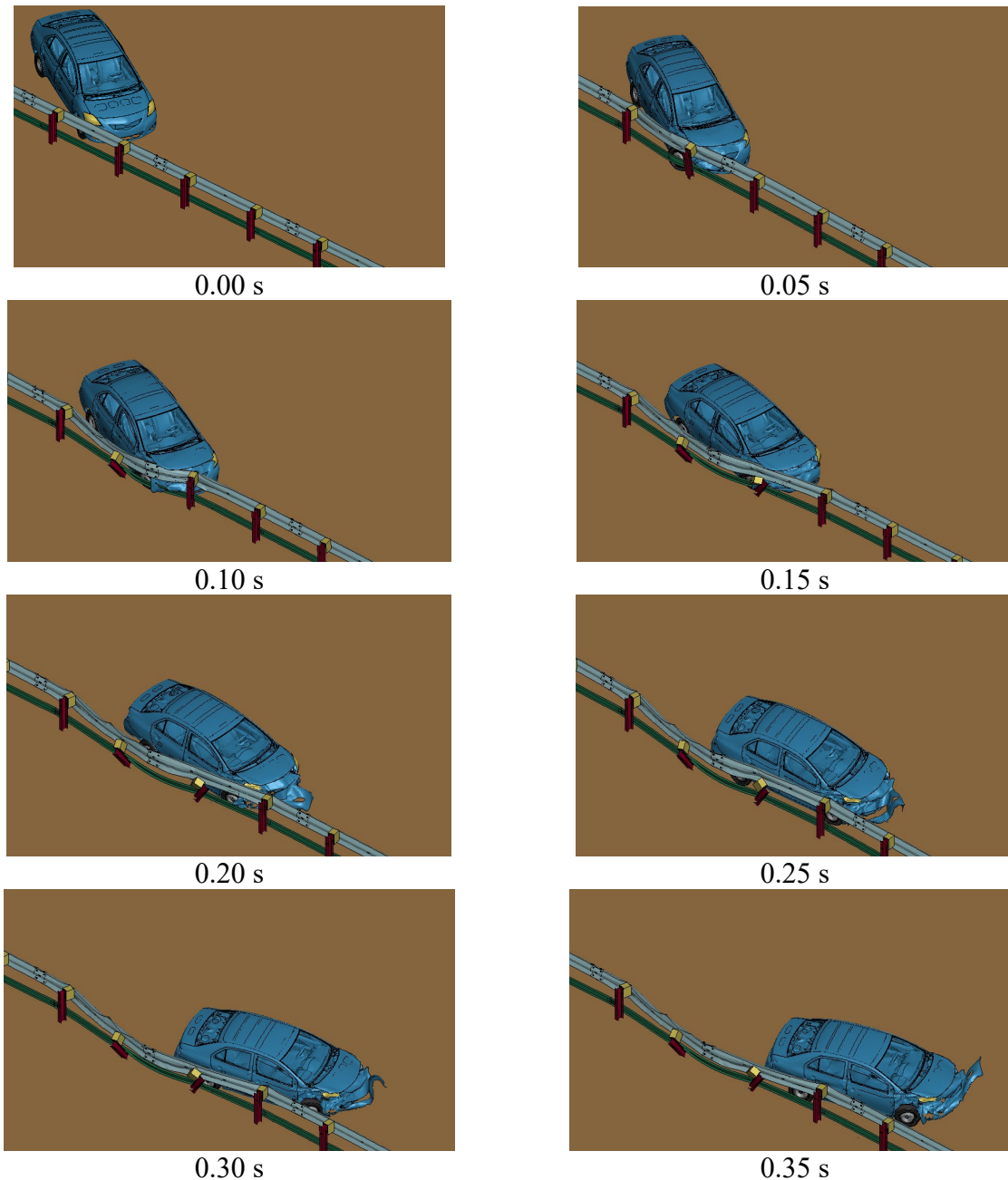
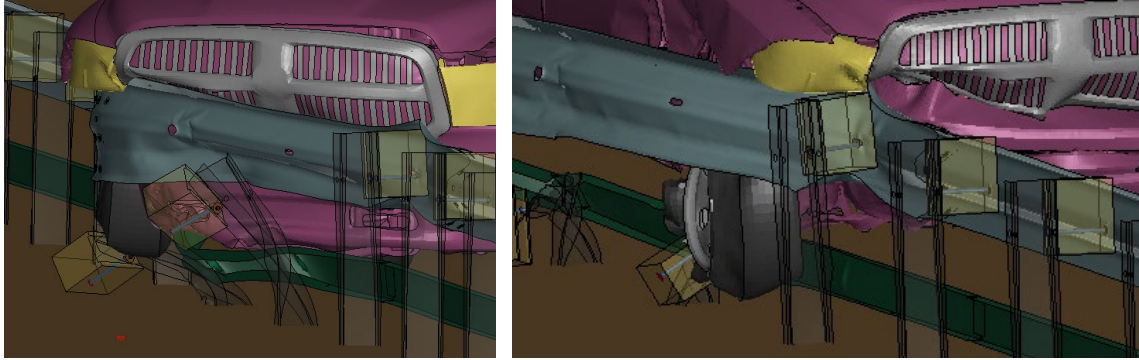
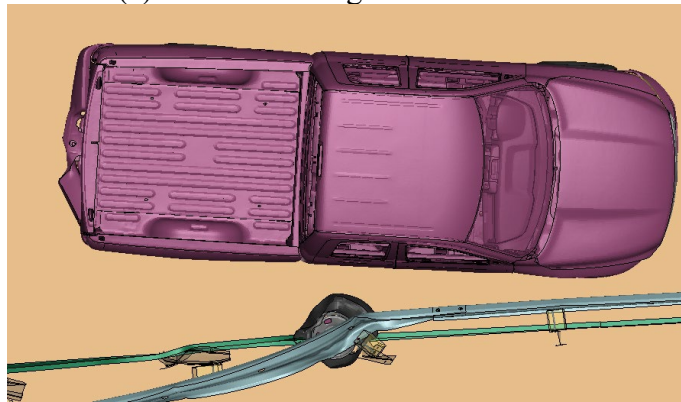


Figure 8.15. Sequential Frames for Small Passenger Car Impact at CIP on 18:1 Flared MGS Retrofitted with Channel Rubrail.

For the pickup truck FE simulations on the flared MGS retrofitted with a channel rubrail, the passenger-side front tire rode on the rubrail, and when the vehicle was exiting, the tire went beyond the rubrail, as shown in Figure 8.16. During this event, a numerical issue was also found, showing a part of the tire element tangled with an edge of the channel rubrail element. However, since the issue was detected after maximum occupant risk factors (e.g., occupant impact velocity and ridedown acceleration) and rail deflection were observed, the numerical issue may not affect the simulation results.



(a) Tire Overriding Channel Rubrail



(b) Tire Tangling

Figure 8.16. FE Pickup Truck Tire Model Behavior.

Since resolving the numerical issue became a concern due to project resource (time and budget) constraints, another simulation for each vehicle type impacting at CIP was performed on the 18:1 flared MGS retrofitted with a channel rubrail. In addition to modifying a contact command between the rubrail and the tire to resolve the numerical issue, the channel rubrail was raised by 3 inches to have a 12-inch distance from the center of the channel to the ground. By raising the rubrail, the gap between the W-beam and channel was decreased, which should reduce the possibility of tire tangling.

Figure 8.17 describes the difference between the initial retrofitted MGS model and the modified retrofitted model. As aforementioned, the vertical location of the channel increased by 3 inches. Figure 8.18 and Figure 8.19 show the close-up view and sequential frames, respectively, for the modified FE pickup truck simulation results to illustrate the improvements. As seen in the figures, the tire overrode the channel less, and it did not tangle with any MGS FE model element. Without tire FE element tangling, the vehicle exited and redirected more smoothly.

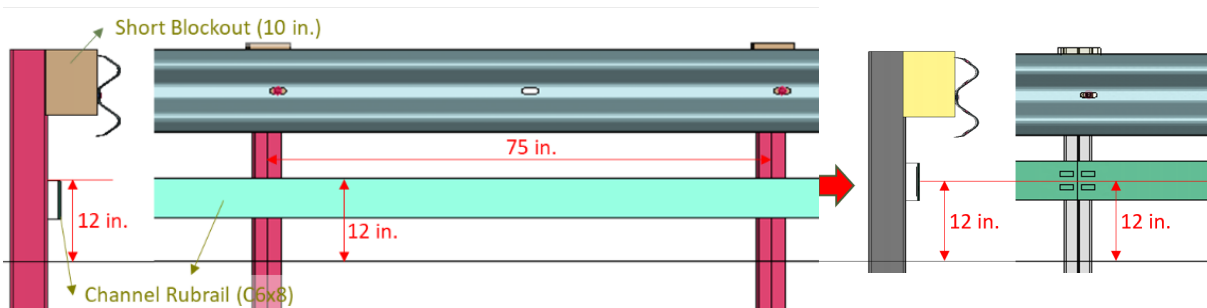
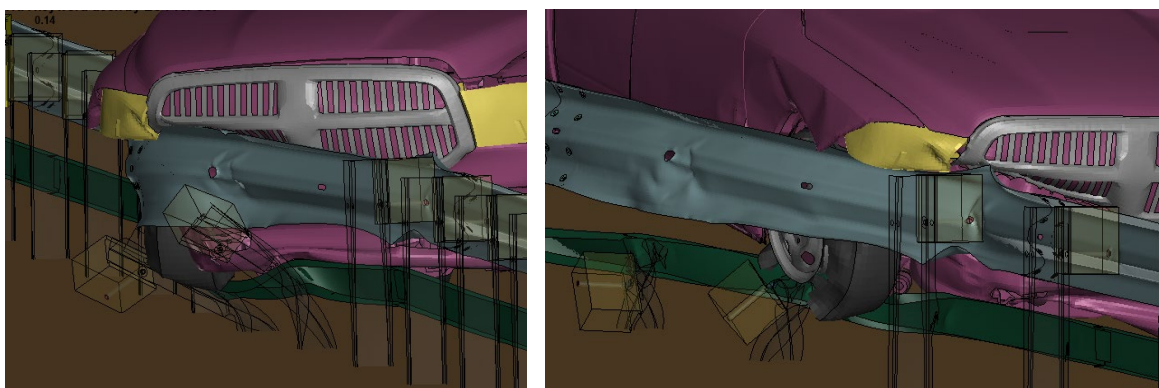
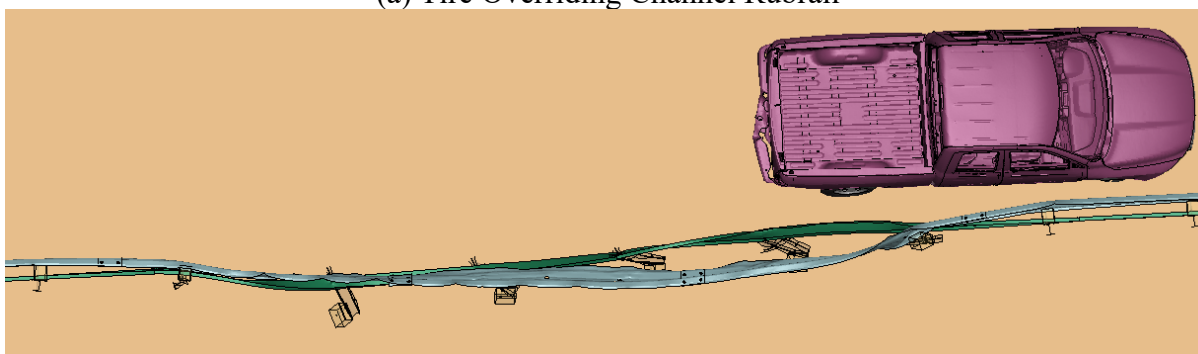


Figure 8.17. Modified Channel Rubrail Location.



(a) Tire Overriding Channel Rubrail



(b) Vehicle Exiting

Figure 8.18. Modified FE Simulation with 18:1 Flared MGS Retrofitted with Channel Rubrail.

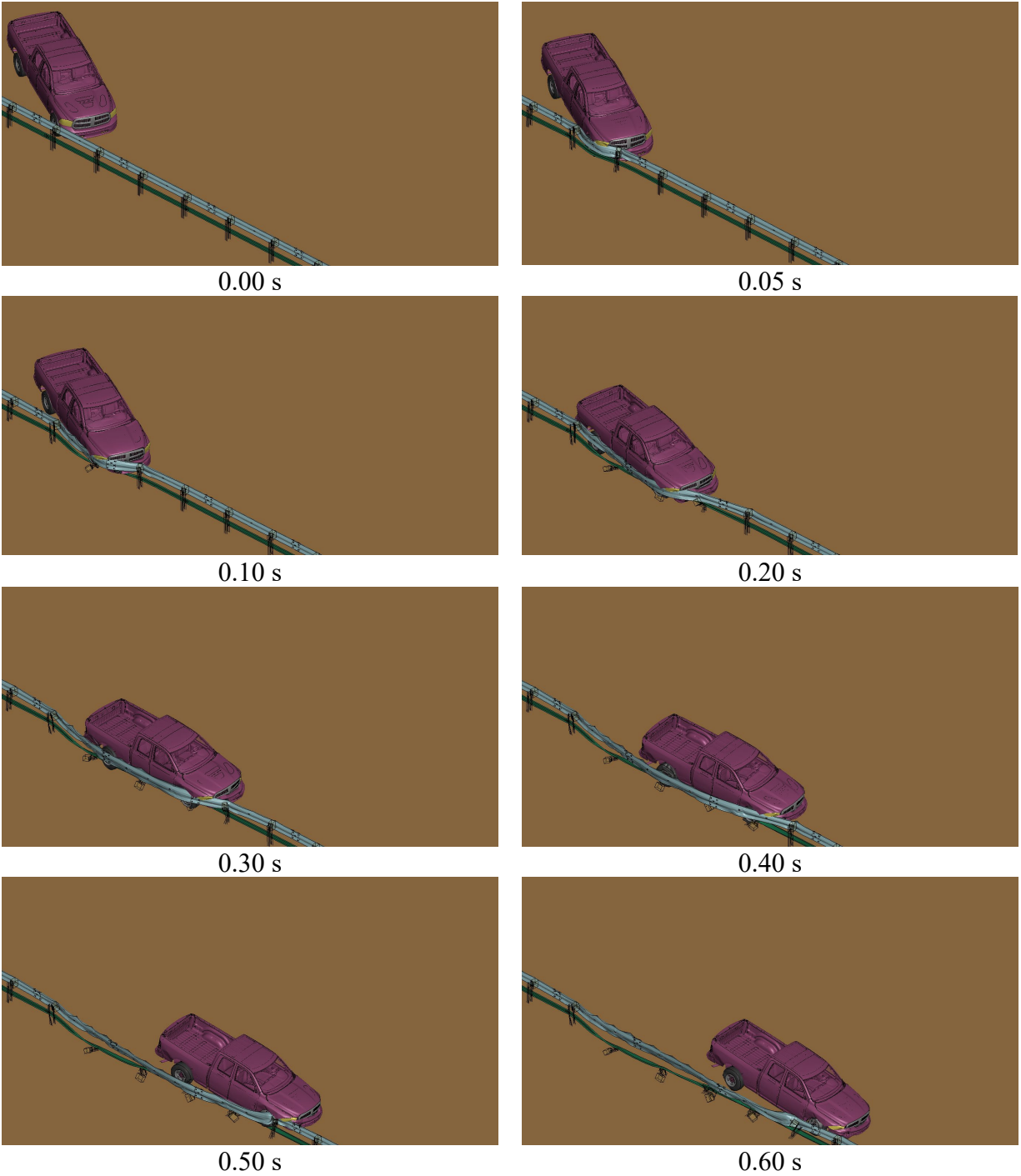


Figure 8.19. Sequential Frames for Pickup Truck Impact at CIP on Modified 18:1 Flared MGS Retrofitted with Channel Rubrail.

To evaluate the modified retrofitted MGS model, a small car impact simulation was also performed under the same TL-3 conditions. Figure 8.20 shows the sequential frames with the small car behavior after impacting the CIP of the modified retrofitted MGS.

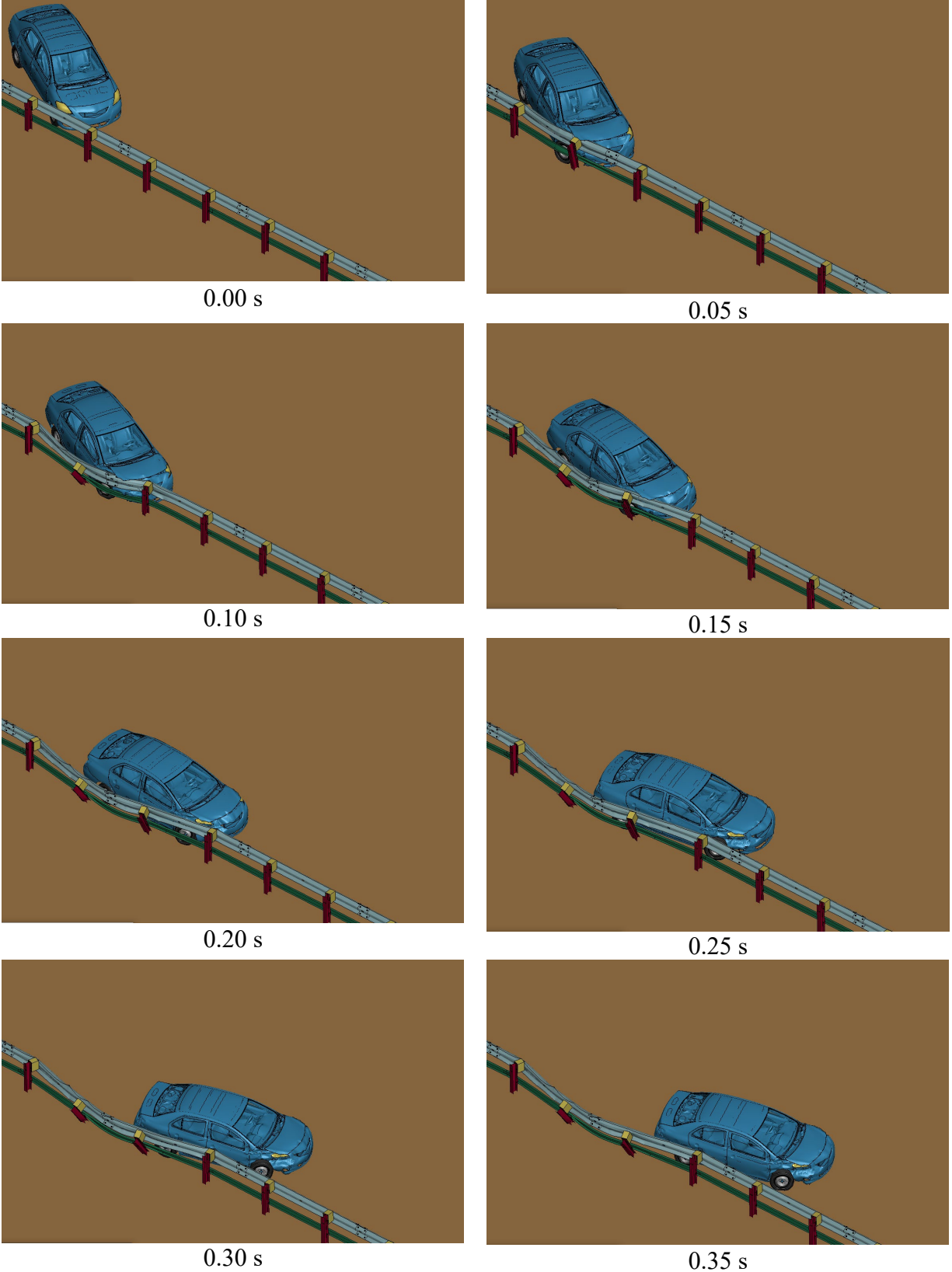


Figure 8.20. Sequential Frames for Small Car Impact at CIP on Modified 18:1 Flared MGS Retrofitted with Channel Rubrail.

Table 8.8 lists the occupant risk factors and maximum lateral dynamic W-beam rail deflection to compare the simulation results of the different channel rubrail heights. For both the pickup truck and small car, the retrofitted MGS with the channel rubrail located higher improved the overall system behavior.

Table 8.8. Comparison of Simulation Results for 18:1 Flared MGS Retrofitted with Channel Rubrail with 12-inch Center-to-Ground Distance.

Vehicle Model			Pickup Truck		Small Car	
Rubrail Height (Channel Top to Ground)			12 in.	15 in.	12 in.	15 in.
Occupant Risk Factors	Occupant Impact Velocity (ft/s)	X	20.3	19.7	32.8	21.7
		Y	16.1	16.7	25.9	24.9
	Ridedown Acceleration (g)	X	12.8	9.6	19.6	13.1
		Y	9.7	8.4	7.2	12.0
	Max. Angle (degrees)	Roll	4.4	8.4	8.3	8.0
		Pitch	8.4	9.8	5.6	2.4
		Yaw	34.7	34.4	50.1	49.2
Maximum Dynamic Lateral Rail Deflection (in.)			48.0	42.7	26.8	26.2

To investigate performance of the system in steeper flare rate, another simulation for each vehicle type impacting at CIP was performed on the 15:1 flared MGS retrofitted with a channel rubrail. Figure 8.21 shows sequential frames, for the modified FE pickup truck. As seen in the figures, without tire FE element issue, the vehicle exited and redirected more smoothly.

With better performance with a pickup truck, a small car impact simulation was also performed under the same TL-3 conditions. Figure 8.22 shows the sequential frames with the small car behavior after impacting the CIP of the modified retrofitted MGS.

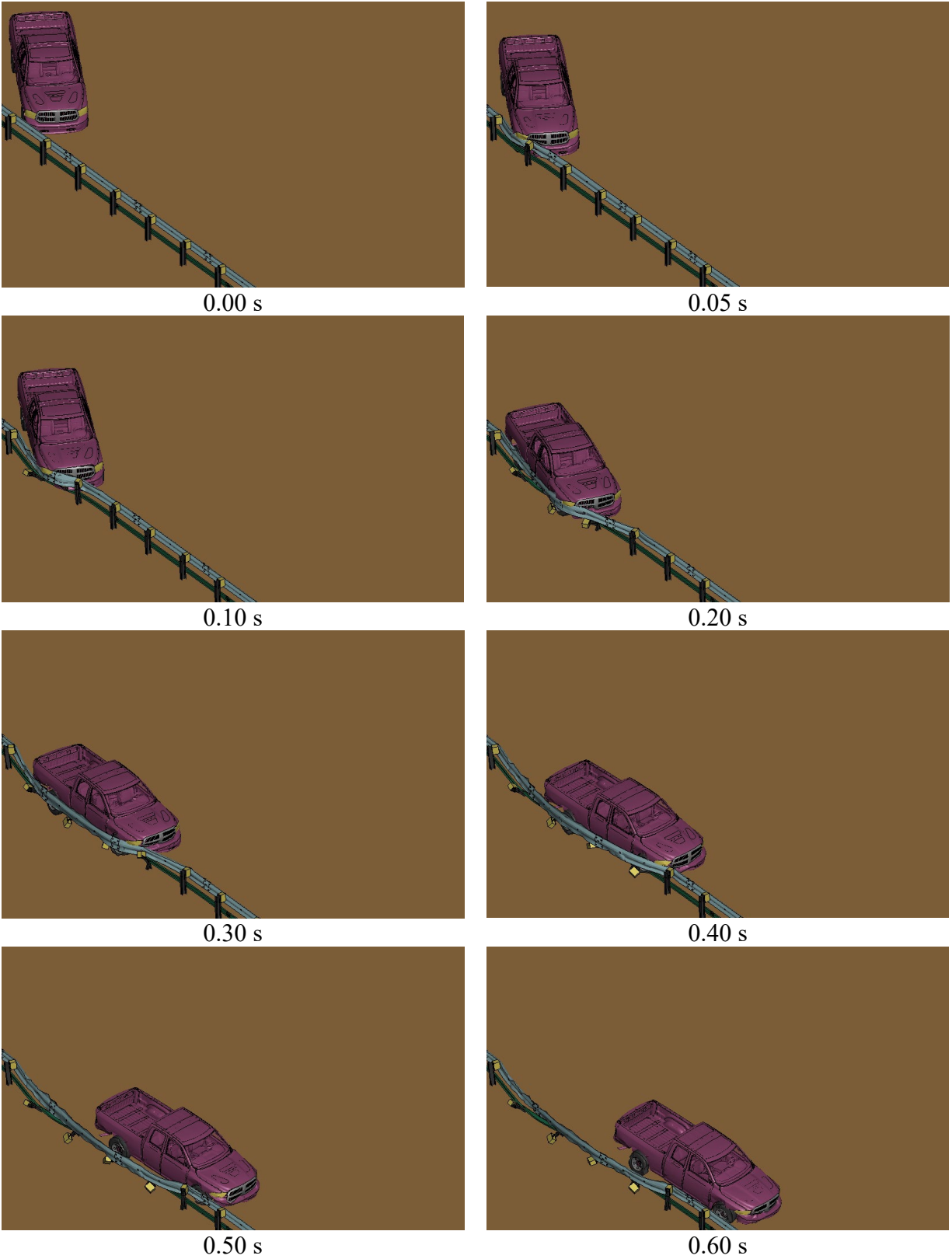


Figure 8.21. Sequential Frames for Pickup Truck Impact at CIP on Modified 15:1 Flared MGS Retrofitted with Channel Rubrail.

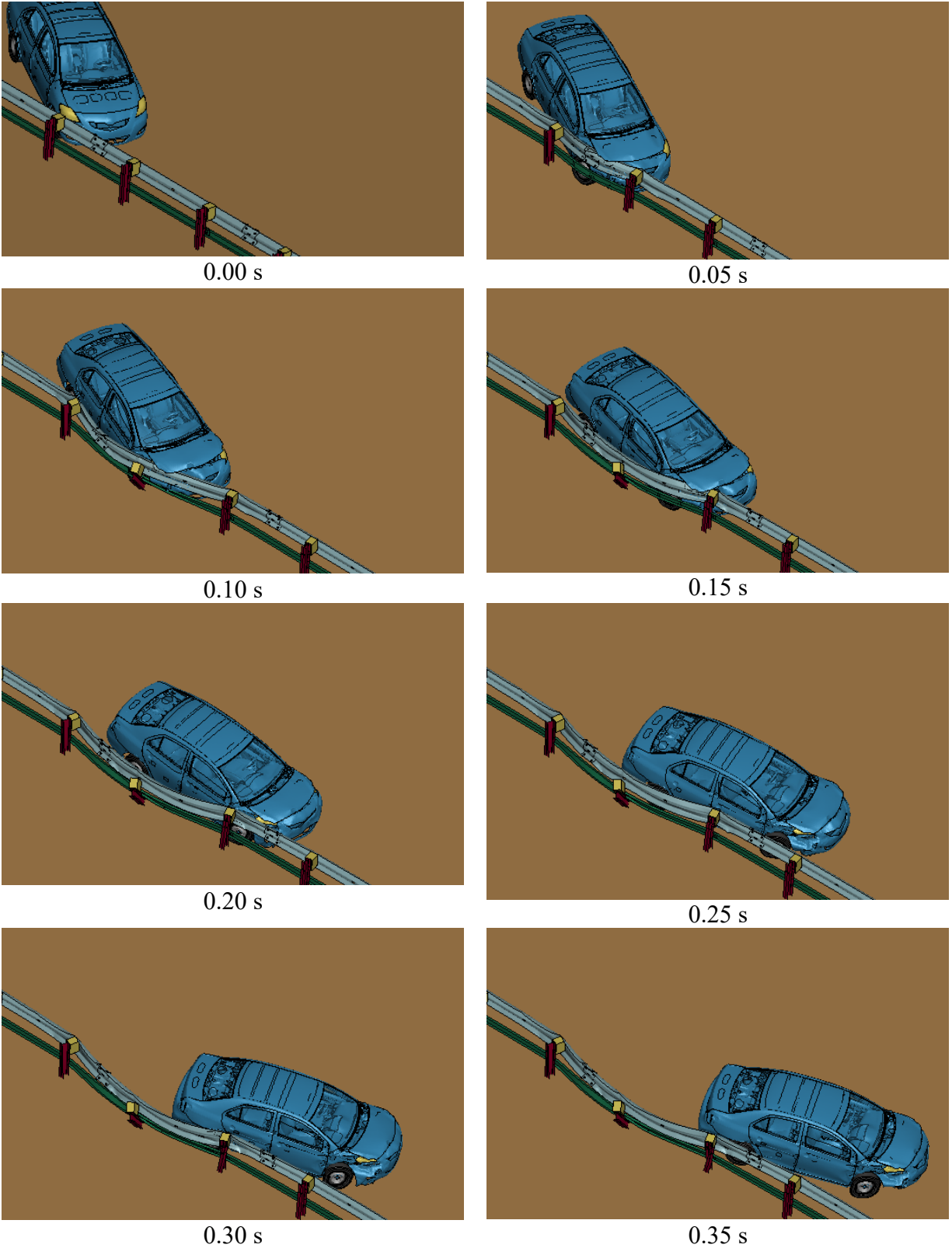


Figure 8.22. Sequential Frames for Small Car Impact at CIP on Modified 15:1 Flared MGS Retrofitted with Channel Rubrail.

Table 8.10 lists the occupant risk factors and maximum lateral dynamic W-beam rail deflection to compare the simulation results of the different channel rubrail heights. For both the pickup truck and small car, the retrofitted MGS with the channel rubrail located higher improved the overall system behavior.

Table 8.9. Comparison of Simulation Results for 15:1 Flared MGS Retrofitted with Channel Rubrail with 12-inch Center-to-Ground Distance.

Vehicle Model			Pickup Truck		Small Car	
Rubrail Height (Channel Top to Ground)			12 in.	15 in.	12 in.	15 in.
Occupant Risk Factors	Occupant Impact Velocity (ft/s)	X	22.3	19.0	32.8	32.5
		Y	14.4	15.7	25.9	17.4
	Ridedown Acceleration (g)	X	11.7	8.1	19.6	11.4
		Y	10.4	9.7	7.2	13.5
	Max. Angle (degrees)	Roll	17.4	12.5	8.3	5.7
		Pitch	4.5	11.1	5.6	5.9
		Yaw	37.1	46.7	50.1	55.0
Maximum Dynamic Lateral Rail Deflection (in.)			49.1	45.5	25.6	24.1

8.2. SUMMARY OF FINITE ELEMENT ANALYSIS

In this chapter, finite element computer modeling and simulations were conducted to investigate predictability of the MGS system crashworthiness when implemented at different flare rates and impacted at TL-3 impact conditions. Two general situations were investigated in parallel: (a) the MGS implemented at shallower flare rates than those already failed under the testing program, and (b) the MGS modified/retrofitted and implemented at different flare rates. For both general cases, a predictive analysis was conducted for impacts at *MASH* TL-3 conditions. Summaries of the performed FE simulation results are included in Table 8.10 and Table 8.11.

The impact behavior of MGS flares with shallower rates than 11:1, including 15:1, 18:1, and 21:1, were investigated and found to not significantly reduce lateral deflection or vehicle interaction compared to an 11:1 flare rate. This could indicate a potential for vehicle pocketing and rail rupture, as seen in a failed crash test.

To address the potential for vehicle pocketing and rail rupture, retrofit options for the MGS system were considered. The first option was to use short blockouts with half-post spacing (37½ inches) to prevent rail high concentration stresses and tearing due to direct contact between the blockout and rail. This retrofit design aimed to reduce lateral deflection and rail stress concentrations during impact to lower the likelihood of vehicle pocketing and rail rupture.

The half-post spacing system with short blockouts was evaluated with flare rates of 11:1 and 15:1 using a pickup truck, but the 11:1 system had increased occupant risks and ridedown acceleration. The 15:1 system showed improvement in both rail deflection and occupant risks.

The system was also evaluated with a small passenger car, but the recorded ridedown acceleration was too high, so a flare rate of 18:1 was evaluated, which showed improved occupant risks but still had a peak ridedown acceleration close to the MASH limit..

The study added a rubrail to a short blockout MGS with regular post spacing of 75 inches to reduce the ridedown acceleration. The rubrail was a typical C6×8 steel channel installed 12 inches from the ground. Flare rates of 15:1 and 18:1 were investigated, and results showed that the retrofitted MGS with a rubrail was able to stably redirect the impacting pickup truck model, but there were numerical issues with the passenger car. Simulations were performed on the 18:1 flare rate retrofitted MGS with raising the rubrail height by 3 inches to reduce the gap between the W-beam and the rubrail. The increased rubrail height prevented the vehicle's tire from overriding the rubrail, which helped to contain and redirect the vehicle. This indicates that the retrofit was successful in reducing ridedown acceleration and improving crashworthiness.

The simulation was conducted on the retrofitted flared MGS system with 15:1 flare rate using a rubrail centered at 12 inches from the ground. The overall system behavior was improved, with maximum rail deflection for the pickup truck simulation being reduced to 45.5 inches, close to the recorded value in the pickup truck full-scale test of the non-flared MGS. Additionally, the ridedown acceleration for the small car simulation was reduced to 11.4 g.

Recommendations for future research include validating the obtained FE analysis results through full-scale testing to verify the crashworthiness of the 15:1 flared, regular post-spacing MGS with inclusion of shorter blockouts and a C6×8 steel channel centered at 12 inches from the ground.

Table 8.10. Summary of FE Analysis for Pickup Truck.

Flare Rate (Effective Angle)		11:1 (30.2°)			15:1 (28.8°)				18:1 (28.4°)			21:1 (27.7°)	
		Test	MGS	Half-Post Spacing	MGS	Half-Post Spacing	Channel Rubrail		MGS	Channel Rubrail		MGS	
12 in.	15 in.						12 in.	15 in.					
Occupant Risk Factors	Occupant Impact Velocity (ft/s)	X	18.7	23.4	29.9	23.6	22.3	22.3	19.0	24.0	20.3	19.7	20.7
		Y	13.9	15.4	17.7	14.8	16.4	14.4	15.7	13.1	16.1	16.7	14.8
	Ridedown Acceleration (g)	X	4.8	8.5	17.1	13.8	11.0	11.7	8.1	14.3	12.8	9.6	10.7
		Y	5.0	9.0	12.4	13.8	10.3	10.4	9.7	7.0	9.7	8.4	9.1
	Max. Angle (degrees)	Roll	8.9	4.76	15.8	8.8	6.8	17.4	12.5	3.1	4.4	8.4	10.2
		Pitch	5.6	1.06	7.4	9.2	2.3	4.5	11.1	5.9	8.4	9.8	3.1
		Yaw	194.4	18.13	58.0	56.2	40.7	37.1	46.7	54.1	34.7	34.4	57.9
Maximum Dynamic Lateral Rail Deflection (in.)		52.9 ^a	52.4	33.5	52.8	33.1	49.1	45.5	49.3	45.5	42.7	48.4	

^a Before rail rupture.

Table 8.11. Summary of FE Analysis for Small Car.

Flare Rate (Effective Angle)			15:1 (28.8°)			18:1 (28.4°)			21:1 (27.7°)	
Design Option			Half-Post Spacing	Channel Rubrail		Half-Post Spacing	Channel Rubrail		MGS	
				12 in.	15 in.		12 in.	15 in.		
Occupant Risk Factors	Occupant Impact Velocity (ft/s)	X	47.2	32.8	32.5	39.4	31.5	21.7	42.0	
		Y	18.0	25.9	17.4	14.1	25.6	24.9	14.4	
	Ridedown Acceleration (g)	X	23.8	19.6	11.4	20.3	19.6	13.1	21.1	
		Y	11.3	7.2	13.5	16.1	7.3	12.0	18.0	
	Max. Angle (degrees)	Roll	14.0	8.3	5.7	10.9	8.1	8.0	19.5	
		Pitch	6.2	5.6	5.9	6.1	5.5	2.4	5.9	
		Yaw	33.6	50.1	55.0	41.3	50.1	49.2	85.7	
	Maximum Dynamic Lateral Rail Deflection (in.)			23.8	25.6	24.1	24.2	24.1	26.2	34.6

Chapter 9. SUMMARY AND CONCLUSIONS

9.1. ASSESSMENT OF TEST RESULTS

A flared strong-post W-beam guardrail system allows for the potential to reduce guardrail installation lengths, which, in turn, would result in decreased guardrail construction and maintenance costs, as well as reduced impact frequency. Stolle et al. (3) conducted a research and test study to investigate the potential to increase flare rates for an MGS according to NCHRP Report 350 criteria. The researchers conducted computer simulations and full-scale crash testing that showed that the MGS could meet NCHRP Report 350 impact criteria when installed at a 5:1 flare rate. Impact severities during testing were found to be greater than intended, yet the MGS passed all NCHRP 350 requirements. The researchers recommended that whenever a guardrail is outside of the shy line for adjacent traffic, and the roadside terrain is sufficiently flat, flare rates should be increased to as high as 5:1 when using the MGS guardrail.

NCHRP Report 350 testing and evaluation criteria were superseded by *MASH*, which was developed to incorporate significant changes and additions to procedures for safety-performance evaluation as well as updates reflecting the changing character of the highway network and the vehicles using it. For example, *MASH* increased the weight of the pickup truck design test vehicle from 4,409 lb to 5,000 lb, changed the body style from a ¾-ton standard cab to a ½-ton four-door, and imposed a minimum height for the vertical CG of 28 inches. The increase in vehicle mass represents an increase in impact severity of approximately 13 percent for Test 3-11 with the pickup truck design test vehicle compared to the impact conditions of NCHRP Report 350. The increased impact severity may therefore result in increased impact forces and larger lateral barrier deflections compared to NCHRP Report 350.

The impact conditions for the small car test have also changed. The weight of the small passenger design test vehicle increased from 1,800 lb to 2,420 lb, and impact angle increased from 20 degrees to 25 degrees with respect to the roadway. These changes represent an increase in impact severity of 105 percent for Test 3-10 with the small car design test vehicle compared to the impact conditions of NCHRP Report 350. This increase in impact severity might result in increased vehicle deformation and could possibly aggravate vehicle stability. Specifically, when a flare rate is included in the guardrail design, there is an increment of the effective impact angle between the vehicle and the guardrail, which results in a considerably higher impact severity and requires an increasing level of demand on the structural capacity of a barrier system. For example, under *MASH* conditions, a 5:1 flare rate would increase the impact severity 196 percent for Test 3-10.

MASH also adopted more quantitative and stringent evaluation criteria for occupant compartment deformation than NCHRP Report 350. An increase in impact severity might result in increased vehicle deformation and could possibly result in failure to meet the latest *MASH* evaluation criteria. For example, NCHRP Report 350 established a 6-inch threshold for occupant compartment deformation or intrusion. *MASH* limited the extent of roof crush to no more than 3.9 inches. In addition, *MASH* requires that the vehicle windshield not sustain a deformation greater than 3 inches and have no holes or tears in the safety lining as a result of the test impact. Although these evaluation criteria are applicable to all roadside safety device testing, they are most relevant for sign support design and testing. In addition, little evaluation of sign supports has been performed with larger vehicles such as the pickup. Systems that have been

demonstrated to be crashworthy for passenger cars may not be geometrically compatible with pickup trucks.

The purpose of this project was to conduct a testing program to assess the performance of the MGS system when implemented with flare conditions according to the safety-performance evaluation guidelines included in *MASH*, Second Edition. The crash tests were performed in accordance with *MASH* TL-3. Two flare conditions were investigated: 7:1 with use of a passenger car, and 11:1 with use of a pickup truck.

The MGS tested at the considered flare conditions did not meet the performance criteria for *MASH* TL-3 guardrails. In the full-scale testing, MGS rail rupture under the higher impact severity and vehicle interaction during impact was the leading reason for system crashworthiness failure. Also, the first test that was conducted with the pickup truck on the 11:1 MGS flare resulted in failure to contain the vehicle due to fracture of the wood-post DAT system used in the test installation. The MGS 11:1 flare was then reinstalled and tested at the same conditions but with the inclusion of a steel-post end terminal system (SoftStop®) to avoid rupture of the wood posts. Although the end terminal did not result in post fracture, the test failed due to MGS rail rupture during the vehicle impact event.

See Table 9.1 for a summary of each test based on the applicable safety evaluation criteria.

Table 9.1. Summary of *MASH* Tests on MGS Guardrail with Flare.

Evaluation Criteria^a	Brief Description	Test No. 609971-01-1	Test No. 609971-03-1	Test No. 609971-03-2
A	Contain, Redirect, or Controlled Stop	Fail	Fail	Fail
D	No Penetration into Occupant Compartment	S	S	S
F	Roll and Pitch Limit	Fail	Fail	S
H	OIV Threshold	S	S	S
I	Ridedown Threshold	S	S	S
Overall		Fail	Fail	Fail

Note: S = Satisfactory.

^a See Table 3.2 for details.

9.2. SUMMARY OF FINITE ELEMENT ANALYSIS RESEARCH

After the full-scale crash tests were completed and determined to be failed, an effort was initiated through finite element modeling and simulations to investigate the crashworthiness of the MGS system at shallower flare rates, and when considering prioritized MGS retrofit options, still under high-speed impact conditions.

The main challenge in evaluating the impact results of a computer simulation for a MGS W-beam rail system was to find a way to predict rail rupture. Element erosion was not considered due to its lack of robustness, so other factors were used, such as the vehicle's interaction with the system, the lateral deflection of the system during impact, predicted rail stresses/strains, and recorded occupant risk values and vehicle stability. The lateral deflection was especially important because it could indicate potential pocketing of the vehicle, which could cause excessive loading on the W-beam railing and ultimate failure.

The impact behavior of MGS flares with shallower rates was investigated and found to not significantly reduce the lateral deflection during impact. Therefore, retrofit options were considered, including the use of short blockouts and half-post spacing and adding a rubrail to short blockout MGS with regular post spacing. The use of short blockouts and half-post spacing improved occupant risk but still had a peak ridedown acceleration that was too close to the MASH allowed limit. Adding a rubrail to a short blockout MGS with regular post spacing and a 15:1 flare rate was found to improve the overall system behavior, reducing the maximum rail deflection and ridedown acceleration.

9.3. CONCLUSIONS

This research has conducted full scale tests and FE analysis on the flared MGS guardrail in accordance with *MASH* Test Level 3. Based on the research presented herein, the following conclusions are drawn:

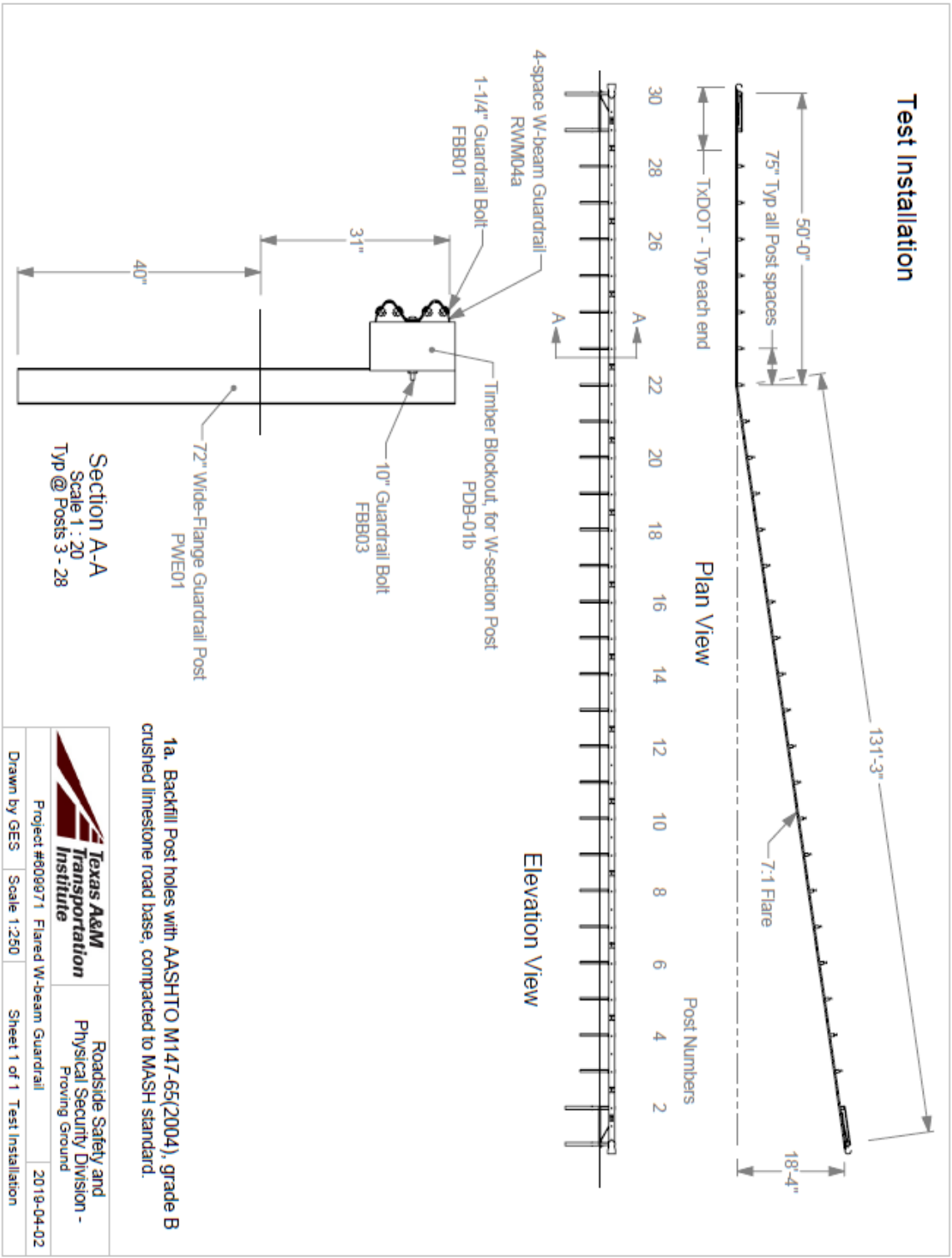
1. To prevent failure to contain the vehicle due to fracture of the wood-post DAT system, a steel-post end terminal system (SoftStop[®]) is recommended for future tests to avoid rupture of the wood posts.
2. None of the three tests conducted on the MGS guardrail with a flare rate of 11:1 met the *MASH* requirements for semi-rigid longitudinal barriers.
3. Standard MGS guardrail with a flare rate of between 11:1 and 21:1 is not expected to meet *MASH* TL 3 requirements.
4. The 15:1 flared regular post-spacing MGS with inclusion of shorter blockouts and a C6×8 steel channel centered at 12 inches from the ground is recommended for future research include validating the obtained FE analysis results through full-scale testing to verify the crashworthiness.

REFERENCES

1. AASHTO. *Manual for Assessing Roadside Safety Hardware*, Second Edition. American Association of State Highway and Transportation Officials, 2016.
2. National Cooperative Highway Research Program (NCHRP). *Recommended Procedures for the Safety Performance Evaluation of Highway Features*. Report 350. Transportation Research Board, National Research Council, Washington, D.C., 1993.
3. Stolle, C.S., Polivka, K.A., Reid, J.D., Faller, R.K., Sicking, D.L., Bielenberg, R.W., and Rohde, J.R., *Evaluation of Critical Flare Rates for the Midwest Guardrail System (MGS)*, TRP-03-191-08, Midwest States' Regional Pooled Fund Program, Lincoln, Nebraska, 2008.
4. Center for Collision Safety & Analysis. *2018 Dodge Ram 1500 FE Detailed Mesh Model v3 Validation*. George Mason University, 2022. <https://www.ccsa.gmu.edu/wp-content/uploads/2022/05/2018-dodge-ram-detailed-validation-v3.pdf>
5. Polivka, K.A., Faller, R.K., Sicking, D.L., Rohde, J.R., Bielenberg, R.W., and Reid, J.D. *Performance Evaluation of the Midwest Guardrail System—Update to NCHRP 350 Test No. 3-11 with 28" CG Height (2214MG-2)*. Mid-America Transportation Center, 2006.
6. Kovar, J.C., Bligh, R.P., Menges, W.L., Schroeder, G.E., Schroeder, W., Wegenast, S., Griffith, B.L., and Kuhn, D.L. *MASH Crash Testing and Evaluation of the MGS with Reduced Post Spacing*. Report No. 610211-01, Texas A&M Transportation Institute, 2021.

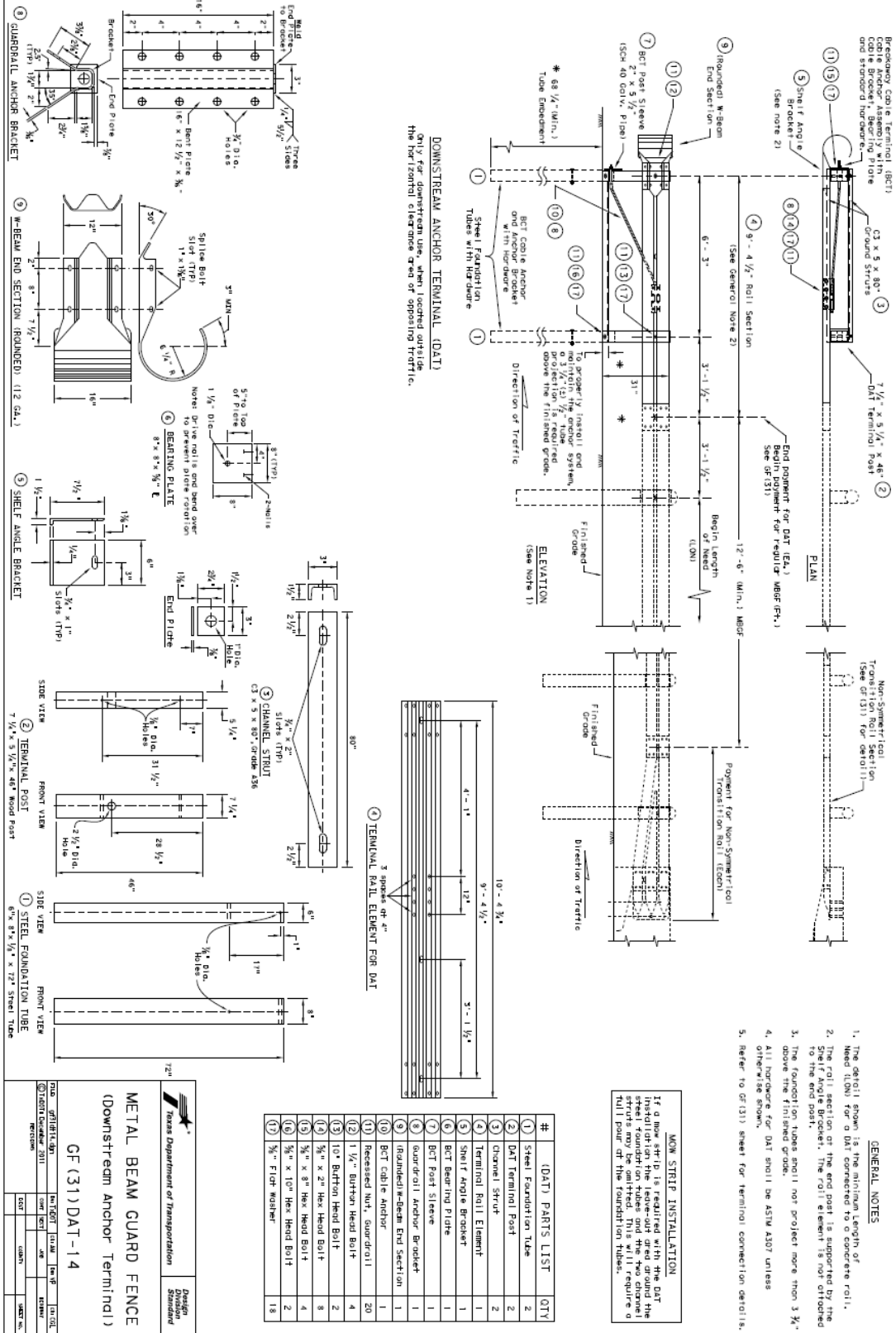
APPENDIX A. DETAILS OF MGS GUARDRAIL WITH FLARE

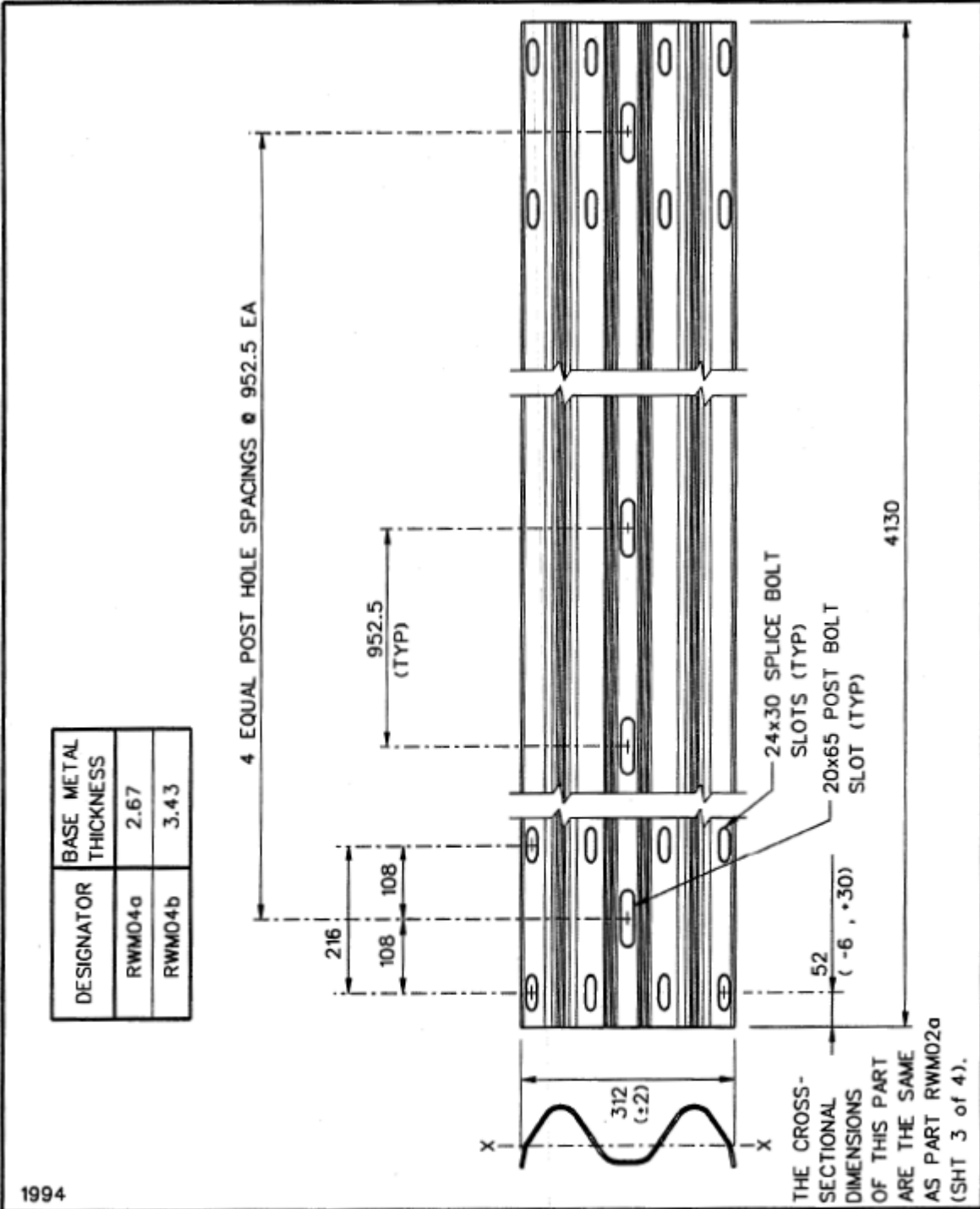
A.1. 6099971-01-1 DRAWINGS



DISCLAIMER
The use of this standard is governed by the "Texas Engineering Practice Act". No warranty of any kind is made by TxDOT for any purpose whatsoever. TxDOT disclaims responsibility for the conversion of this standard to other formats or for incorrect results or damages resulting from its use.

DATE: _____
FILE: _____





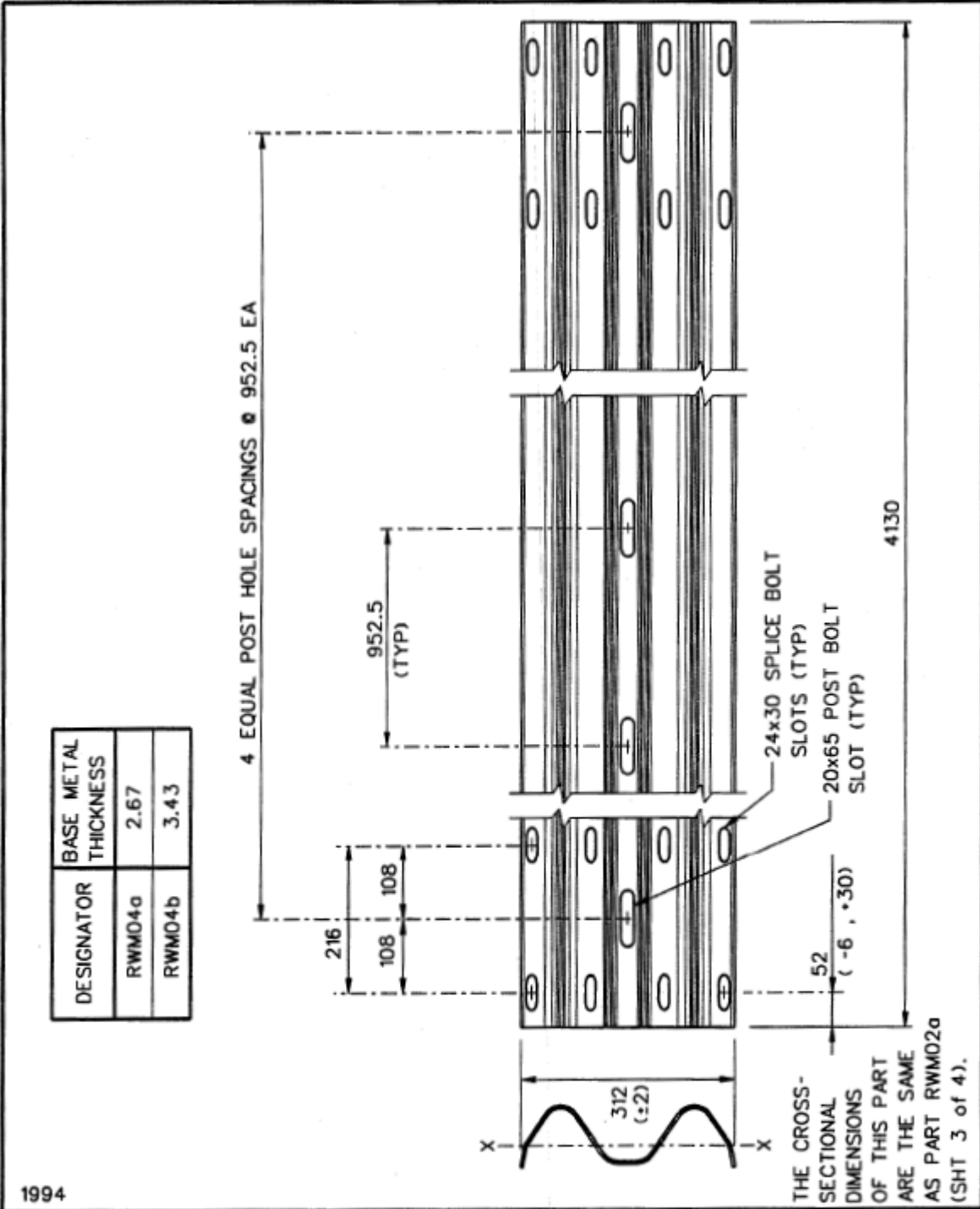
1994

4-SPACE W-BEAM GUARDRAIL



RWM04a-b

SHEET NO.	REF. NO.
1 of 2	RE-3-73



1994

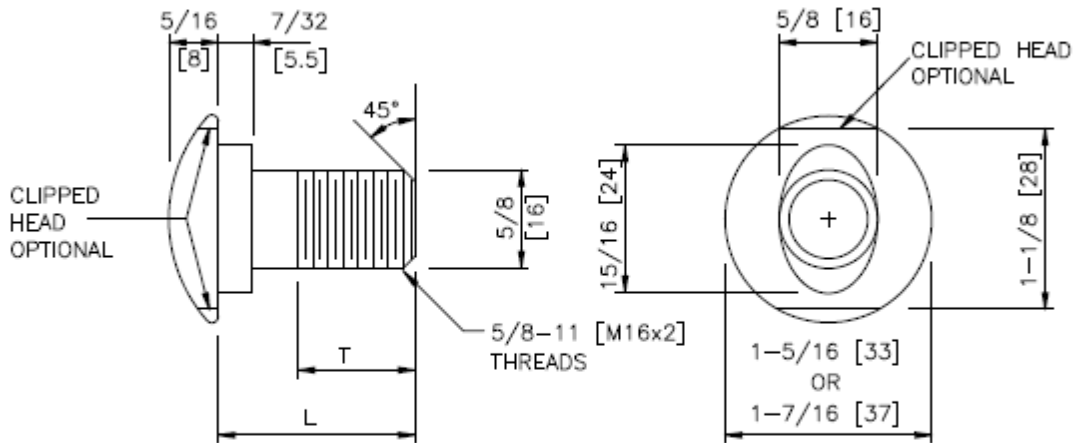
4-SPACE W-BEAM GUARDRAIL



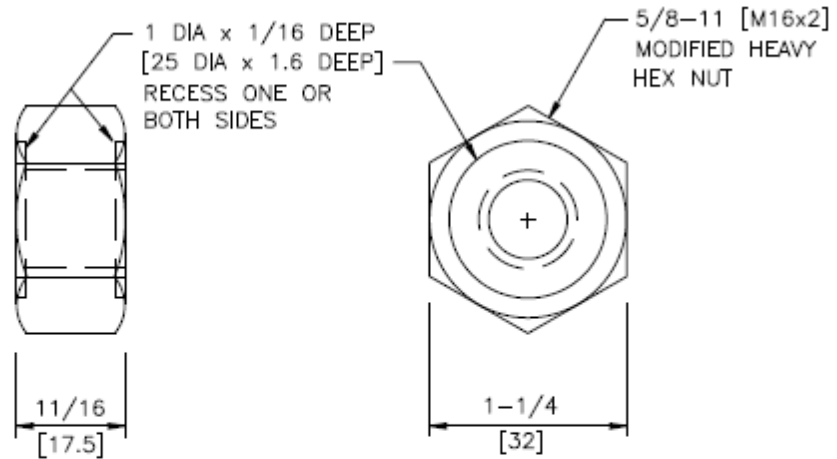
RWM04a-b

SHEET NO.	REF. NO.
1 of 2	RE-3-73

- NOTES:** 1. ALL FILLETS SHALL HAVE A MINIMUM RADIUS OF 1/16 [2].
 2. IF THE BOLT EXTENDS MORE THAN 1/4 [6] FROM THE NUT THE BOLT SHOULD BE TRIMMED BACK.



DESIGNATOR	L	T (MIN)
FBB01	1-1/4 [32]	1-1/8 [28]
FBB02	2 [51]	1-3/4 [44]
FBB03	10 [254]	4 [102]
FBB04	18 [457]	4 [102]
FBB05	25 [635]	4 [102]



GUARDRAIL BOLT AND RECESSED NUT



FBB01-05

SHEET NO.	DATE:
1 of 2	5/2/2018

SPECIFICATIONS

The geometry and material specifications for this oval shoulder button-headed bolt and hex nut are found in AASHTO M 180. The bolt shall have 5/8-11 [M16x2] threads as defined in ANSI B1.1 [ANSI B1.13M] for Class 2A [6g] tolerances. Bolt material shall conform to ASTM A307 Grade A [ASTM F 568M Class 4.6], with a tensile strength of 60 ksi [400 MPa] and yield strength of 36 ksi [240 MPa]. Material for corrosion-resistant bolts shall conform to ASTM A325 Type 3 [ASTM F 568M Class 8.8.3], with tensile strength of 120 ksi [830 MPa] and yield strength of 92 ksi [660 MPa]. This bolt material has corrosion resistance comparable to ASTM A588 steels. Metric zinc-coated bolt heads shall be marked as specified in ASTM F 568 Section 9 with the symbol "4.6."

Nuts shall have ANSI B1.1 Class 2B [ANSI B1.13M Class 6h] 5/8-11 [M16x2] threads. The geometry of the nuts, with the exception of the recess shown in the drawing, shall conform to ANSI B18.2.2 [ANSI B18.2.4.1M Style 1] for zinc-coated hex nuts (shown in drawing) and ANSI B18.2.2 [ANSI B18.2.4.6M] for heavy hex corrosion-resistant nuts (not shown in drawing). Material for zinc-coated nuts shall conform to the requirements of AASHTO M 291 (ASTM A 563) Grade A [AASHTO M 291M (ASTM A 563M) Class 5], and material for corrosion-resistant nuts shall conform to the requirements of AASHTO M 291 (ASTM A 563) Grade C3 [AASHTO M 291M (ASTM A 563M) Class 8S3].

When zinc-coated bolts and nuts are required, the coating shall conform to either AASHTO M 232 (ASTM A 153/A 153M) for Class C or AASHTO M 298 (ASTM B 695) for Class 50. Zinc-coated nuts shall be tapped over-size as specified in AASHTO M 291 (ASTM A 563) [AASHTO M 291M (ASTM A 563M)], except that a diametrical allowance of 0.020 inch [0.510 mm] shall be used instead of 0.016 inches [0.420 mm].

Designator	Stress Area of Threaded Bolt Shank (in ² [mm ²])	Min. Bolt Tensile Strength (kips [kN])
FBB01-05	0.226 [157.0]	13.6 [62.8]

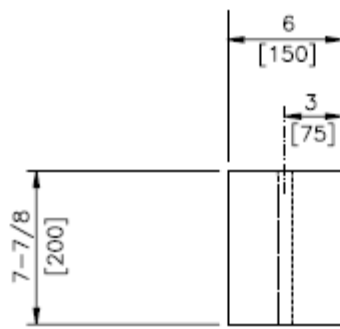
Dimensional tolerances not shown or implied are intended to be those consistent with the proper functioning of the part, including its appearance and accepted manufacturing practices.

INTENDED USE

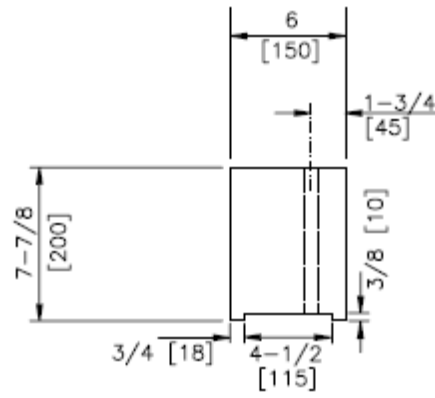
These bolts and nuts are used in numerous guardrail and median barrier designs.

GUARDRAIL BOLT AND RECESSED NUT

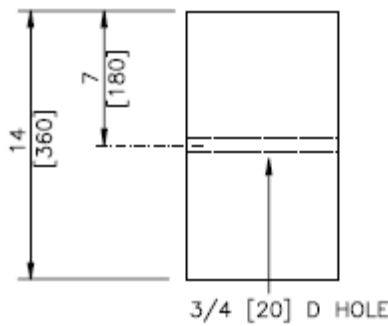
FBB01-05		
SHEET NO.	DATE	
2 of 2	5/2/2018	



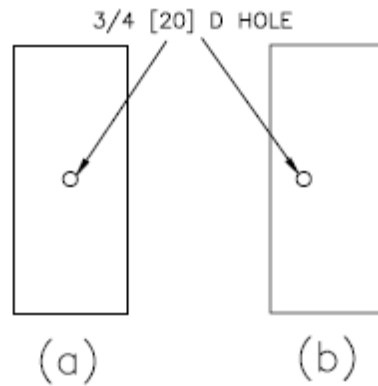
PLAN (a)



PLAN (b)



SIDE



FRONT

1994

W-BEAM TIMBER BLOCKOUT

PDB01a-b

SHEET NO.	DATE:
1 of 2	6/30/2005

SPECIFICATIONS

Blockouts shall be made of timber with a stress grade of at least 1160 psi [8 MPa]. Grading shall be in accordance with the rules of the West Coast Lumber Inspection Bureau, Southern Pine Inspection Bureau, or other appropriate timber association. Timber for blockouts shall be either rough-sawn (unplaned) or S4S (surfaced four sides) with nominal dimensions indicated. The variation in size of blockouts in the direction parallel to the axis of the bolt holes shall not be more than $\pm \frac{1}{4}$ inch [6 mm]. Only one type of surface finish shall be used for posts and blockouts in any one continuous length of guardrail.

All timber shall receive a preservation treatment in accordance with AASHTO M 133 after all end cuts are made and holes are drilled.

Dimensional tolerances not shown or implied are intended to be those consistent with the proper functioning of the part, including its appearance and accepted manufacturing practices.

INTENDED USE

Blockout PDB01a is used with wood post PDE01 or PDE02 in the SGR04b strong-post W-beam guardrail and the SGM04b median barrier. Blockout PDB01b is routed to be used with steel post PWE01 or PWE02 in the SGR04c guardrail and the SGM04a median barrier.

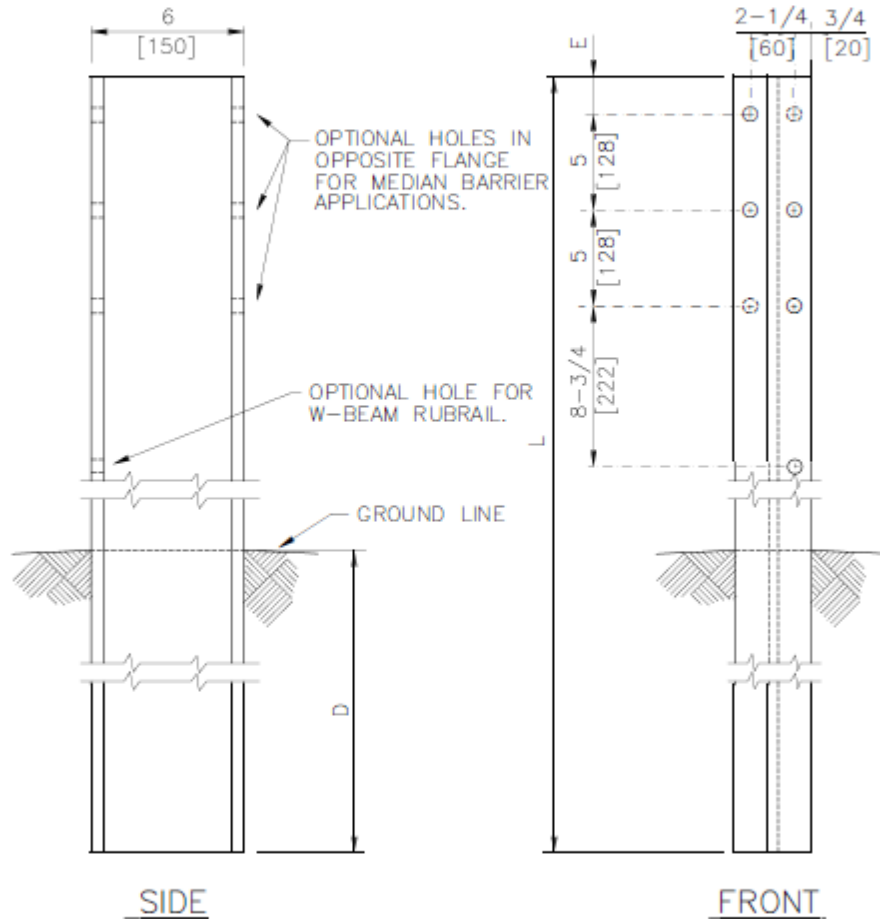
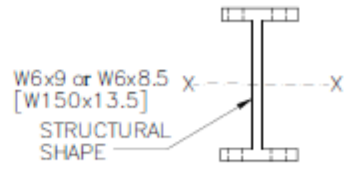
W-BEAM TIMBER BLOCKOUT

PDB01a-b

SHEET NO.	DATE
2 of 2	7/06/2005

DESIGNATOR	L	D	E
PWE01	72 [1830]	43-1/4 [1100]	2 [52]
PWE02	78 [1980]	49-1/4 [1250]	2 [52]
PWE03	78 [1980]	45-3/8 [1153]	5-7/8 [149]
PWE04	81 [2060]	46-1/8 [1173]	5-7/8 [149]

NOTE: ALL HOLES ARE 3/4 [20] D.



1994

WIDE-FLANGE GUARDRAIL POST

PWE01-04

SHEET NO.	DATE:
1 of 2	7/27/2005

SPECIFICATIONS

W-beam and thrie-beam guardrail posts shall be manufactured using AASHTO M 270 / M 270M (ASTM A 709 / A 709M) Grade 36 [250] steel unless corrosion-resistant steel is required, in which case the post shall be manufactured from AASHTO M 270 / M 270M (ASTM A 709 / A 709M) Grade 50W [345W] steel. The dimensions of the cross-section shall conform to a W6x9 [W150x13.5] section as defined in AASHTO M 160 / M 160M (ASTM A 6 / A 6M). [W150x12.6] wide flange posts are an acceptable alternative that is considered equivalent to the [W150x13.5].

After the section is cut and all holes are drilled or punched, the component should be zinc-coated according to AASHTO M 111 (ASTM A 123) unless corrosion-resistant steel is used. When corrosion-resistant steel is used, the portion of the post to be embedded in soil shall be zinc-coated according to AASHTO M 111 (ASTM A 123) and the portion above the soil shall not be zinc-coated, painted or otherwise treated.

Designator	Area in ² [10 ³ mm ²]	I _x in ⁴ [10 ⁶ mm ⁴]	I _y in ⁴ [10 ⁶ mm ⁴]	S _x in ³ [10 ³ mm ³]	S _y in ³ [10 ³ mm ³]
PWE01-04	2.63 [1.7]	16.43 [6.84]	2.19 [0.91]	5.57 [91.2]	1.11 [18.2]

Dimensional tolerances not shown or implied are intended to be those consistent with the proper functioning of the part, including its appearance and accepted manufacturing practices.

INTENDED USE

Posts PWE01 and PWE02 are used with the SGR04a and SGR04c guardrails and the SGM04a median barrier. Blockouts like PWB01 (steel) or PDB01 (wood) are attached to each post.

Post PWE03 is used with the SGR09a guardrail and the SGM09a median barrier. Wood or plastic blockouts like the PWB02 are attached to each post with FBB03 bolts and FWC16a washers under the nuts.

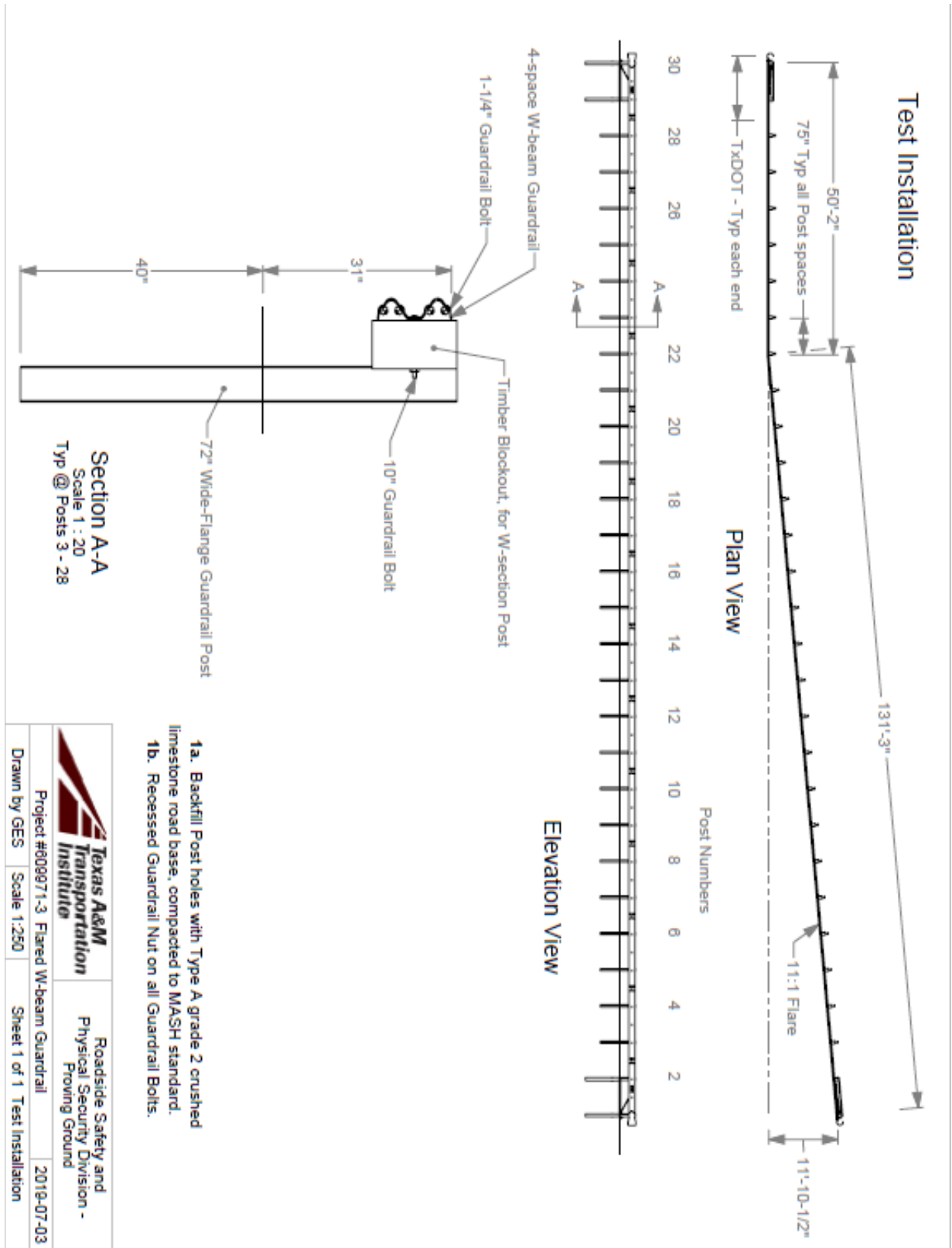
Post PWE04 is used with the SGR09b guardrail and the SGM09b median barrier. A modified steel blockout PWB03 is attached to each post with at least two 1.5-inch [40 mm] long FBX16a bolts and nuts.

WIDE-FLANGE GUARDRAIL POST

PWE01-04

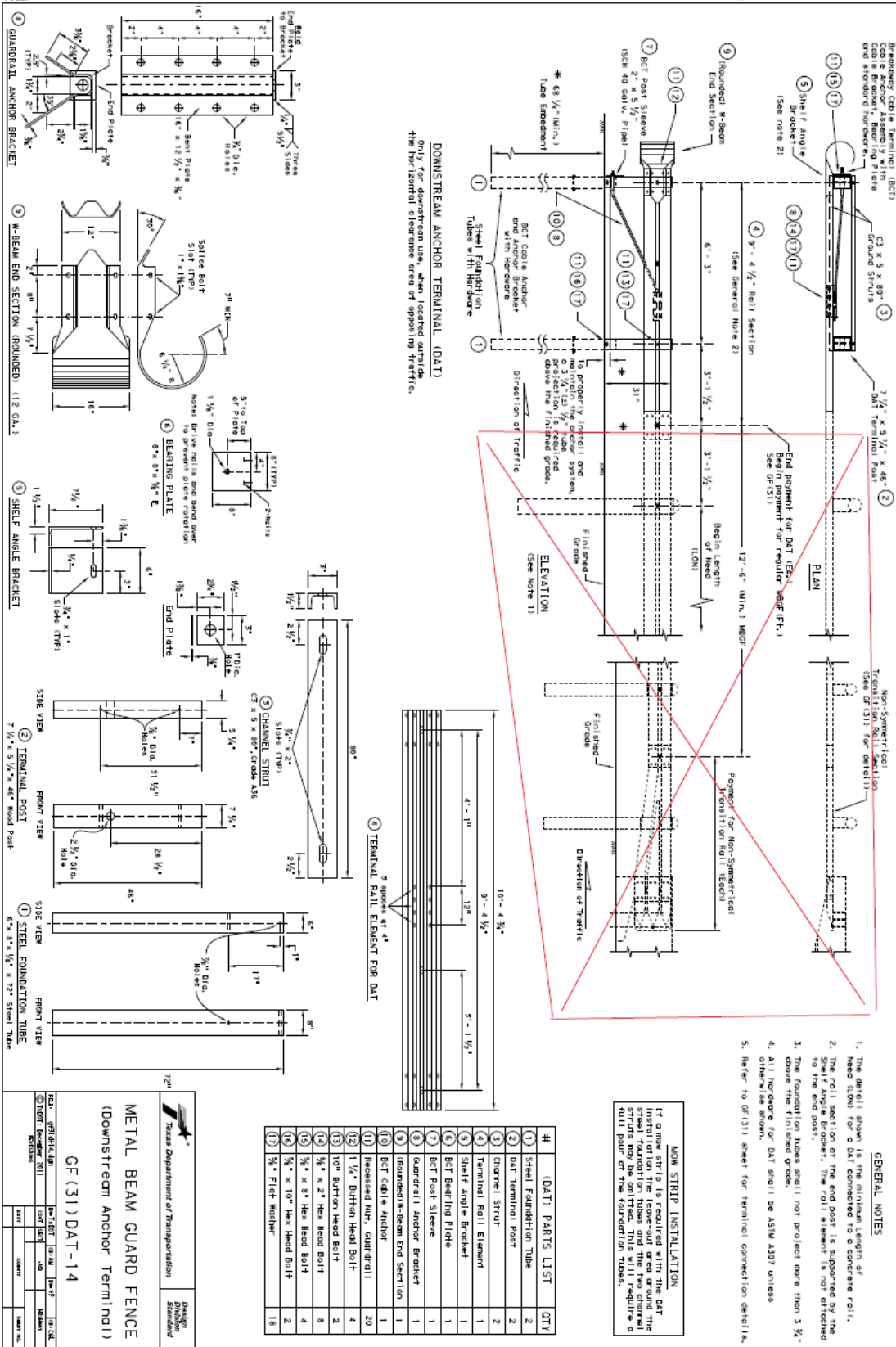
SHEET NO.	DATE
2 of 2	7/06/2005

A.2. 6099971-03-1 DRAWINGS

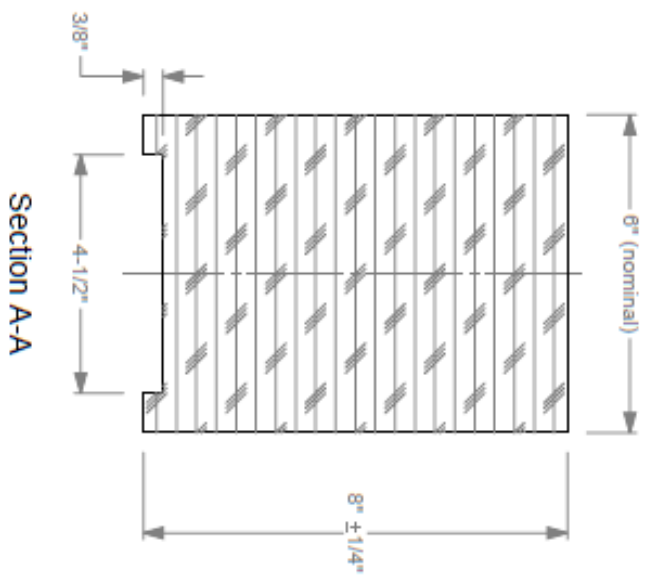
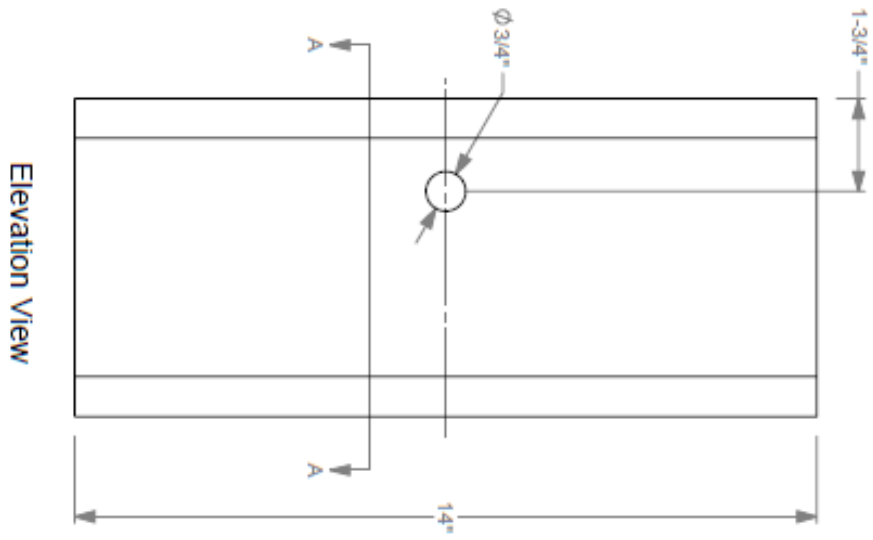


The use of this standard is governed by the "Texas Engineering Practice Act". No warranty of any kind is made by TxDOT for any purpose whatsoever. TxDOT disclaims responsibility for the conversion of this standard to other formats or for incorrect results or damage resulting from its use.

DATE
FILED

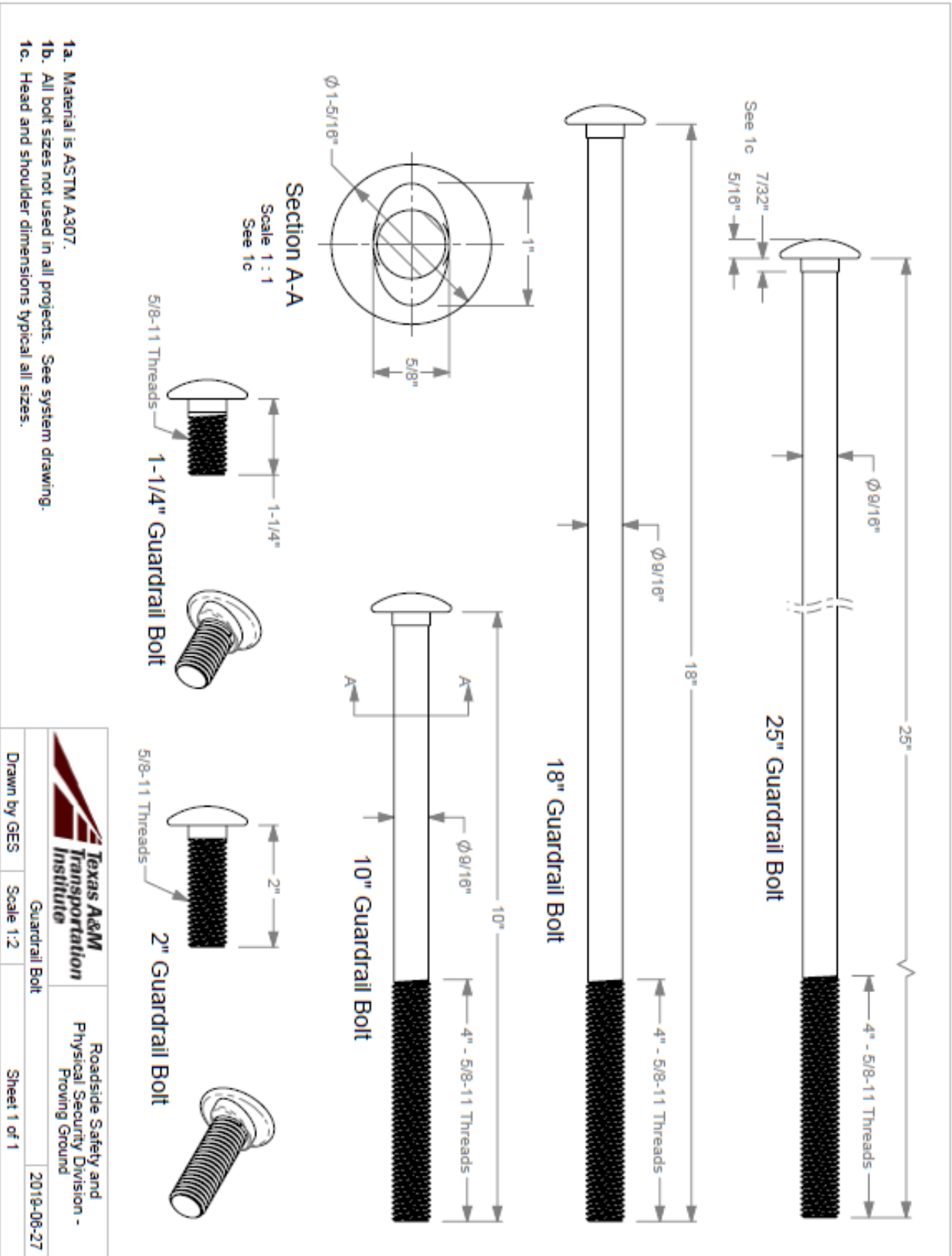


Timber Blockout for W-section Post

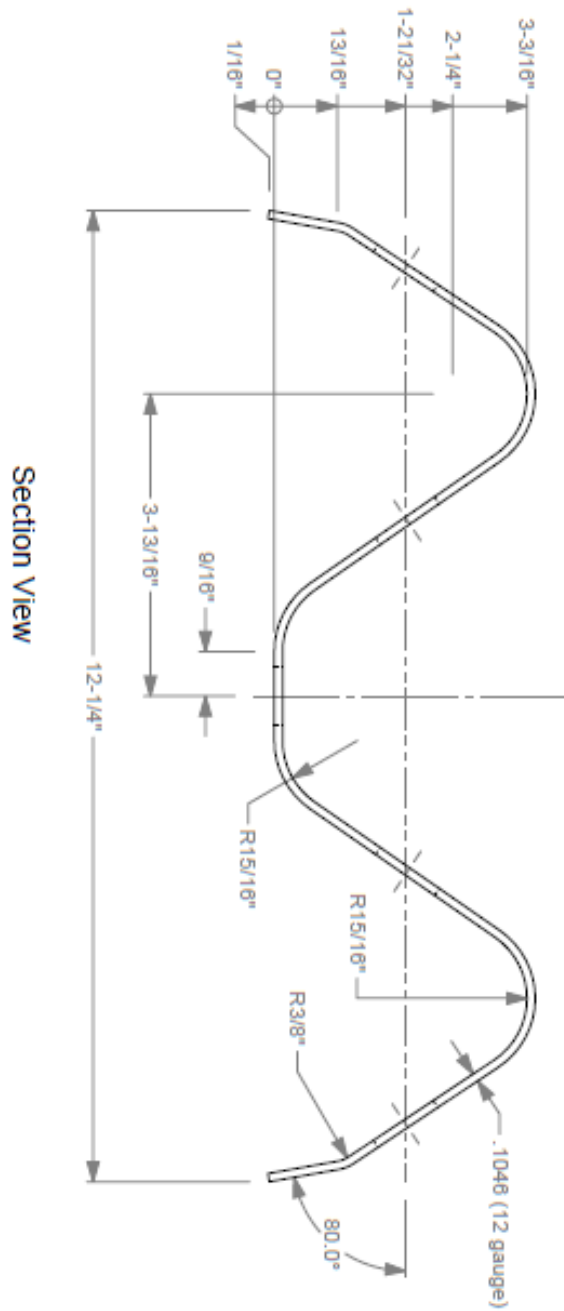
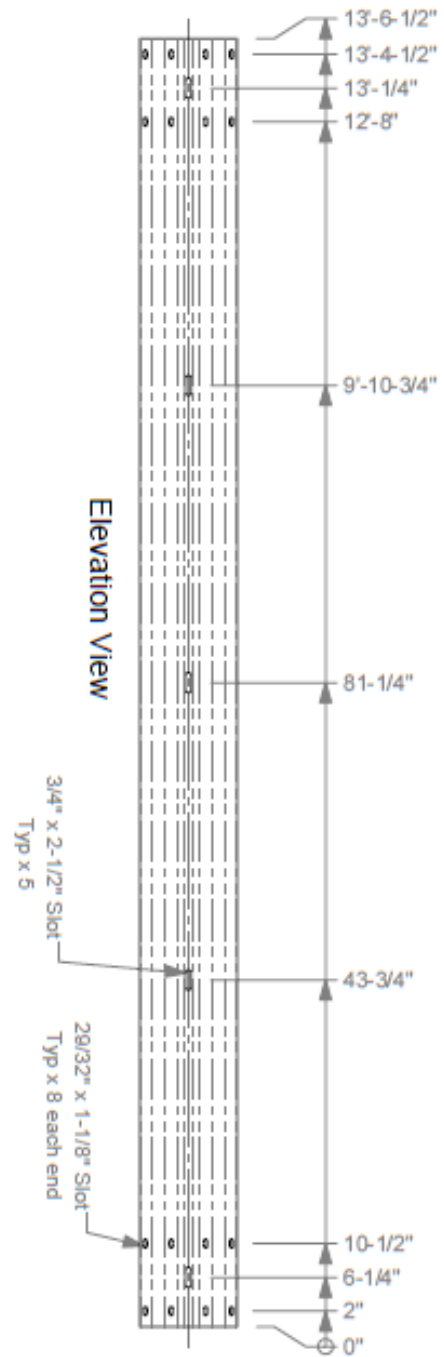


1a. Timber blockouts are treated with a preservative in accordance with AASHTO M 133 after all cutting and drilling.

	Texas A&M Transportation Institute	Roadside Safety and Physical Security Division - Proving Ground
	Timber Blockout, for W-section Post	2019-07-03
Drawn by GES	Scale 1:3	Sheet 1 of 1

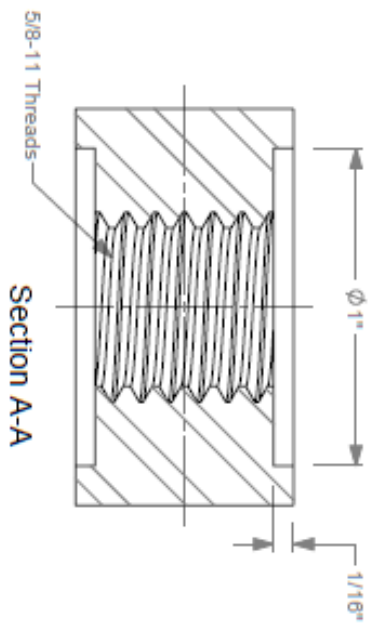
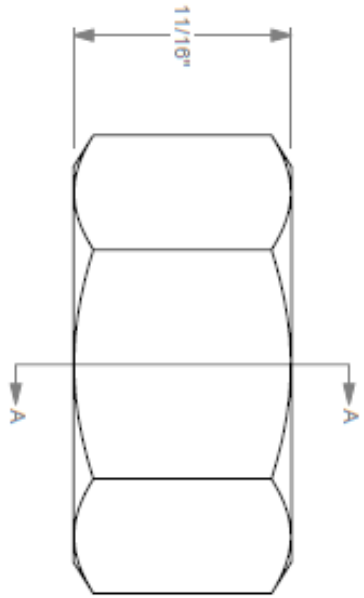
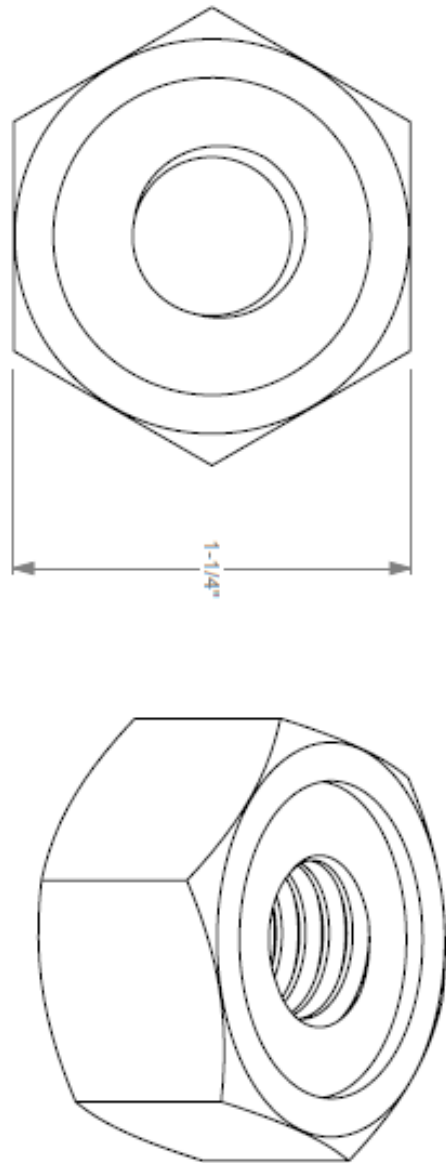


	Roadside Safety and Physical Security Division - Proving Ground
Drawn by GES	Scale 1:2
Sheet 1 of 1	2019-06-27



 <p>Texas A&M Transportation Institute</p>	<p>Roadside Safety and Physical Security Division - Proving Ground</p>
<p>Drawn by GES</p>	<p>Scale 1:20</p>
<p>Sheet 1 of 1</p>	<p>2019-06-26</p>

Recessed Guardrail Nut



1a. Material is ASTM A 563 Grade A.



Roadside Safety and
Physical Security Division -
Proving Ground

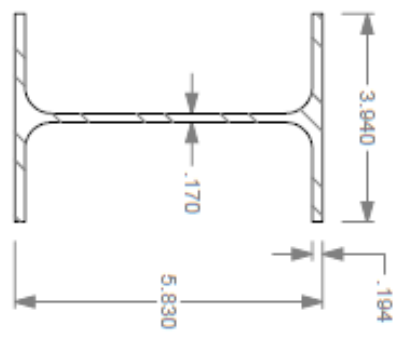
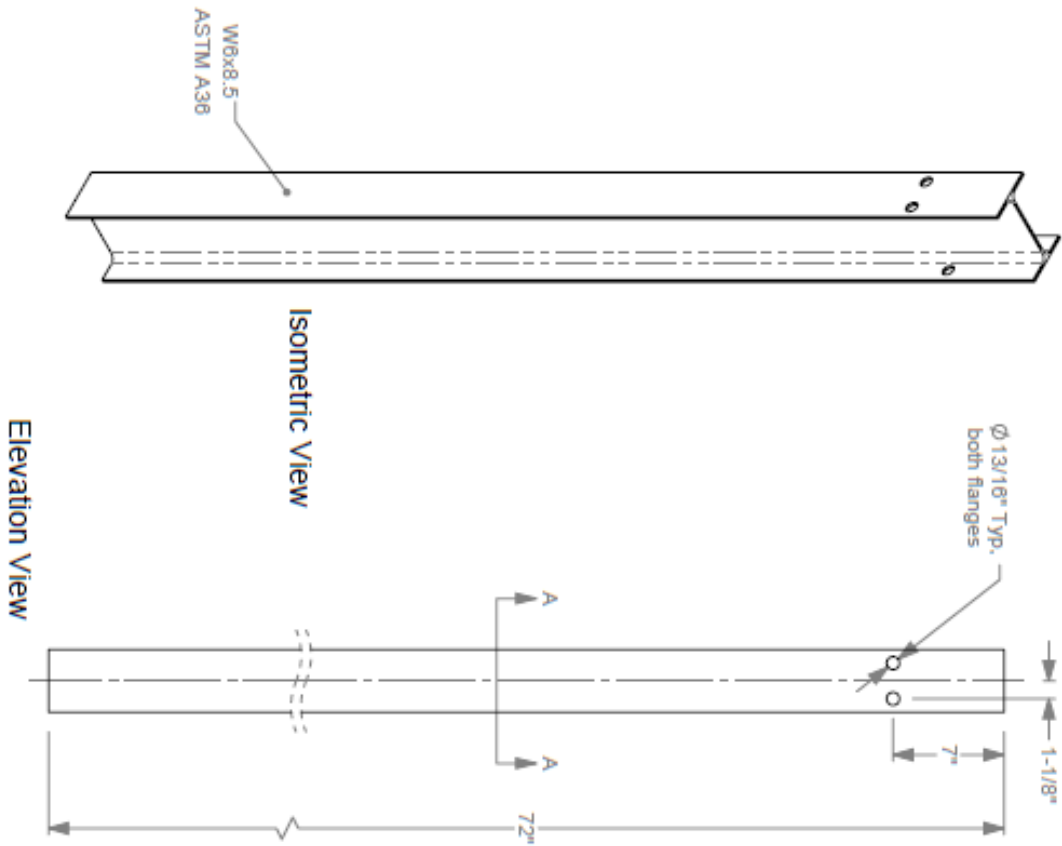
Drawn by GES

Scale 2:1

Sheet 1 of 1

2019-06-27

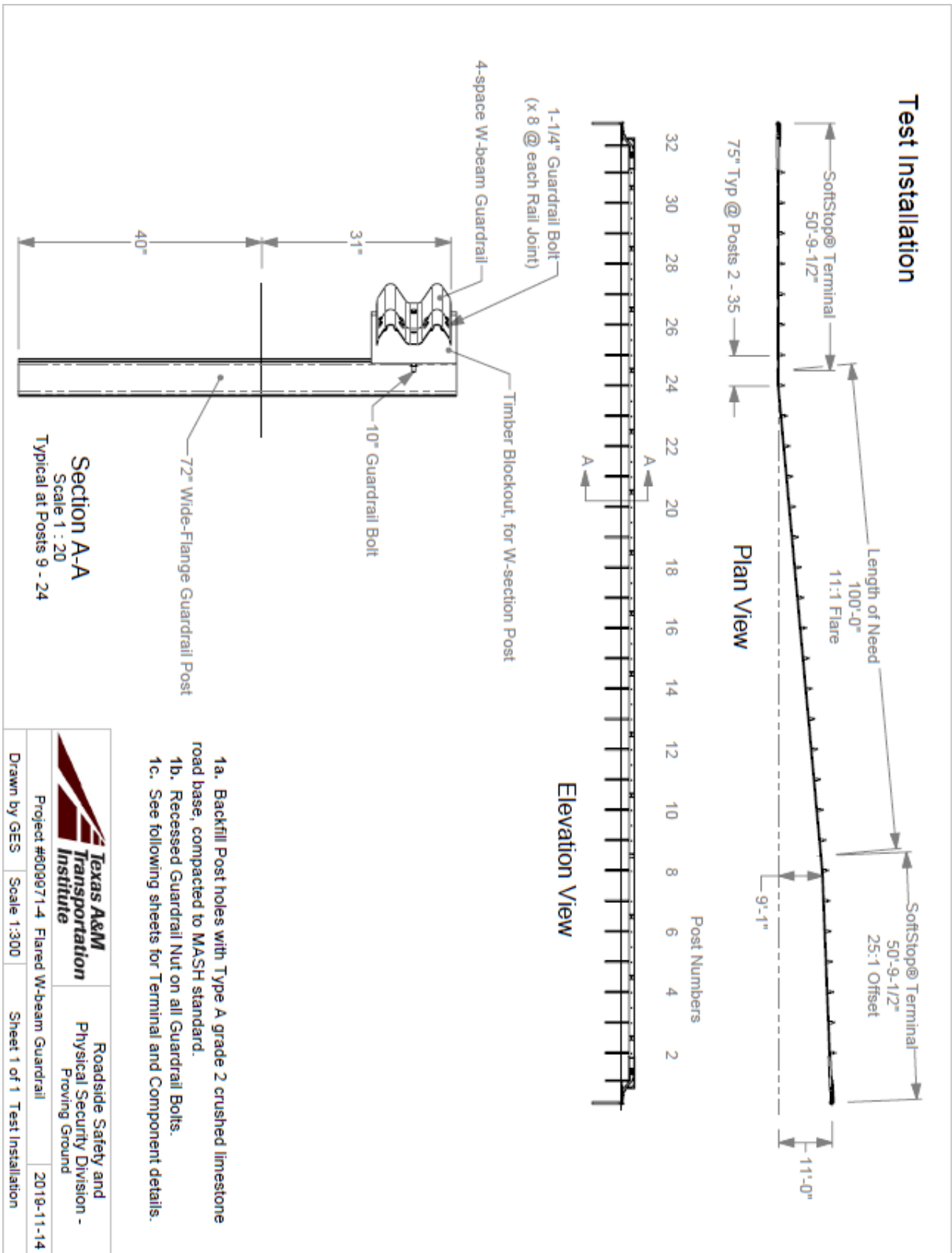
72" Wide Flange Guardrail Post

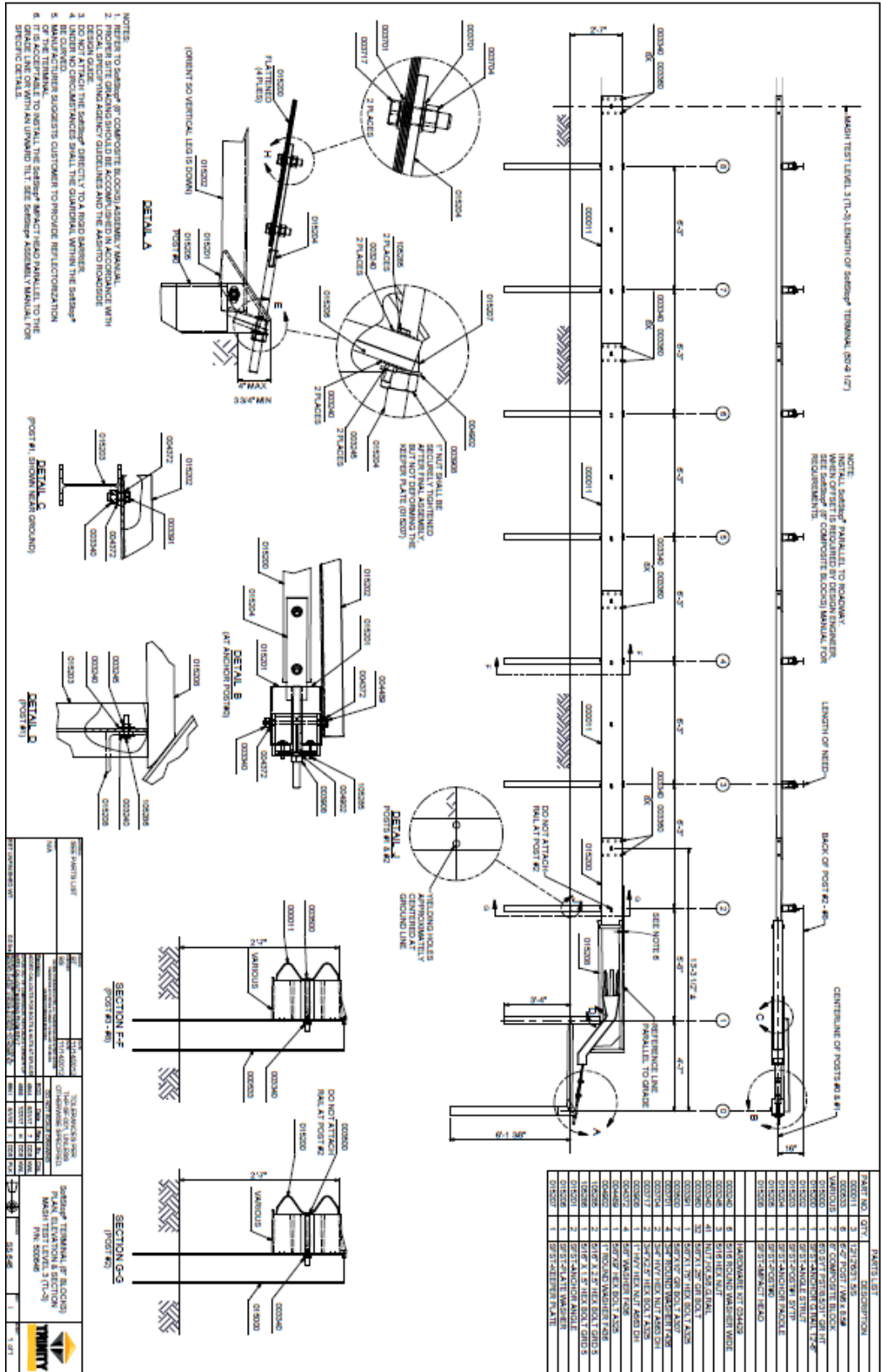


Section A-A
Scale 1 : 3

	Roadside Safety and Physical Security Division - Proving Ground	72" Wide-Flange Guardrail Post	2019-07-01
		Drawn by GES Scale 1:10	Sheet 1 of 1

A.3. 6099971-03-2 DRAWINGS





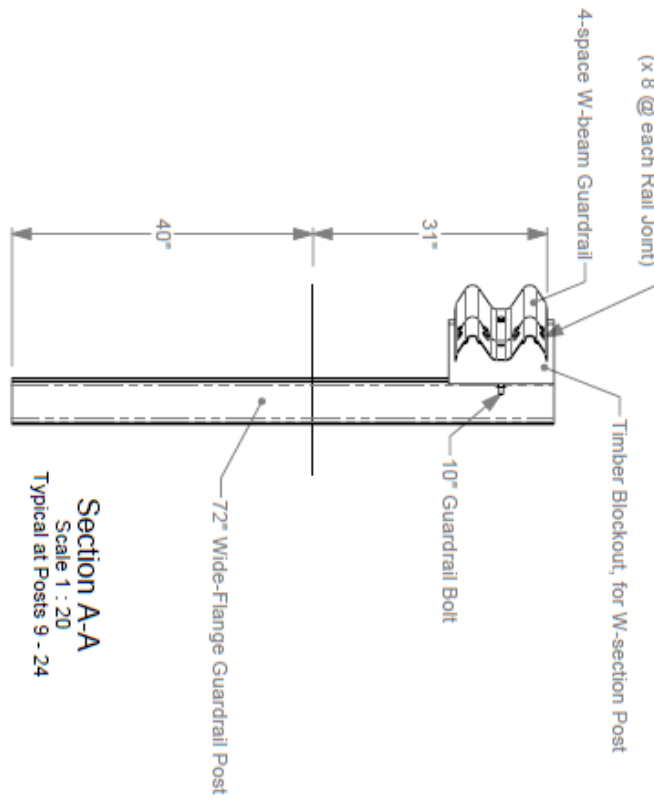
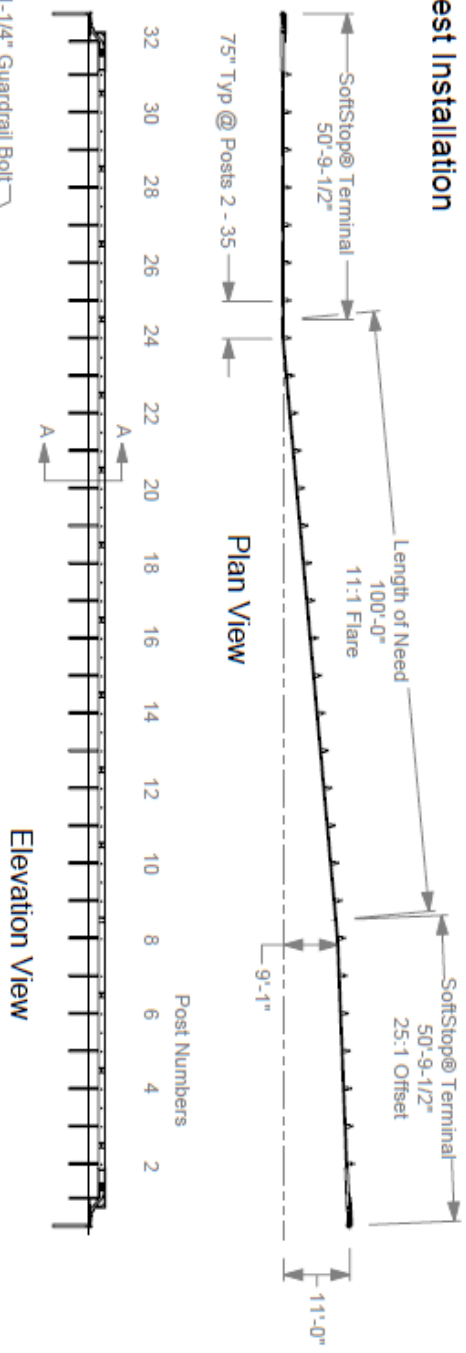
- NOTES
1. REFER TO BARRIER OR COMPOSITE BLOCK ASSEMBLY MANUAL.
 2. PROPER SITE GRADING SHOULD BE ACCOMPLISHED IN ACCORDANCE WITH LOCAL SPECIFIC AGENCY GUIDELINES AND THE ASHRAE HANDBOOK.
 3. DO NOT ATTACH THE BARRIER DIRECTLY TO A ROAD SURFACE.
 4. UNDER NO CIRCUMSTANCES SHALL THE GUARDRAIL WITHIN THE BARRIER BE ATTACHED TO THE ROAD SURFACE.
 5. MANUFACTURER SUGGESTS CUSTOMER TO PROVIDE REFLECTORIZATIONS OF THE TERMINAL TO RETAIL THE BARRIER IMPACT HEAD PARALLEL TO THE GRADE LINE OR WITH AN UPWARD TILT. SEE BARRIER ASSEMBLY MANUAL FOR SPECIFIC DETAIL.

NOTE: INITIAL BARRIER PARALLEL TO ROADWAY. SEE BARRIER OR COMPOSITE BLOCK MANUAL FOR REQUIREMENTS.

PARTS LIST

PART NO.	QTY.	DESCRIPTION
00001	1	POST #1-4
00002	1	POST #5-8
00003	1	POST #1-4 NUT & WASHER
00004	1	POST #5-8 NUT & WASHER
00005	1	POST #1-4 WASHER
00006	1	POST #5-8 WASHER
00007	1	POST #1-4 LOCK WASHER
00008	1	POST #5-8 LOCK WASHER
00009	1	POST #1-4 WASHER
00010	1	POST #5-8 WASHER
00011	1	POST #1-4 WASHER
00012	1	POST #5-8 WASHER
00013	1	POST #1-4 WASHER
00014	1	POST #5-8 WASHER
00015	1	POST #1-4 WASHER
00016	1	POST #5-8 WASHER
00017	1	POST #1-4 WASHER
00018	1	POST #5-8 WASHER
00019	1	POST #1-4 WASHER
00020	1	POST #5-8 WASHER
00021	1	POST #1-4 WASHER
00022	1	POST #5-8 WASHER
00023	1	POST #1-4 WASHER
00024	1	POST #5-8 WASHER
00025	1	POST #1-4 WASHER
00026	1	POST #5-8 WASHER
00027	1	POST #1-4 WASHER
00028	1	POST #5-8 WASHER
00029	1	POST #1-4 WASHER
00030	1	POST #5-8 WASHER
00031	1	POST #1-4 WASHER
00032	1	POST #5-8 WASHER
00033	1	POST #1-4 WASHER
00034	1	POST #5-8 WASHER
00035	1	POST #1-4 WASHER
00036	1	POST #5-8 WASHER
00037	1	POST #1-4 WASHER
00038	1	POST #5-8 WASHER
00039	1	POST #1-4 WASHER
00040	1	POST #5-8 WASHER
00041	1	POST #1-4 WASHER
00042	1	POST #5-8 WASHER
00043	1	POST #1-4 WASHER
00044	1	POST #5-8 WASHER
00045	1	POST #1-4 WASHER
00046	1	POST #5-8 WASHER
00047	1	POST #1-4 WASHER
00048	1	POST #5-8 WASHER
00049	1	POST #1-4 WASHER
00050	1	POST #5-8 WASHER
00051	1	POST #1-4 WASHER
00052	1	POST #5-8 WASHER
00053	1	POST #1-4 WASHER
00054	1	POST #5-8 WASHER
00055	1	POST #1-4 WASHER
00056	1	POST #5-8 WASHER
00057	1	POST #1-4 WASHER
00058	1	POST #5-8 WASHER
00059	1	POST #1-4 WASHER
00060	1	POST #5-8 WASHER
00061	1	POST #1-4 WASHER
00062	1	POST #5-8 WASHER
00063	1	POST #1-4 WASHER
00064	1	POST #5-8 WASHER
00065	1	POST #1-4 WASHER
00066	1	POST #5-8 WASHER
00067	1	POST #1-4 WASHER
00068	1	POST #5-8 WASHER
00069	1	POST #1-4 WASHER
00070	1	POST #5-8 WASHER
00071	1	POST #1-4 WASHER
00072	1	POST #5-8 WASHER
00073	1	POST #1-4 WASHER
00074	1	POST #5-8 WASHER
00075	1	POST #1-4 WASHER
00076	1	POST #5-8 WASHER
00077	1	POST #1-4 WASHER
00078	1	POST #5-8 WASHER
00079	1	POST #1-4 WASHER
00080	1	POST #5-8 WASHER
00081	1	POST #1-4 WASHER
00082	1	POST #5-8 WASHER
00083	1	POST #1-4 WASHER
00084	1	POST #5-8 WASHER
00085	1	POST #1-4 WASHER
00086	1	POST #5-8 WASHER
00087	1	POST #1-4 WASHER
00088	1	POST #5-8 WASHER
00089	1	POST #1-4 WASHER
00090	1	POST #5-8 WASHER
00091	1	POST #1-4 WASHER
00092	1	POST #5-8 WASHER
00093	1	POST #1-4 WASHER
00094	1	POST #5-8 WASHER
00095	1	POST #1-4 WASHER
00096	1	POST #5-8 WASHER
00097	1	POST #1-4 WASHER
00098	1	POST #5-8 WASHER
00099	1	POST #1-4 WASHER
00100	1	POST #5-8 WASHER

Test Installation

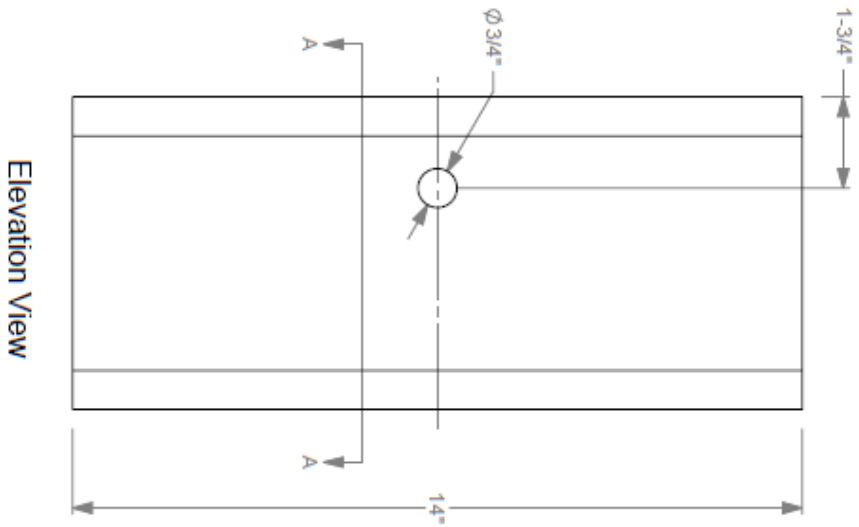


Section A-A
Scale 1 : 20
Typical at Posts 9 - 24

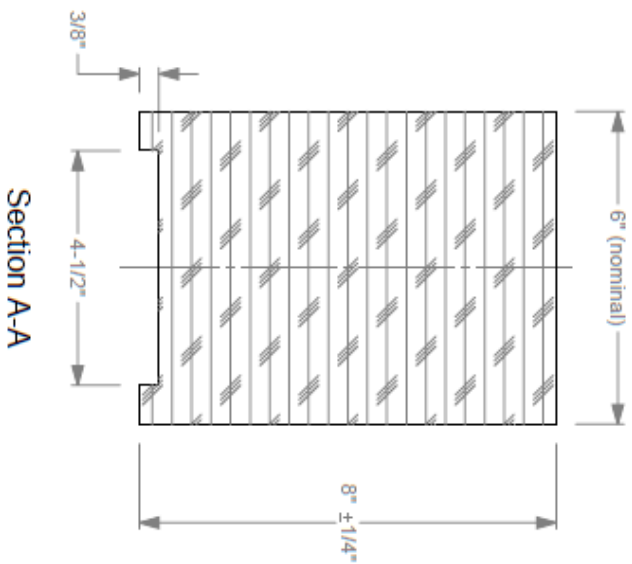
- 1a. Backfill Post holes with Type A grade 2 crushed limestone road base, compacted to MASH standard.
- 1b. Recessed Guardrail Nut on all Guardrail Bolts.
- 1c. See following sheets for Terminal and Component details.

	Roadside Safety and Physical Security Division - Proving Ground	
	Project #009971-4 Flared W-beam Guardrail	2019-11-14
Drawn by GES	Scale 1:300	Sheet 1 of 1 Test Installation

Timber Blockout for W-section Post



Elevation View

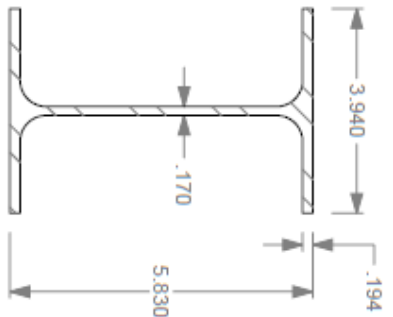
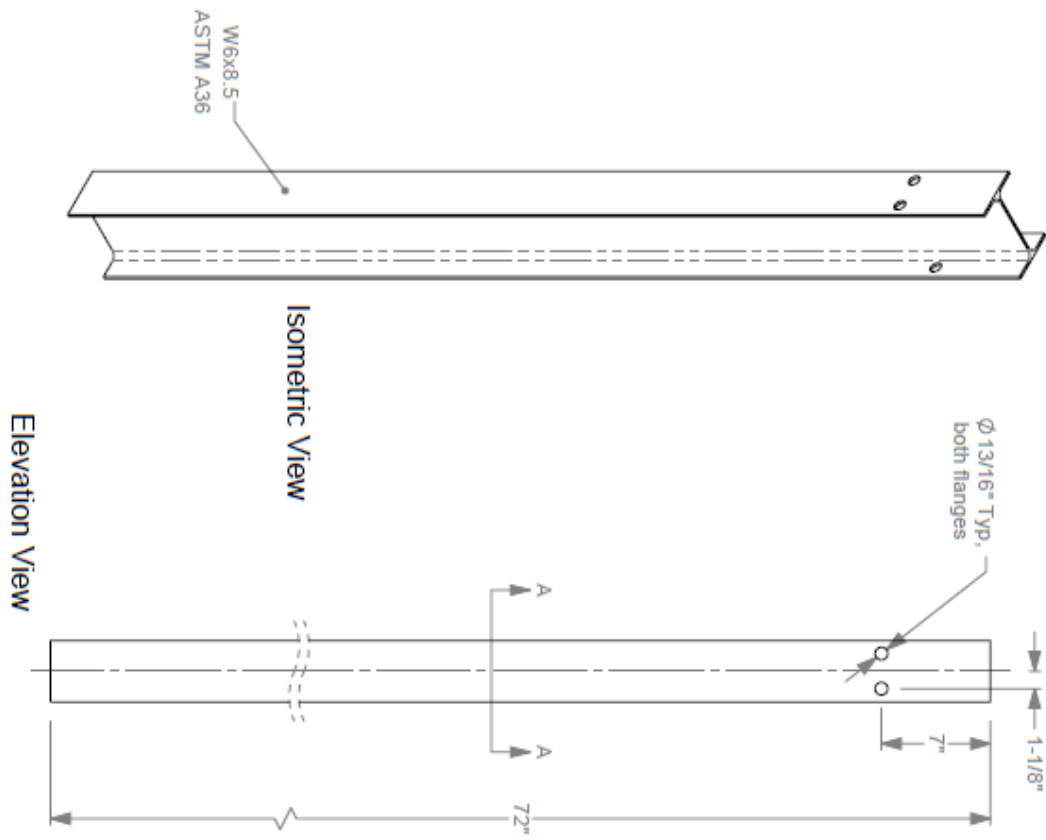


Section A-A

1a. Timber blockouts are treated with a preservative in accordance with AASHTO M 133 after all cutting and drilling.

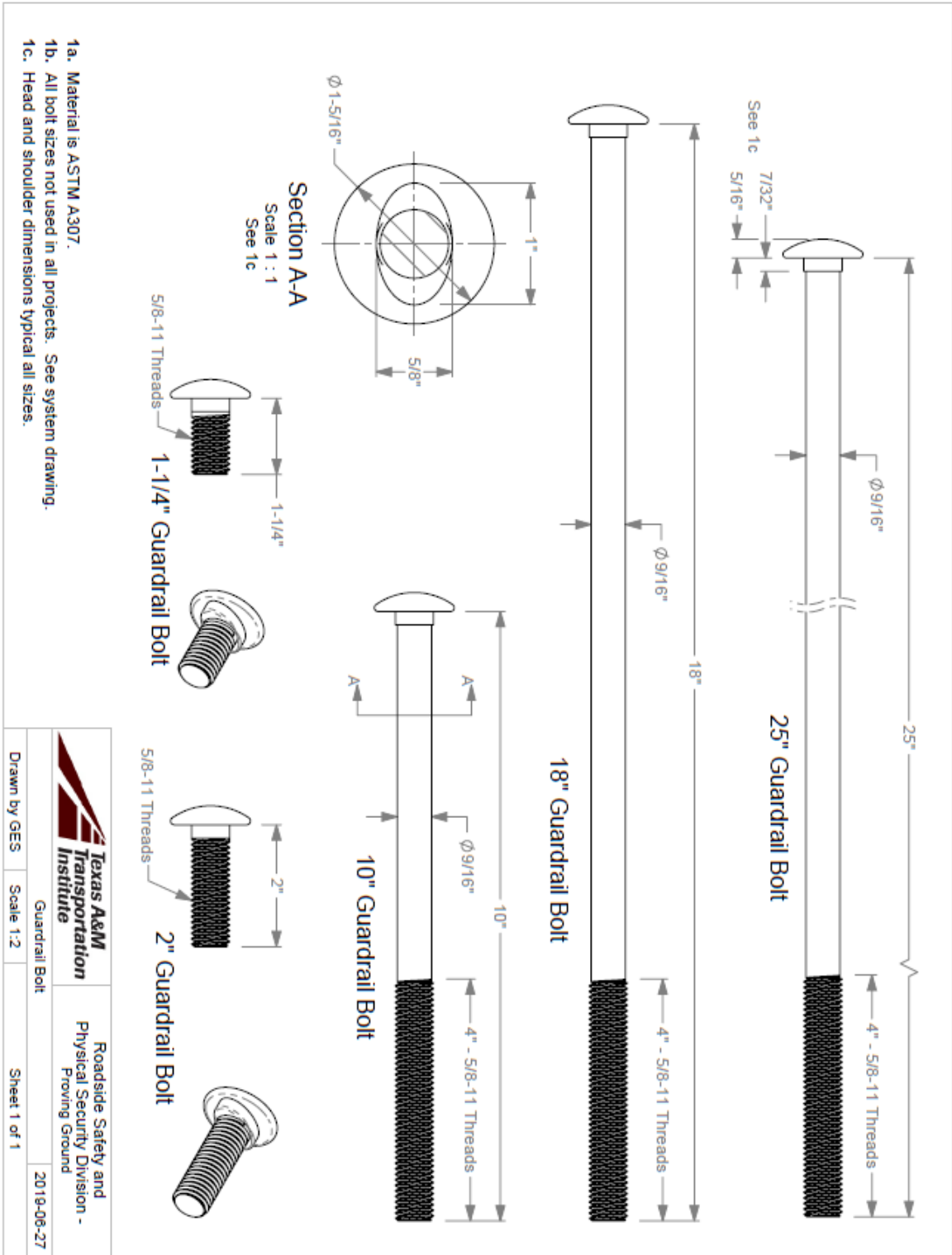
	Roadside Safety and Physical Security Division - Proving Ground	
	Timber Blockout, for W-section Post	Sheet 1 of 1
Drawn by GES	Scale 1:3	2019-07-03

Standard Wide-Flange Guardrail Post



Section A-A
Scale 1 : 3

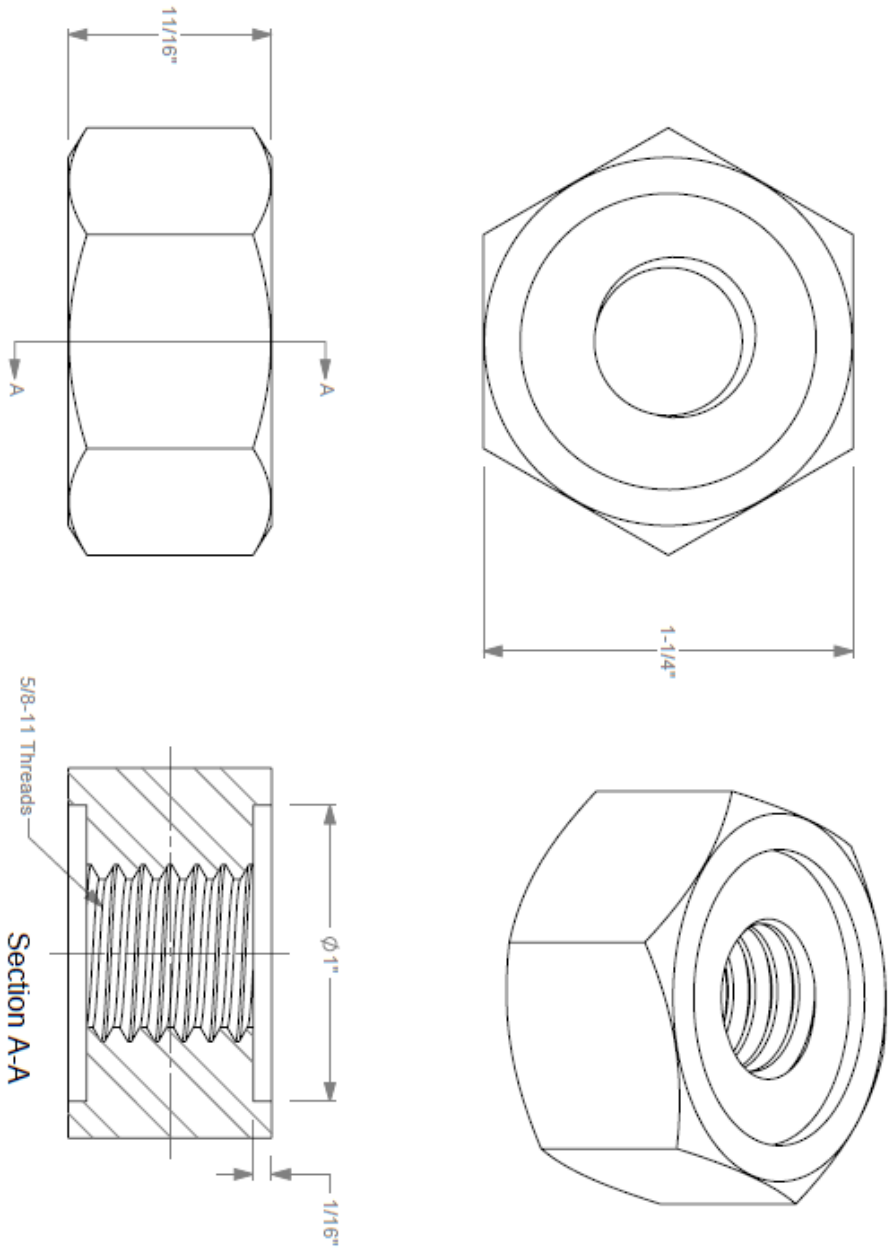
	Roadside Safety and Physical Security Division - Proving Ground
	Standard Wide-Flange Guardrail Post
Drawn by GES	Scale 1:10
	Sheet 1 of 1
	2019-08-28



- 1a. Material is ASTM A307.
- 1b. All bolt sizes not used in all projects. See system drawing.
- 1c. Head and shoulder dimensions typical all sizes.

	Roadsides Safety and Physical Security Division - Proving Ground
Drawn by GES	Scale 1:2
Sheet 1 of 1	2019-06-27

Recessed Guardrail Nut



1a. Material is ASTM A 563 Grade A.

	Roadside Safety and Physical Security Division - Proving Ground		
		Recessed Guardrail Nut	
Drawn by GES	Scale 2:1	Sheet 1 of 1	2019-06-27

APPENDIX B. SUPPORTING CERTIFICATION DOCUMENTS

Certified Analysis



Trinity Highway Products LLC
 2548 N.E. 28th St.
 Ft Worth (THP), TX 76111 Phn:(817) 665-1499

Order Number: 1309704 Prod Ln Grp: 3-Guardrail (Dom)

Customer PO: 609971 - ALASKA

As of: 5/8/19

Customer: SAMPLES, TESTING MATERIALS

BOL Number: 76112

Ship Date:

2525 STEMMONS FRWY

Document #: 1

Shipped To: TX

DALLAS, TX 75207

Use State: TX



Project: ALASKA DOT PROJECT #609971

Qty	Part #	Description	Spec	CL	TY	Heat Code/Heat	Yield	TS	Eig	C	Mn	P	S	Si	Cu	Cr	Vn	ACW	
40	11G	12/126/31.5/S	M-180	A	2	FT1819	60,900	82,100	26.0	0.210	0.750	0.008	0.002	0.030	0.090	0.004	0.040	0.002	4
			M-180	A	2	1191763	53,000	80,800	20.0	0.220	0.810	0.009	0.002	0.030	0.100	0.004	0.050	0.003	4
			M-180	A	2	1191766	53,800	78,100	30.0	0.210	0.770	0.009	0.002	0.030	0.090	0.000	0.040	0.002	4
			M-180	A	2	1292230	62,600	84,100	22.0	0.220	0.760	0.007	0.002	0.020	0.090	0.000	0.040	0.002	4
			M-180	B	2	235485	58,920	78,610	25.6	0.190	0.730	0.010	0.005	0.010	0.110	0.000	0.060	0.001	4
			A-36			55060347	60,200	76,500	27.5	0.130	0.860	0.014	0.017	0.190	0.310	0.009	0.140	0.001	4
12	724G	6/0 TUBE SIL/125X8X6	A-500			A92132	55,160	74,134	27.0	0.200	0.470	0.010	0.003	0.040	0.080	0.000	0.050	0.001	4
6	830G	12/BUFFER/ROLLED	M-180	A	2	31847970	48,400	62,300	35.0	0.060	0.450	0.015	0.001	0.030	0.090	0.001	0.070	0.002	4
6	3000G	CBL 3/4X6/6/DRL	HW			132915													
405	3340G	5/8" GR HEX NUT	HW			19-42-014													
320	3360G	5/8"x1.25" GR BOLT	HW			20190107811													
85	3500G	5/8"x1.0" GR BOLT A307	HW			31732-B													
85	4076B	WD BLK RTD 6X8X14	HW			174													
12	4140B	WD 4/0.25 POST 5.5X7.5	HW			197													
12	19481G	C3X5#X6"-8" RUBRAL	A-36			3086788	56,100	76,200	31.0	0.170	0.650	0.014	0.033	0.210	0.360	0.015	0.090	0.000	4
6	20207G	12/9/4.5/8-HOLE ANCHS	RHC	A	2	L14818	61,710	79,460	28.7	0.180	0.720	0.012	0.005	0.020	0.120	0.000	0.070	0.002	4

Certified Analysis



Trinity Highway Products LLC
2548 N.E. 28th St.

Order Number: 1309704 Prod Ln Grp: 3-Guardrail (Dom)

Ft Worth (THP), TX 76111 Phn:(817) 665-1499

As of: 5/8/19

Customer: SAMPLES, TESTING MATERIALS

Customer PO: 609971 - ALASKA

Shipped To: TX

2525 STEMMONS FRWY

Document #: 1

DALLAS, TX 75207

Use State: TX



Project: ALASKA DOT PROJECT #609971

Qty	Part #	Description	Spec	CL	TY	Heat Code/Heat	Yield	TS	Eig	C	Mn	P	S	SI	Cu	CB	Cr	Vn	ACW
	M-180		M-180	A	2	233123	63,570	82,430	22.7	0.190	0.720	0.013	0.004	0.020	0.110	0.000	0.070	0.000	4
	M-180		M-180	A	2	233124	62,720	82,150	24.5	0.190	0.720	0.011	0.003	0.010	0.130	0.001	0.060	0.000	4
	M-180		M-180	A	2	233125	63,900	83,490	21.4	0.200	0.730	0.018	0.004	0.020	0.110	0.000	0.090	0.001	4
	M-180		M-180	A	2	A90778	65,800	86,800	20.7	0.210	0.680	0.012	0.003	0.030	0.120	0.000	0.070	0.001	4
	M-180		M-180	A	2	A90779	55,100	78,200	20.6	0.190	0.660	0.010	0.002	0.020	0.120	0.000	0.070	0.001	4
	M-180		M-180	A	2	C88581	59,000	79,100	16.3	0.210	0.690	0.009	0.002	0.030	0.110	0.000	0.060	0.001	4
	M-180		M-180	A	2	C88582	63,500	82,200	23.6	0.200	0.710	0.011	0.001	0.040	0.090	0.000	0.060	0.001	4
6	36120A	DAT-31-TX-HDW-CAN	M-180	A	2	4174233	48,700	68,700	34.0	0.200	0.400	0.011	0.010	0.010	0.040	0.001	0.050	0.001	4
	A-500		A-500			A809937	61,500	67,000	31.0	0.060	0.330	0.011	0.003	0.020	0.090	0.003	0.050	0.001	4
	36120A		HW			P38498 R70030-02													
	36120A		HW			19-42-014													
	36120A		HW			20190107811													
	36120A		HW			848773-8													
	36120A		HW			31732-B													
	36120A		HW			P38729 R71181-01													
	36120A		HW			P38562 R70589-01													
	36120A		HW			31654													
	36120A		HW			31433													

Certified Analysis



Trinity Highway Products LLC

2548 N.E. 28th St.

Ft Worth (THP), TX 76111 Phn:(817) 665-1499

Customer: SAMPLES, TESTING MATERIALS

2525 STEMMONS FRWY

DALLAS, TX 75207

Project: ALASKA DOT PROJECT #609971

Order Number: 1309704 Prod Ln Grp: 3-Guardrail (Dom)

Customer PO: 609971 - ALASKA

BOL Number: 76112

Document #: 1

Shipped To: TX

Use State: TX

As of: 5/8/19



Qty	Part #	Description	Spec	CL	TY	Heat Code/Heat	Yield	TS	Eig	C	Mn	P	S	SI	Cu	Cr	Va	ACW	
	36120A		A-36			1058859	56,400	76,100	25.0	0.140	0.710	0.012	0.019	0.190	0.370	0.015	0.180	0.003	4
	36120A		A-36			83187C	51,500	75,000	31.0	0.200	1.000	0.014	0.003	0.013	0.040	0.003	0.060	0.000	4

Upon delivery, all materials subject to Trinity Highway Products, LLC Storage Stain Policy QMS-IG-002.

ALL STEEL USED WAS MELTED AND MANUFACTURED IN USA AND COMPLIES WITH THE BUY AMERICA ACT, 23 CFR 635.410.

ALL GUARDRAIL MEETS AASHTO M-180. ALL STRUCTURAL STEEL MEETS ASTM A36 UNLESS OTHERWISE STATED.

ALL COATINGS PROCESSES OF THE STEEL OR IRON ARE PERFORMED IN USA AND COMPLIES WITH THE "BUY AMERICA ACT", 23 CFR 635.410.

ALL GALVANIZED MATERIAL CONFORMS WITH ASTM A-123 (US DOMESTIC SHIPMENTS)

ALL GALVANIZED MATERIAL CONFORMS WITH ASTM A-123 & ISO 1461 (INTERNATIONAL SHIPMENTS)

FINISHED GOOD PART NUMBERS ENDING IN SUFFIX B.P. OR S, ARE UNCOATED

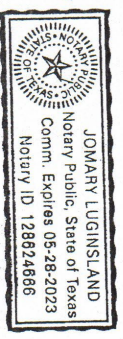
BOLTS COMPLY WITH ASTM A-307 SPECIFICATIONS AND ARE GALVANIZED IN ACCORDANCE WITH ASTM A-153, UNLESS OTHERWISE STATED.

NUTS COMPLY WITH ASTM A-563 SPECIFICATIONS AND ARE GALVANIZED IN ACCORDANCE WITH ASTM A-153, UNLESS OTHERWISE STATED.

WASHERS COMPLY WITH ASTM F-436 SPECIFICATION AND/OR F-844 AND ARE GALVANIZED IN ACCORDANCE WITH ASTM F-2329, UNLESS OTHERWISE STATED.

3/4" DIA CABLE 6X19 ZINC COATED SWAGED END AISI C-1035 STEEL, ANNEALED STUD 1" DIA ASTM 449 AASHTO M30, TYPE II BREAKING STRENGTH - 46000 LB

State of Texas, County of Tarrant. Sworn and subscribed before me this 8th day of May, 2019.



Jomary Luginsland

Notary Public:
Commission Expires:

Certified By:

Jerry Curtis

Quality Assurance

Certified Analysis



Trinity Highway Products LLC
 2548 N.E. 28th St.
 Ft Worth (THP), TX 76111 Phn:(817) 665-1499
 Customer: SAMPLES, TESTING MATERIALS
 2525 STEMMONS FRWY
 DALLAS, TX 75207
 Project: POOLED FUND PROJECT 609971

Order Number: 1319212 Prod Ln Grp: 9-End Terminals (Dom)
 Customer PO: POOLED FUND
 BOL Number: 78438
 Document #: 1
 Shipped To: TX
 Use State: TX

As of: 12/31/19



Qty	Part #	Description	Spec	CL	TY	Heat Code/Heat	Yield	TS	Elg	C	Mn	P	S	Si	Cu	Cb	Cr	Vn	ACW
16	11G	12/12/631.5/S	RHC		2	L14619													
			M-180	A	2	244186	63,390	81,850	24.5	0.190	0.730	0.008	0.002	0.020	0.110	0.001	0.050	0.002	4
			M-180	A	2	245247	63,510	82,890	24.6	0.190	0.740	0.011	0.002	0.030	0.110	0.000	0.070	0.001	4
			M-180	A	2	245248	61,270	79,830	27.8	0.190	0.720	0.010	0.005	0.020	0.100	0.000	0.060	0.002	4
			M-180	A	2	245249	61,940	82,830	26.0	0.200	0.720	0.010	0.004	0.010	0.100	0.000	0.060	0.000	4
			M-180	A	2	245250	61,610	91,910	25.4	0.190	0.740	0.010	0.004	0.010	0.110	0.000	0.070	0.002	4
			M-180	B	2	241647	56,310	76,620	29.1	0.190	0.730	0.012	0.003	0.020	0.100	0.000	0.060	0.001	4
			M-180	A	2	1297897	62,400	84,900	21.0	0.220	0.810	0.009	0.001	0.030	0.080	0.000	0.050	0.003	4
			M-180	A	2	1197276	56,100	82,200	22.0	0.220	1.000	0.005	0.003	0.030	0.170	0.000	0.050	0.000	4
			A-36			2817878	59,800	71,100	25.0	0.070	0.860	0.007	0.030	0.160	0.260	0.014	0.050	0.004	4
			A-36			1801947	55,000	68,200	25.6	0.070	0.830	0.007	0.028	0.250	0.090	0.014	0.040	0.003	4
			A-36			59089368													
			F844-3300			P39066 R72634-01	61,274	74,311	26.3	0.090	0.930	0.018	0.031	0.230	0.440	0.000	0.210	0.002	4
			FAST			19-35-008													
			A307-3360			879381-2													
			A307-3500			881353-1													
			WOOD			736													
			WD BLK RTD 6X8X14																
			REFL-SHT 5X24 Y/B LT			192571													



Certified Analysis

Trinity Highway Products LLC

2548 N.E. 28th St.

Ft Worth (THP), TX 76111 Phn:(817) 665-1499

Customer: SAMPLES, TESTING MATERIALS

2525 STEMMONS FRWY

DALLAS, TX 75207

Project: POOLED FUND PROJECT 609971

Order Number: 1319212 Prod Ln Grp: 9-End Terminals (Dom)

Customer PO: POOLED FUND

BOL Number: 78438

Document #: 1

Shipped To: TX

Use State: TX

As of: 12/31/19



Qty	Part #	Description	Spec	CL	TY	Heat Code/Heat	Yield	TS	Elg	C	Mn	P	S	Si	Cu	Cb	Cr	Vn	ACW	
2	5852B	REFL SHT 5X24 Y/B RT	LABELS			192571														
4	500646B	SOFTSTOP MASH TL3	RHC		2	L14619	63,390	81,850	24.5	0.190	0.730	0.008	0.002	0.020	0.110	0.001	0.050	0.002		
			M-180	A	2	244186	63,510	82,890	24.6	0.190	0.740	0.011	0.002	0.030	0.110	0.000	0.070	0.001		
			M-180	A	2	245247	61,270	79,830	27.8	0.190	0.720	0.010	0.005	0.020	0.100	0.000	0.060	0.002		
			M-180	A	2	245248	61,940	82,830	26.0	0.200	0.720	0.010	0.004	0.010	0.100	0.000	0.060	0.000		
			M-180	A	2	245249	61,610	91,910	25.4	0.190	0.740	0.010	0.004	0.010	0.110	0.000	0.070	0.002		
			M-180	B	2	241647	56,310	76,620	29.1	0.190	0.730	0.012	0.003	0.020	0.100	0.000	0.060	0.001		
			A-36			1801947	55,000	68,200	25.6	0.070	0.830	0.007	0.028	0.250	0.090	0.014	0.040	0.003		
			A-36			2817878	59,800	71,100	25.0	0.070	0.860	0.007	0.030	0.160	0.260	0.014	0.050	0.004		
			F436-3240			P38754 R71028-01														
			A563-3354			P38401 R70911-01														
			FAST			19-35-008														
			A307-3360			879381-2														
			F3125-3391			8604648-1														
			A307-3500			881353-1														
			F436-3701			P38468 R69526														

Certified Analysis



Trinity Highway Products LLC

2548 N.E. 28th St.

Ft Worth (THP), TX 76111 Phn:(817) 665-1499

Customer: SAMPLES, TESTING MATERIALS

2525 STEMMONS FRWY

Order Number: 1319212 Prod Ln Grp: 9-End Terminals (Dom)

Customer PO: POOLED FUND

BOL Number: 78438

Document #: 1

Shipped To: TX

Use State: TX

As of: 12/31/19



DALLAS, TX 75207

Project: POOLED FUND PROJECT 609971

Qty	Part #	Description	Spec	CL	TV	Heat Code/Heat	Yield	TS	Elg	C	Mn	P	S	Si	Cu	Cr	Vn	ACW
	500646B		A563-3704			P38836 R71968												
	500646B		F3125-3717			884309-1												
	500646B		A563-3908			P38841												
	500646B		F436-4372			P38874 R71569-01												
	500646B		F3125-4489			31848-B												
	500646B		B18 21.1-49			[38984 R72012												
	500646B		PLAST			36510												
	500646B		MISC			54923												
	500646B		MISC			33933-12												
	500646B		A-36			13870	53,000	78,000	22.0	0.180	0.890	0.014	0.027	0.240	0.320	0.002	0.150	0.005

Upon delivery, all materials subject to Trinity Highway Products, LLC Storage Stain Policy QMS-LG-002.

ALL STEEL USED WAS MELTED AND MANUFACTURED IN USA AND COMPLIES WITH THE BUY AMERICA ACT, 23 CFR 635.410.
ALL GUARDRAIL MEETS AASHTO M-180, ALL STRUCTURAL STEEL MEETS ASTM A36 UNLESS OTHERWISE STATED.



Certified Analysis

Trinity Highway Products LLC

2548 N.E. 28th St.

Ft Worth (THP), TX 76111 Phn:(817) 665-1499

Customer: SAMPLES, TESTING MATERIALS

2525 STEMMONS FRWY

Order Number: 1319212 Prod Ln Grp: 9-End Terminals (Dom)

Customer PO: POOLED FUND

BOL Number: 78438

As of: 12/31/19

Document #: 1 Ship Date:

Shipped To: TX

Use State: TX



Project: POOLED FUND PROJECT 609971

ALL COATINGS PROCESSES OF THE STEEL OR IRON ARE PERFORMED IN USA AND COMPLIES WITH THE "BUY AMERICA ACT", 23 CFR 635.410.

ALL GALVANIZED MATERIAL CONFORMS WITH ASTM A-123 (US DOMESTIC SHIPMENTS)

ALL GALVANIZED MATERIAL CONFORMS WITH ASTM A-123 & ISO 1461 (INTERNATIONAL SHIPMENTS)

FINISHED GOOD PART NUMBERS ENDING IN SUFFIX B,P, OR S, ARE UNCOATED

BOLTS COMPLY WITH ASTM A-307 SPECIFICATIONS AND ARE GALVANIZED IN ACCORDANCE WITH ASTM A-153, UNLESS OTHERWISE STATED.

NUTS COMPLY WITH ASTM A-563 SPECIFICATIONS AND ARE GALVANIZED IN ACCORDANCE WITH ASTM A-153, UNLESS OTHERWISE STATED.

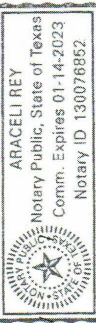
WASHERS COMPLY WITH ASTM F-436 SPECIFICATION AND/OR F-844 AND ARE GALVANIZED IN ACCORDANCE WITH ASTM F-2329, UNLESS

OTHERWISE STATED.

3/4" DIA CABLE 6X19 ZINC COATED SWAGED END AISI C-1035 STEEL ANNEALED STUD 1" DIA ASTM 449 AASHTO M30, TYPE II BREAKING

STRENGTH - 46000 LB

State of Texas, County of Tarrant. Sworn and subscribed before me this 31st day of December, 2019.



Notary Public:

Commission Expires:

Trinity Highway Products LLC

Certified By:

Quality Assurance

Araceli Rey

Table B.1. Test Day Static Soil Strength Documentation for Test No. 609971-01-1.

Date	4-22-2019
Test Facility and Site Location	TTI Proving Ground 3100 SH 47 Bryan, TX 77807
In Situ Soil Description (ASTM D2487)	Sandy gravel with silty fines
Fill Material Description (ASTM D2487) and sieve analysis	AASHTO M147 Grade B Crushed Limestone Road Base
Description of Fill Placement Procedure	6-inch lifts tamped with a pneumatic compactor for 40 s

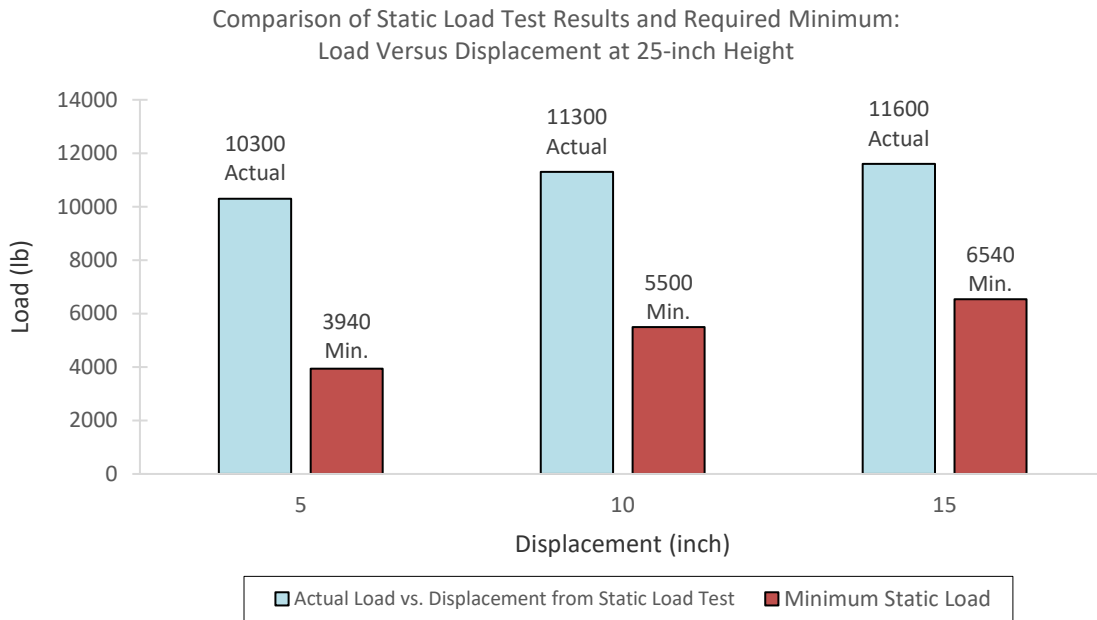


Figure B.1. Test Day Static Soil Strength Documentation for Test No. 609971-01-1.

Table B.2. Test Day Static Soil Strength Documentation for Test No. 609971-03-1.

Date	7-22-2019
Test Facility and Site Location	TTI Proving Ground 3100 SH 47 Bryan, TX 77807
In Situ Soil Description (ASTM D2487)	Sandy gravel with silty fines
Fill Material Description (ASTM D2487) and sieve analysis	AASHTO M147 Type A Grade 2 Crushed Limestone Road Base
Description of Fill Placement Procedure	6-inch lifts tamped with a pneumatic compactor for 40 s

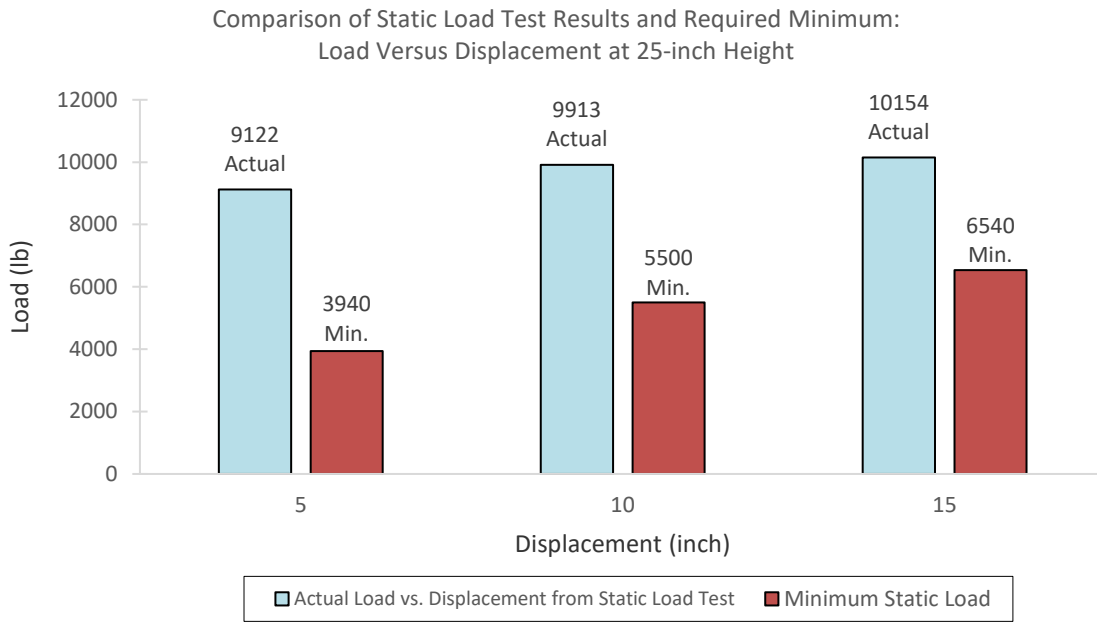


Figure B.2. Test Day Static Soil Strength Documentation for Test No. 609971-03-1.

Table B.3. Test Day Static Soil Strength Documentation for Test No. 609971-03-2.

Date	3-18-2020
Test Facility and Site Location	TTI Proving Ground 3100 SH 47 Bryan, TX 77807
In Situ Soil Description (ASTM D2487)	Sandy gravel with silty fines
Fill Material Description (ASTM D2487) and sieve analysis	AASHTO M147 Type A Grade 2 Crushed Limestone Road Base
Description of Fill Placement Procedure	6-inch lifts tamped with a pneumatic compactor for 40 s

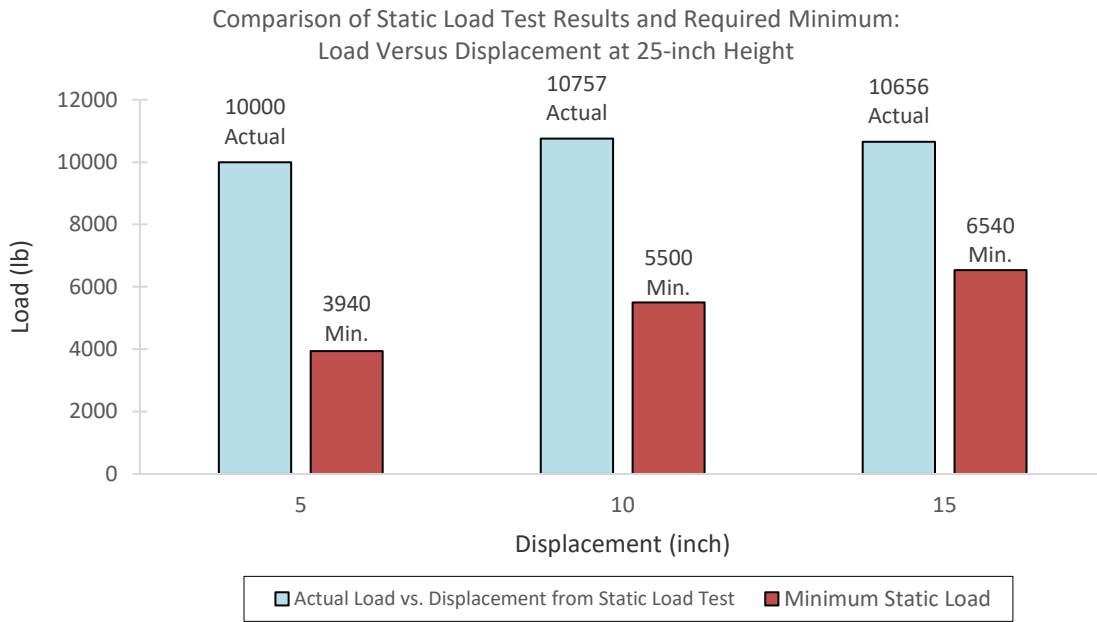


Figure B.3. Test Day Static Soil Strength Documentation for Test No. 609971-03-2.

APPENDIX C. MASH TEST 3-10 (CRASH TEST NO. 609971-01-1)

C.1. VEHICLE PROPERTIES AND INFORMATION

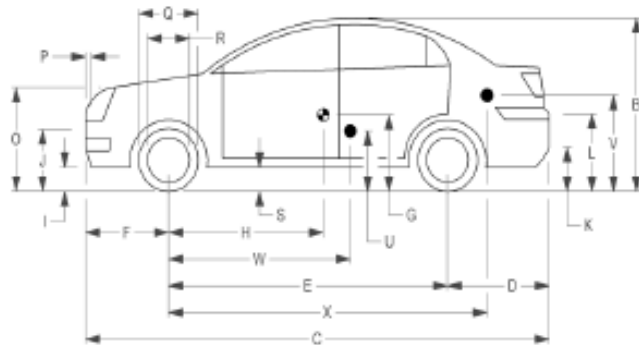
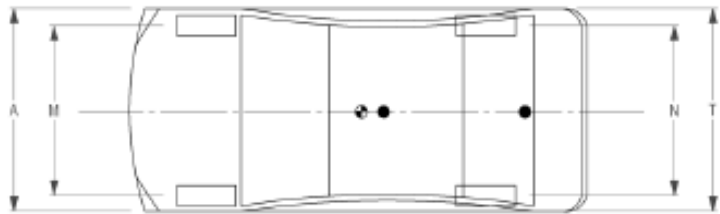
Date: 2019-04-18 Test No.: 609971-01-1 VIN No.: KNADE123886404640
 Year: 2008 Make: Kia Model: Rio
 Tire Inflation Pressure: 32 PSI Odometer: 150972 Tire Size: 185/65R14

Describe any damage to the vehicle prior to test: None

• Denotes accelerometer location.

NOTES: None

Engine Type: 4 CYL
 Engine CID: 1.6 L
 Transmission Type:
 Auto or Manual
 FWD RWD 4WD
 Optional Equipment:
None



Dummy Data:
 Type: 50th Percentile Male
 Mass: 165 lb
 Seat Position: Impact Side

Geometry: inches

A <u>66.38</u>	F <u>33.00</u>	K <u>12.25</u>	P <u>4.12</u>	U <u>14.75</u>
B <u>51.50</u>	G _____	L <u>25.25</u>	Q <u>22.50</u>	V <u>20.50</u>
C <u>165.75</u>	H <u>35.61</u>	M <u>57.75</u>	R <u>15.50</u>	W <u>35.60</u>
D <u>34.00</u>	I <u>7.75</u>	N <u>57.70</u>	S <u>8.25</u>	X <u>102.00</u>
E <u>98.75</u>	J <u>21.50</u>	O <u>27.00</u>	T <u>66.20</u>	
Wheel Center Ht Front <u>11.00</u>	Wheel Center Ht Rear <u>11.00</u>	W-H <u>0.00</u>		

RANGE LIMIT: A = 65 ±3 inches; C = 169 ±8 inches; E = 98 ±5 inches; F = 35 ±4 inches; H = 39 ±4 inches; O (Bottom of Hood Lip) = 24 ±4 inches
 TOP OF RADIATOR SUPPORT = $\frac{E+O}{2}$ inches; (M+N)/2 = 56 ±2 inches; W-H < 2 inches or use MASH Paragraph A4.3.2

GVWR Ratings:	Mass: lb	Curb	Test Inertial	Gross Static
Front <u>1718</u>	M _{front}	<u>1589</u>	<u>1560</u>	<u>1645</u>
Back <u>1874</u>	M _{rear}	<u>854</u>	<u>880</u>	<u>960</u>
Total <u>3638</u>	M _{Total}	<u>2443</u>	<u>2440</u>	<u>2805</u>

Allowable TIM = 2420 lb ±55 lb | Allowable GSM = 2585 lb ± 55 lb

Mass Distribution:
 lb LF: 780 RF: 780 LR: 460 RR: 420

Figure C.1. Vehicle Properties for Test No. 609971-01-1.

Date: 2019-04-18 Test No.: 609971-01-1 VIN No.: KNADE123886404640
 Year: 2008 Make: Kia Model: Rio

VEHICLE CRUSH MEASUREMENT SHEET¹

Complete When Applicable	
End Damage	Side Damage
Undeformed end width _____ Corner shift: A1 _____ A2 _____ End shift at frame (CDC) (check one) < 4 inches _____ ≥ 4 inches _____	Bowing: B1 _____ X1 _____ B2 _____ X2 _____ Bowing constant $\frac{X1 + X2}{2} = \underline{\hspace{2cm}}$

Note: Measure C₁ to C₆ from Driver to Passenger Side in Front or Rear Impacts – Rear to Front in Side Impacts.

Specific Impact Number	Plane* of C-Measurements	Direct Damage		Field L**	C ₁	C ₂	C ₃	C ₄	C ₅	C ₆	±D
		Width** (CDC)	Max*** Crush								
1	AT FT BUMPER		6								
2	SAME		9								
	Measurements recorded										
	<input checked="" type="checkbox"/> inches or <input type="checkbox"/> mm										

¹Table taken from National Accident Sampling System (NASS).

*Identify the plane at which the C-measurements are taken (e.g., at bumper, above bumper, at sill, above sill, at beltline, etc.) or label adjustments (e.g., free space).

Free space value is defined as the distance between the baseline and the original body contour taken at the individual C locations. This may include the following: bumper lead, bumper taper, side protrusion, side taper, etc. Record the value for each C-measurement and maximum crush.

**Measure and document on the vehicle diagram the beginning or end of the direct damage width and field L (e.g., side damage with respect to undamaged axle).

***Measure and document on the vehicle diagram the location of the maximum crush.

Note: Use as many lines/columns as necessary to describe each damage profile.

Figure C.2. Exterior Crush Measurements for Test No. 609971-01-1.

C.2. SEQUENTIAL PHOTOGRAPHS

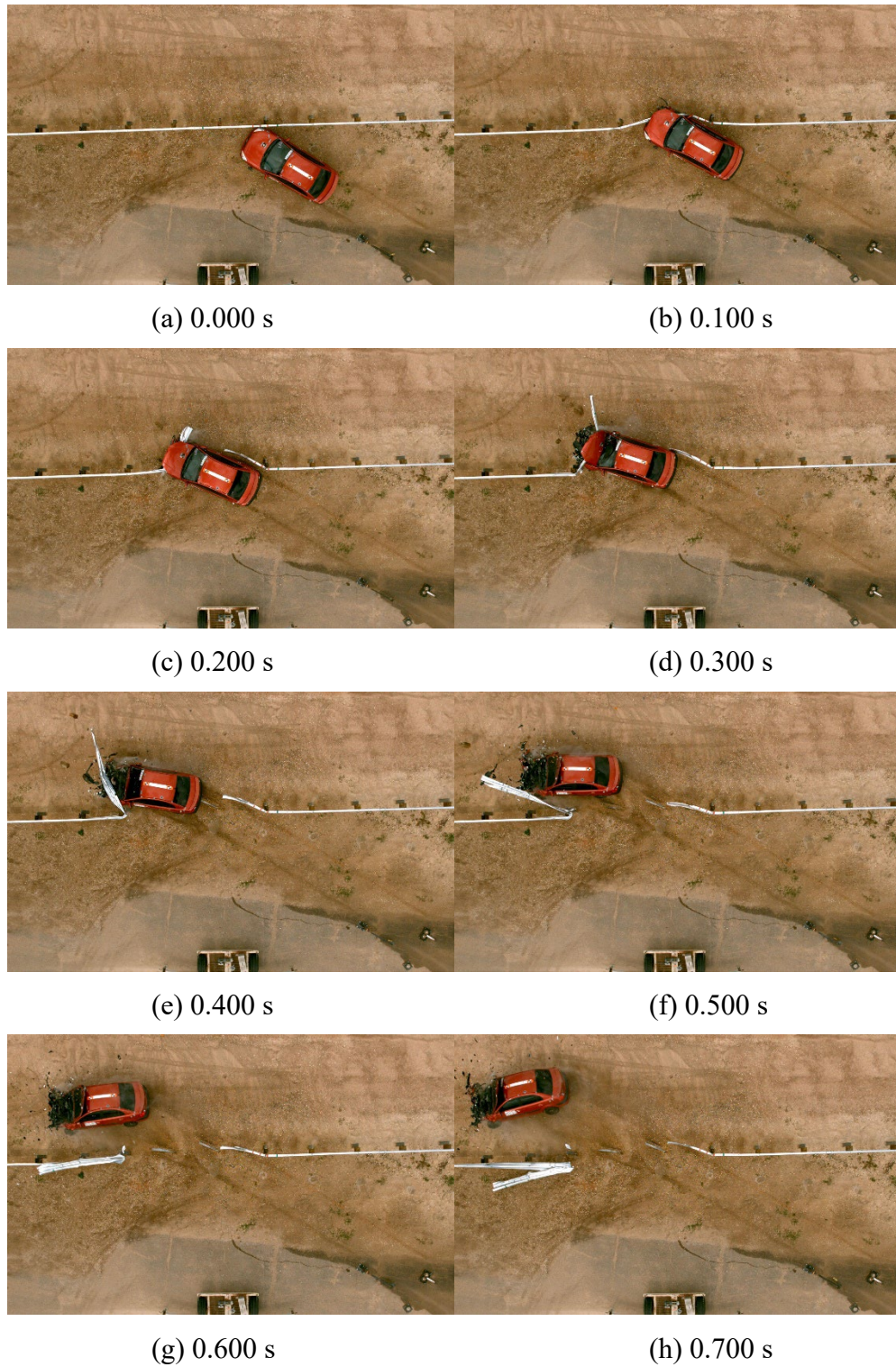


Figure C.3. Sequential Photographs for Test No. 609971-01-1 (Overhead Views).



(a) 0.000 s

(b) 0.100 s



(c) 0.200 s

(d) 0.300 s



(e) 0.400 s

(f) 0.500 s



(g) 0.600 s

(h) 0.700 s

Figure C.4. Sequential Photographs for Test No. 609971-01-1 (Frontal Views).



(a) 0.000 s

(b) 0.100 s



(c) 0.200 s

(d) 0.300 s



(e) 0.400 s

(f) 0.500 s

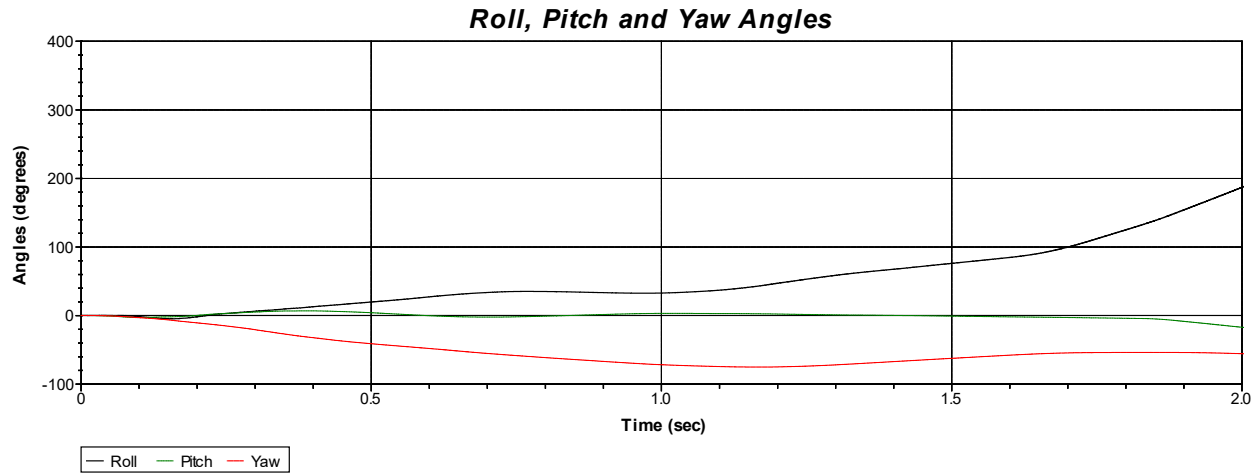


(g) 0.600 s

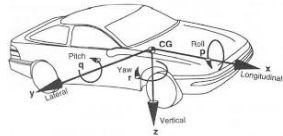
(h) 0.700 s

Figure C.5. Sequential Photographs for Test No. 609971-01-1 (Rear Views).

C.3. VEHICLE ANGULAR DISPLACEMENTS



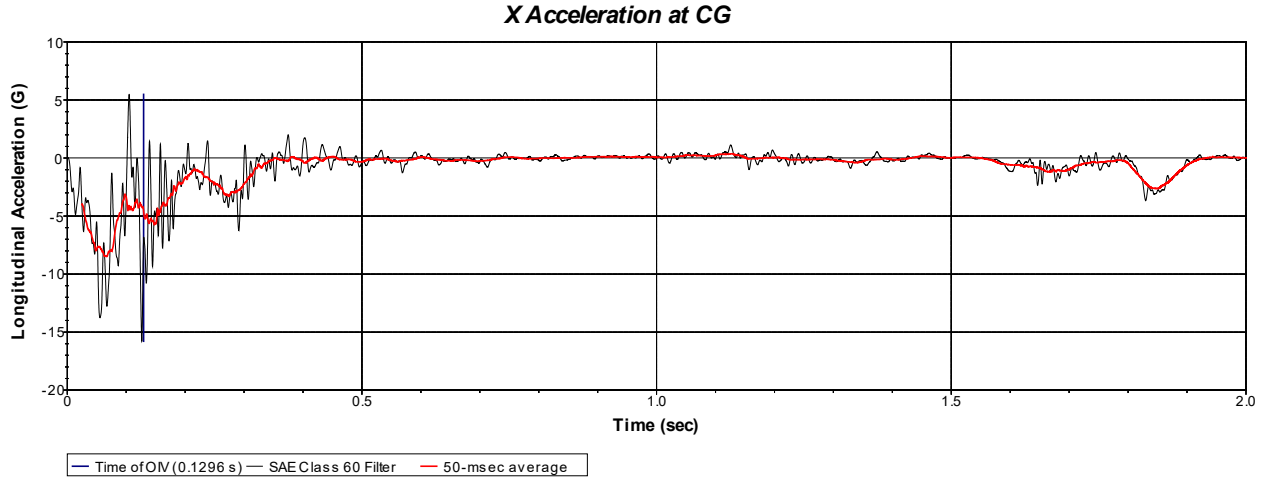
Axes are vehicle-fixed.
 Sequence for determining orientation:
 1. Yaw.
 2. Pitch.
 3. Roll.



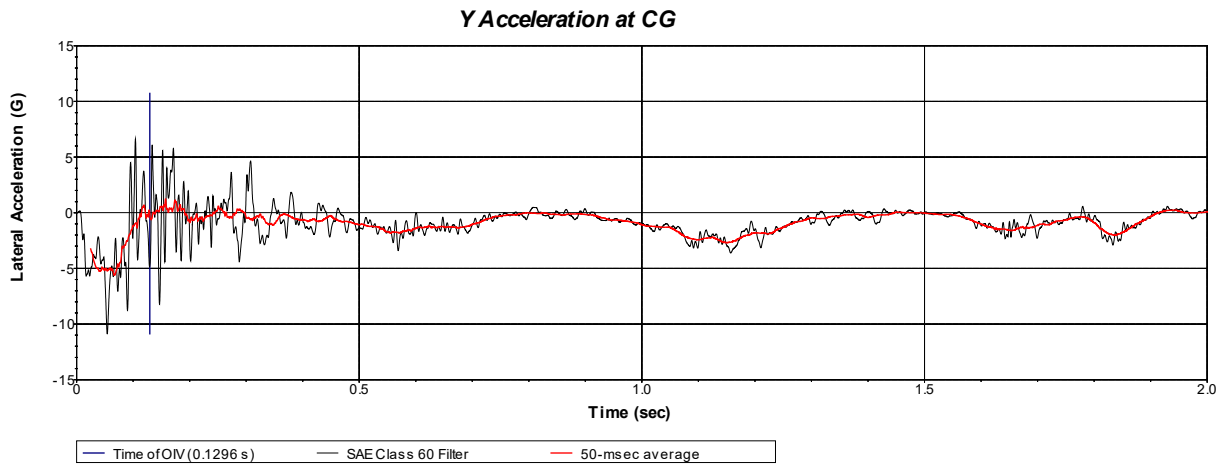
Test Number: 609971-01-1
 Test Standard Test Number: MASH Test 3-10
 Test Article: MGS Guardrail with Flare
 Test Vehicle: 2008 Kia Rio
 Inertial Mass: 2440 lb
 Gross Mass: 2605 lb
 Impact Speed: 61.8 mph
 Impact Angle: 24.8 degrees

Figure C.6. Vehicle Angular Displacements for Test No. 609971-01-1.

C.4. VEHICLE ACCELERATIONS



**Figure C.7. Vehicle Longitudinal Accelerometer Trace for Test No. 609971-01-1
(Accelerometer Located at Center of Gravity).**



**Figure C.8. Vehicle Lateral Accelerometer Trace for Test No. 609971-01-1
(Accelerometer Located at Center of Gravity).**

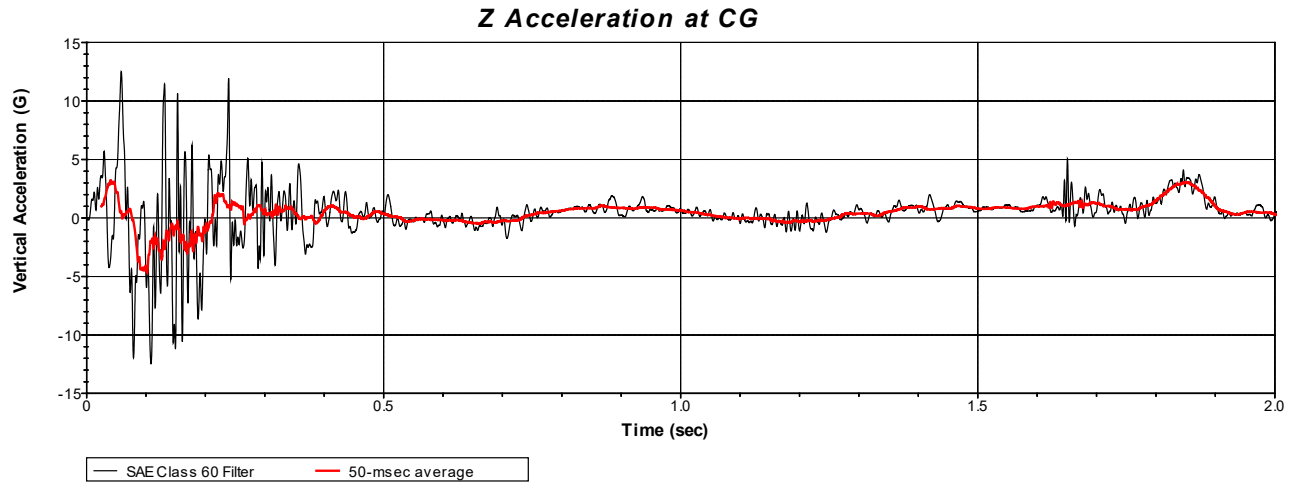


**Figure C.9. Vehicle Vertical Accelerometer Trace for Test No. 609971-01-1
(Accelerometer Located at Center of Gravity).**

APPENDIX D. MASH TEST 3-11 (CRASH TEST NO. 609971-03-1)

D.1. VEHICLE PROPERTIES AND INFORMATION

Date: 2019-07-22 Test No.: 609971-03-01 VIN No.: 1C6RR6GT2DS693414
 Year: 2013 Make: RAM Model: 1500
 Tire Size: 265/70 R 17 Tire Inflation Pressure: 35 psi
 Tread Type: Highway Odometer: 126643
 Note any damage to the vehicle prior to test: None

• Denotes accelerometer location.

NOTES: None

Engine Type: V-8
 Engine CID: 4.7 liter

Transmission Type:
 Auto or Manual
 FWD RWD 4WD

Optional Equipment:
None

Dummy Data:
 Type: No dummy
 Mass: 0 lb
 Seat Position: NA

Geometry: inches

A	<u>78.50</u>	F	<u>40.00</u>	K	<u>20.00</u>	P	<u>3.00</u>	U	<u>26.75</u>
B	<u>74.00</u>	G	<u>28.25</u>	L	<u>30.00</u>	Q	<u>30.50</u>	V	<u>30.25</u>
C	<u>227.50</u>	H	<u>59.60</u>	M	<u>68.50</u>	R	<u>18.00</u>	W	<u>59.60</u>
D	<u>44.00</u>	I	<u>11.75</u>	N	<u>68.00</u>	S	<u>13.00</u>	X	<u>79.00</u>
E	<u>140.50</u>	J	<u>27.00</u>	O	<u>46.00</u>	T	<u>77.00</u>		
Wheel Center Height Front	<u>14.75</u>	Wheel Well Clearance (Front)	<u>6.00</u>	Bottom Frame Height - Front	<u>12.50</u>				
Wheel Center Height Rear	<u>14.75</u>	Wheel Well Clearance (Rear)	<u>9.25</u>	Bottom Frame Height - Rear	<u>22.50</u>				

RANGE LIMIT: A=78 ±2 inches; C=237 ±13 inches; E=148 ±12 inches; F=39 ±3 inches; G = > 28 inches; H = 63 ±4 inches; O=43 ±4 inches; (M+N)/2=67 ±1.5 inches

GVWR Ratings:	Mass: lb	Curb	Test Inertial	Gross Static
Front	<u>3700</u>	<u>M_{front}</u>	<u>2968</u>	<u>2906</u>
Back	<u>3900</u>	<u>M_{rear}</u>	<u>2084</u>	<u>2141</u>
Total	<u>6700</u>	<u>M_{Total}</u>	<u>5052</u>	<u>5047</u>

(Allowable Range for TIM and GSM = 5000 lb ±110 lb)

Mass Distribution:
 lb LF: 1465 RF: 1441 LR: 1097 RR: 1044

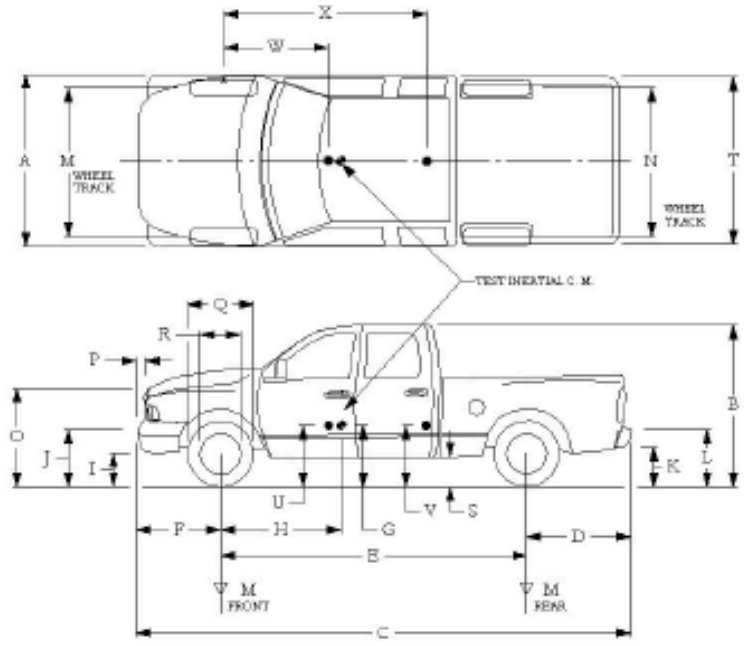


Figure D.1. Vehicle Properties for Test No. 609971-03-1.

Date: 2019-07-22 Test No.: 609971-03-01 VIN No.: 1C6RR6GT2DS693414
 Year: 2013 Make: RAM Model: 1500

VEHICLE CRUSH MEASUREMENT SHEET¹

Complete When Applicable	
End Damage	Side Damage
Undeformed end width _____ Corner shift: A1 _____ A2 _____ End shift at frame (CDC) (check one) < 4 inches _____ ≥ 4 inches _____	Bowing: B1 _____ X1 _____ B2 _____ X2 _____ Bowing constant $\frac{X1 + X2}{2} = \underline{\hspace{2cm}}$

Note: Measure C₁ to C₆ from Driver to Passenger Side in Front or Rear Impacts – Rear to Front in Side Impacts.

Specific Impact Number	Plane* of C-Measurements	Direct Damage		Field L**	C ₁	C ₂	C ₃	C ₄	C ₅	C ₆	±D
		Width** (CDC)	Max*** Crush								
1	AT FT BUMPER	16	11								
2	SAME	16	10								
	Measurements recorded										
	<input type="checkbox"/> inches or <input type="checkbox"/> mm										

¹Table taken from National Accident Sampling System (NASS).

*Identify the plane at which the C-measurements are taken (e.g., at bumper, above bumper, at sill, above sill, at beltline, etc.) or label adjustments (e.g., free space).

Free space value is defined as the distance between the baseline and the original body contour taken at the individual C locations. This may include the following: bumper lead, bumper taper, side protrusion, side taper, etc. Record the value for each C-measurement and maximum crush.

**Measure and document on the vehicle diagram the beginning or end of the direct damage width and field L (e.g., side damage with respect to undamaged axle).

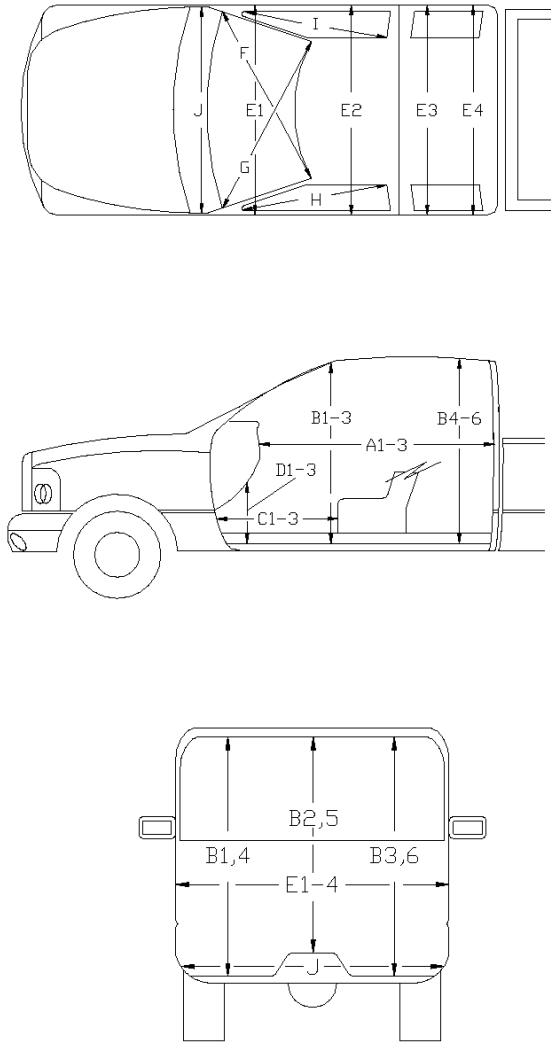
***Measure and document on the vehicle diagram the location of the maximum crush.

Note: Use as many lines/columns as necessary to describe each damage profile.

Figure D.2. Exterior Crush Measurements for Test No. 609971-03-1.

Date: 2019-07-22 Test No.: 609971-03-01 VIN No.: 1C6RR6GT2DS693414
 Year: 2013 Make: RAM Model: 1500

OCCUPANT COMPARTMENT DEFORMATION MEASUREMENT



	Before	After (inches)	Differ.
A1	65.00	65.00	0.00
A2	63.00	63.00	0.00
A3	65.50	65.50	0.00
B1	45.00	45.00	0.00
B2	38.00	38.00	0.00
B3	45.00	45.00	0.00
B4	39.50	39.50	0.00
B5	43.00	43.00	0.00
B6	39.50	39.50	0.00
C1	26.00	26.00	0.00
C2	0.00	0.00	0.00
C3	26.00	26.00	0.00
D1	11.00	11.00	0.00
D2	0.00	0.00	0.00
D3	11.50	11.50	0.00
E1	58.50	58.50	0.00
E2	63.50	63.50	0.00
E3	63.50	63.50	0.00
E4	63.50	63.50	0.00
F	59.00	59.00	0.00
G	59.00	59.00	0.00
H	37.50	37.50	0.00
I	37.50	37.50	0.00
J*	25.00	25.00	0.00

*Lateral area across the cab from driver's side kickpanel to passenger's side kickpanel.

Figure D.3. Occupant Compartment Measurements for Test No. 609971-03-1.

D.2. SEQUENTIAL PHOTOGRAPHS

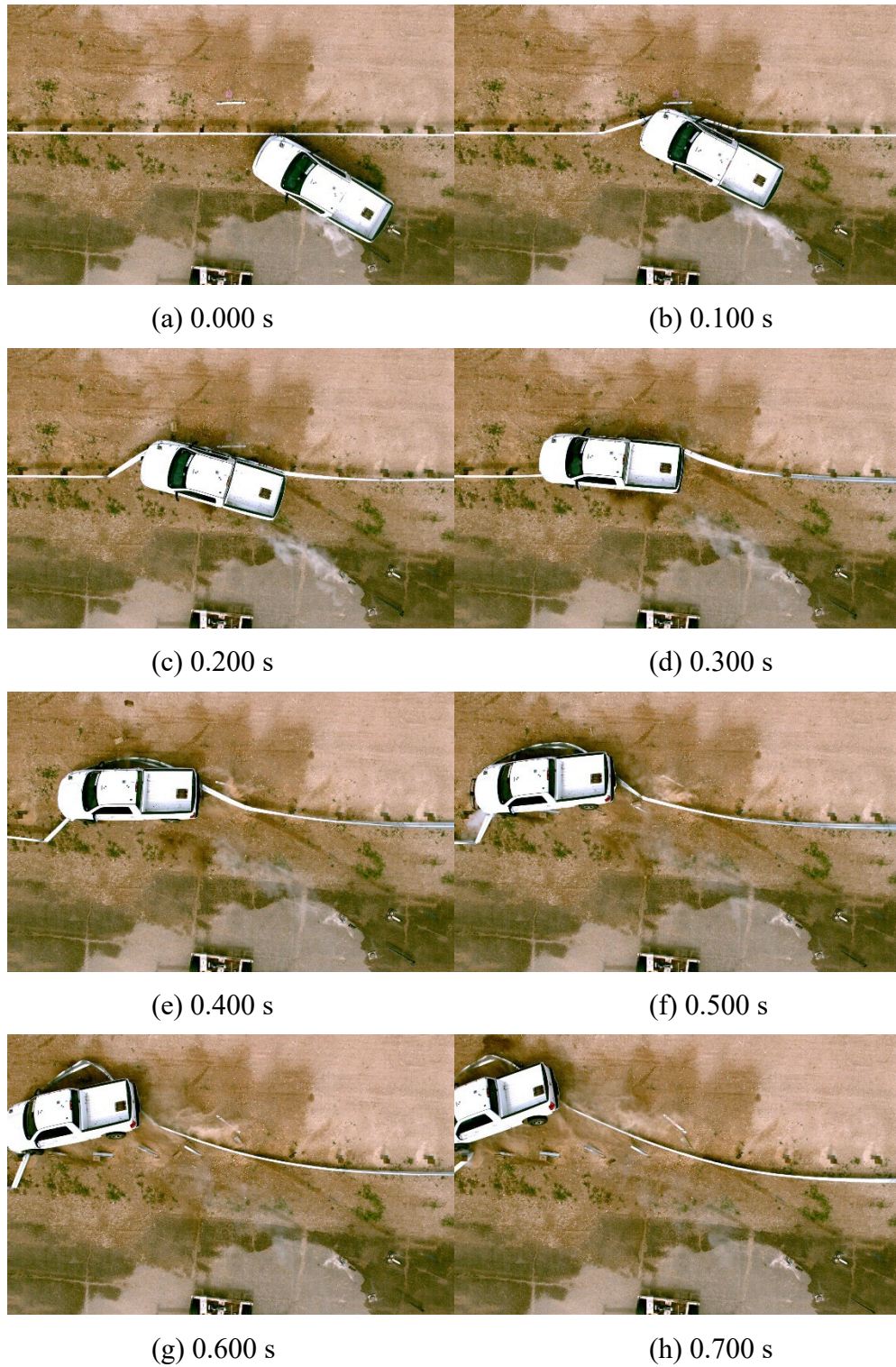


Figure D.4. Sequential Photographs for Test No. 609971-03-1 (Overhead Views).



(a) 0.000 s

(b) 0.100 s



(c) 0.200 s

(d) 0.300 s



(e) 0.400 s

(f) 0.500 s



(g) 0.600 s

(h) 0.700 s

Figure D.5. Sequential Photographs for Test No. 609971-03-1 (Frontal Views).



(a) 0.000 s

(b) 0.100 s



(c) 0.200 s

(d) 0.300 s



(e) 0.400 s

(f) 0.500 s

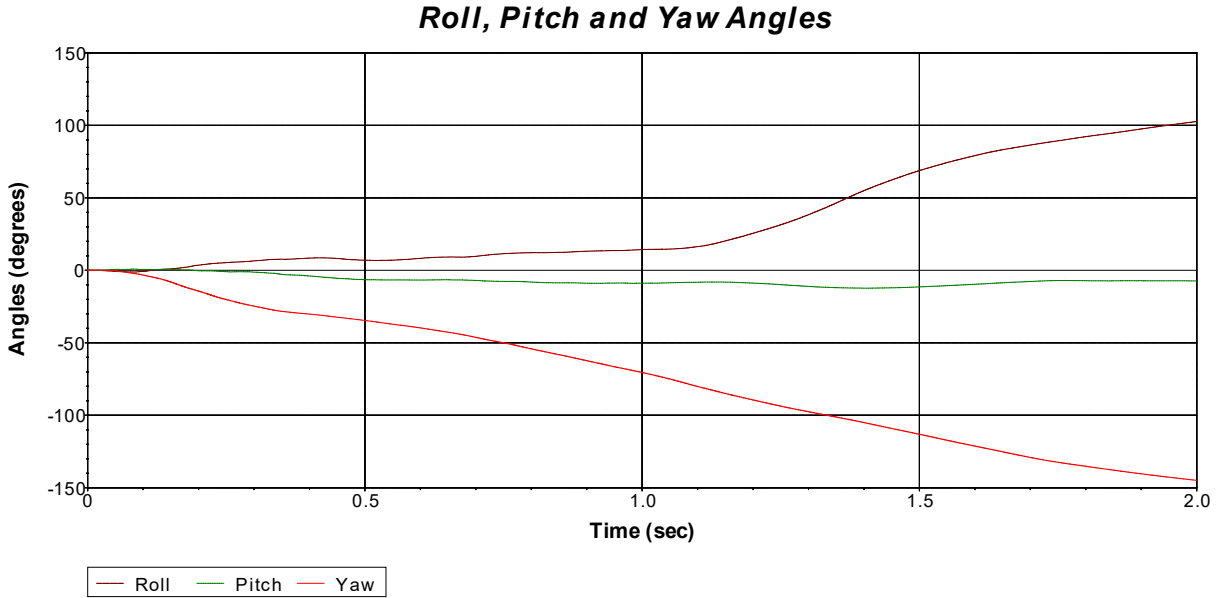


(g) 0.600 s

(h) 0.700 s

Figure D.6. Sequential Photographs for Test No. 609971-03-1 (Rear Views).

D.3. VEHICLE ANGULAR DISPLACEMENTS



Axes are vehicle-fixed.
Sequence for determining orientation:

1. Yaw.
2. Pitch.
3. Roll.

Test Number: 609971-03-1
 Test Standard Test Number: *MASH* Test 3-11
 Test Article: MGS Guardrail with Flare
 Test Vehicle: 2013 RAM 1500
 Inertial Mass: 5047 lb
 Gross Mass: 5047 lb
 Impact Speed: 62.6 mi/s
 Impact Angle: 25.7°

Figure D.7. Vehicle Angular Displacements for Test No. 609971-03-1.

D.4. VEHICLE ACCELERATIONS

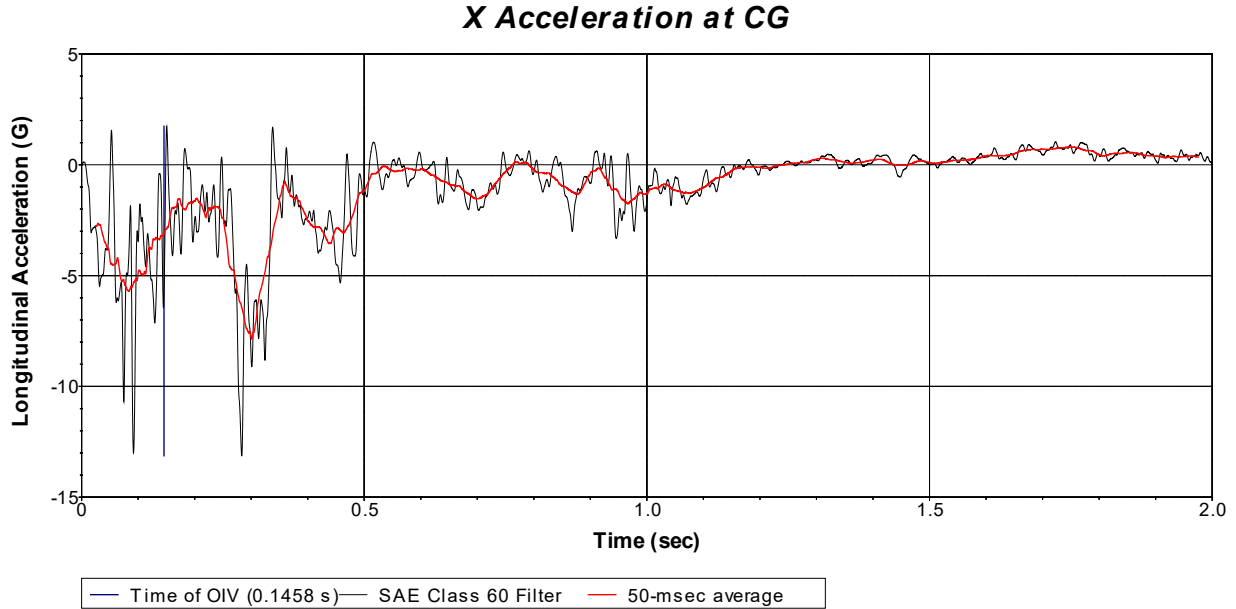


Figure D.8. Vehicle Longitudinal Accelerometer Trace for Test No. 609971-03-1 (Accelerometer Located at Center of Gravity).

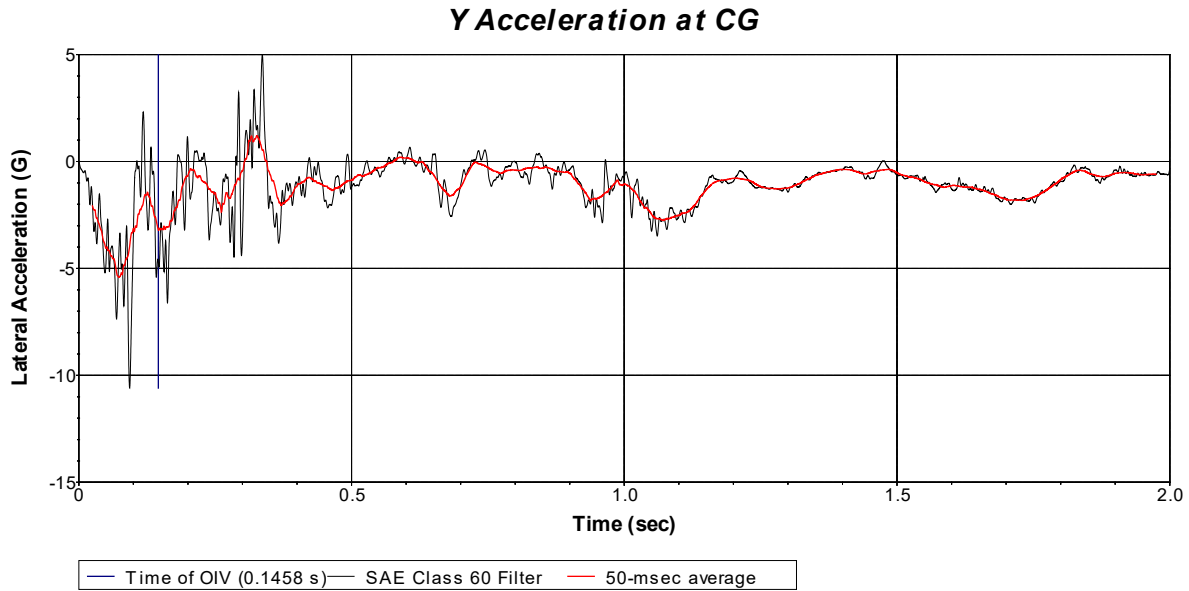
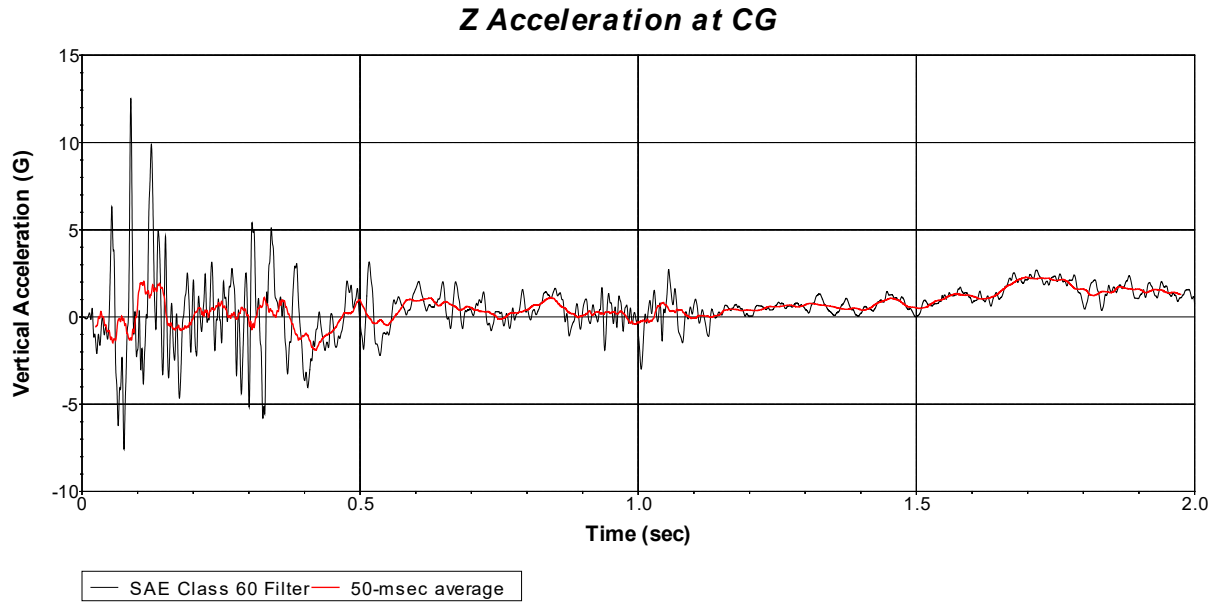


Figure D.9. Vehicle Lateral Accelerometer Trace for Test No. 609971-03-1 (Accelerometer Located at Center of Gravity).



**Figure D.10. Vehicle Vertical Accelerometer Trace for Test No. 609971-03-1
(Accelerometer Located at Center of Gravity).**

APPENDIX E. MASH TEST 3-11 (CRASH TEST NO. 609971-03-2)

E.1. VEHICLE PROPERTIES AND INFORMATION

Date: 2020-3-18 Test No.: 609971-03-2 VIN No.: 1C6RR6GT2ES286071
 Year: 2014 Make: RAM Model: _____
 Tire Size: 265/70 R 17 Tire Inflation Pressure: 35 psi
 Tread Type: Highway Odometer: 156583
 Note any damage to the vehicle prior to test: None

• Denotes accelerometer location.

NOTES: None

Engine Type: V-8
 Engine CID: 5.7 L

Transmission Type:
 Auto or Manual
 FWD RWD 4WD

Optional Equipment:
None

Dummy Data:
 Type: NONE
 Mass: 0 lb
 Seat Position: _____

Geometry: inches

A	<u>78.50</u>	F	<u>40.00</u>	K	<u>20.00</u>	P	<u>3.00</u>	U	<u>26.75</u>
B	<u>74.00</u>	G	<u>29</u>	L	<u>30.00</u>	Q	<u>30.50</u>	V	<u>30.25</u>
C	<u>227.50</u>	H	<u>59.54</u>	M	<u>68.50</u>	R	<u>18.00</u>	W	<u>59.5</u>
D	<u>44.00</u>	I	<u>11.75</u>	N	<u>68.00</u>	S	<u>13.00</u>	X	<u>79</u>
E	<u>140.50</u>	J	<u>27.00</u>	O	<u>46.00</u>	T	<u>77.00</u>		
Wheel Center Height Front	<u>14.75</u>	Wheel Well Clearance (Front)	<u>6.00</u>	Bottom Frame Height - Front	<u>12.50</u>				
Wheel Center Height Rear	<u>14.75</u>	Wheel Well Clearance (Rear)	<u>9.25</u>	Bottom Frame Height - Rear	<u>22.50</u>				

RANGE LIMIT: A=78 ±2 inches; C=237 ±13 inches; E=148 ±12 inches; F=39 ±3 inches; G = > 28 inches; H = 63 ±4 inches; O=43 ±4 inches; (M+N)/2=67 ±1.5 inches

GVWR Ratings:	Mass: lb	Curb	Test Inertial	Gross Static
Front <u>3700</u>	M _{front}	<u>2985</u>	<u>2892</u>	
Back <u>3900</u>	M _{rear}	<u>2161</u>	<u>2127</u>	
Total <u>6700</u>	M _{Total}	<u>5146</u>	<u>5019</u>	<u>0</u>

(Allowable Range for TIM and GSM = 5000 lb ±110 lb)

Mass Distribution:
 lb LF: 1450 RF: 1442 LR: 1073 RR: 1054

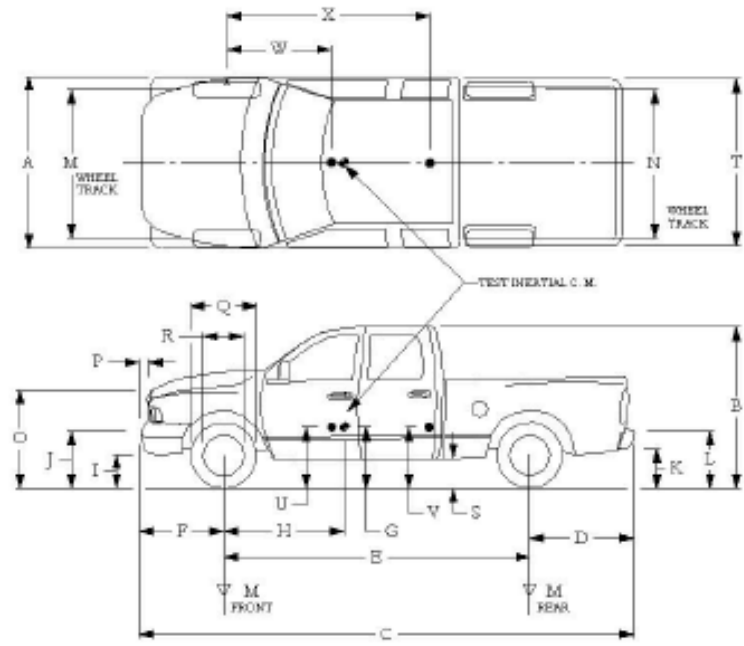


Figure E.1. Vehicle Properties for Test No. 609971-03-2.

Date: 2020-3-18 Test No.: 609971-03-2 VIN No.: 1C6RR6GT2ES286071
 Year: 2014 Make: RAM Model: _____

VEHICLE CRUSH MEASUREMENT SHEET¹

Complete When Applicable	
End Damage	Side Damage
Undeformed end width _____	Bowing: B1 _____ X1 _____
Corner shift: A1 _____	B2 _____ X2 _____
A2 _____	
End shift at frame (CDC)	Bowing constant
(check one)	$\frac{X1 + X2}{2} =$ _____
< 4 inches _____	
≥ 4 inches _____	

Note: Measure C₁ to C₆ from Driver to Passenger Side in Front or Rear Impacts – Rear to Front in Side Impacts.

Specific Impact Number	Plane* of C-Measurements	Direct Damage		Field L**	C ₁	C ₂	C ₃	C ₄	C ₅	C ₆	±D
		Width** (CDC)	Max*** Crush								
1	AT FT BUMPER	18	10								
2	SAME	18	10								
	Measurements recorded										
	<input checked="" type="checkbox"/> inches or <input type="checkbox"/> mm										

¹Table taken from National Accident Sampling System (NASS).

*Identify the plane at which the C-measurements are taken (e.g., at bumper, above bumper, at sill, above sill, at beltline, etc.) or label adjustments (e.g., free space).

Free space value is defined as the distance between the baseline and the original body contour taken at the individual C locations. This may include the following: bumper lead, bumper taper, side protrusion, side taper, etc. Record the value for each C-measurement and maximum crush.

**Measure and document on the vehicle diagram the beginning or end of the direct damage width and field L (e.g., side damage with respect to undamaged axle).

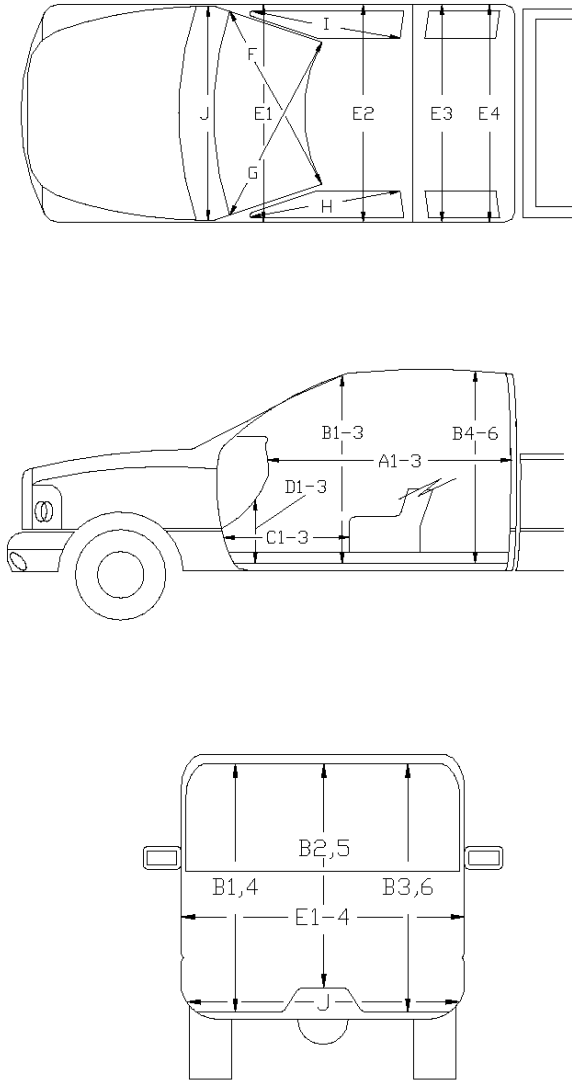
***Measure and document on the vehicle diagram the location of the maximum crush.

Note: Use as many lines/columns as necessary to describe each damage profile.

Figure E.2. Exterior Crush Measurements for Test No. 609971-03-2.

Date: 2020-3-18 Test No.: 609971-03-2 VIN No.: 1C6RR6GT2ES286071
 Year: 2014 Make: RAM Model: _____

OCCUPANT COMPARTMENT DEFORMATION MEASUREMENT

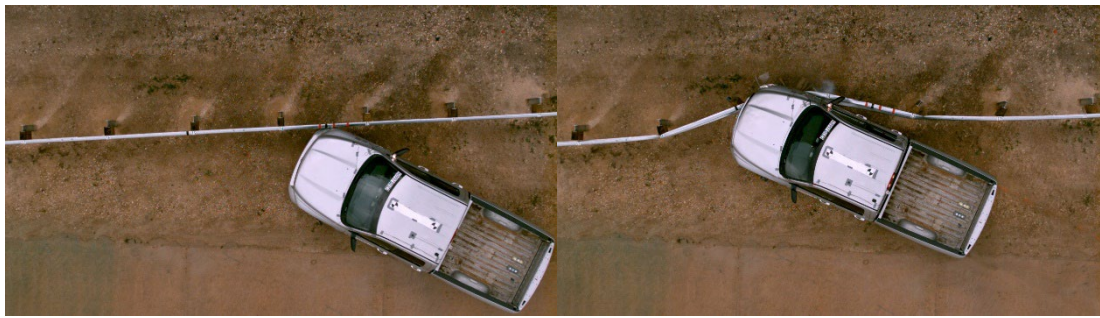


	Before	After (inches)	Differ.
A1	65.00	65.00	0.00
A2	63.00	63	0.00
A3	65.50	65.50	0.00
B1	45.00	45.00	0.00
B2	38.00	38.00	0.00
B3	45.00	45.00	0.00
B4	39.50	39.50	0.00
B5	43.00	43.00	0.00
B6	39.50	39.50	0.00
C1	26.00	26.00	0.00
C2	0.00	0.00	0.00
C3	26.00	26.00	0.00
D1	11.00	11.00	0.00
D2	0.00	0.00	0.00
D3	11.50	11.50	0.00
E1	58.50	58.50	0.00
E2	63.50	63.50	0.00
E3	63.50	63.50	0.00
E4	63.50	63.50	0.00
F	59.00	59.00	0.00
G	59.00	59.00	0.00
H	37.50	37.50	0.00
I	37.50	37.50	0.00
J*	25.00	25.00	0.00

*Lateral area across the cab from driver's side kickpanel to passenger's side kickpanel.

Figure E.3. Occupant Compartment Measurements for Test No. 609971-03-2.

E.2. SEQUENTIAL PHOTOGRAPHS



(a) 0.000 s

(b) 0.100 s



(c) 0.200 s

(d) 0.300 s



(e) 0.400 s

(f) 0.500 s



(g) 0.600 s

(h) 0.700 s

Figure E.4. Sequential Photographs for Test No. 609971-03-2 (Overhead Views).



(a) 0.000 s

(b) 0.100 s



(c) 0.200 s

(d) 0.300 s



(e) 0.400 s

(f) 0.500 s

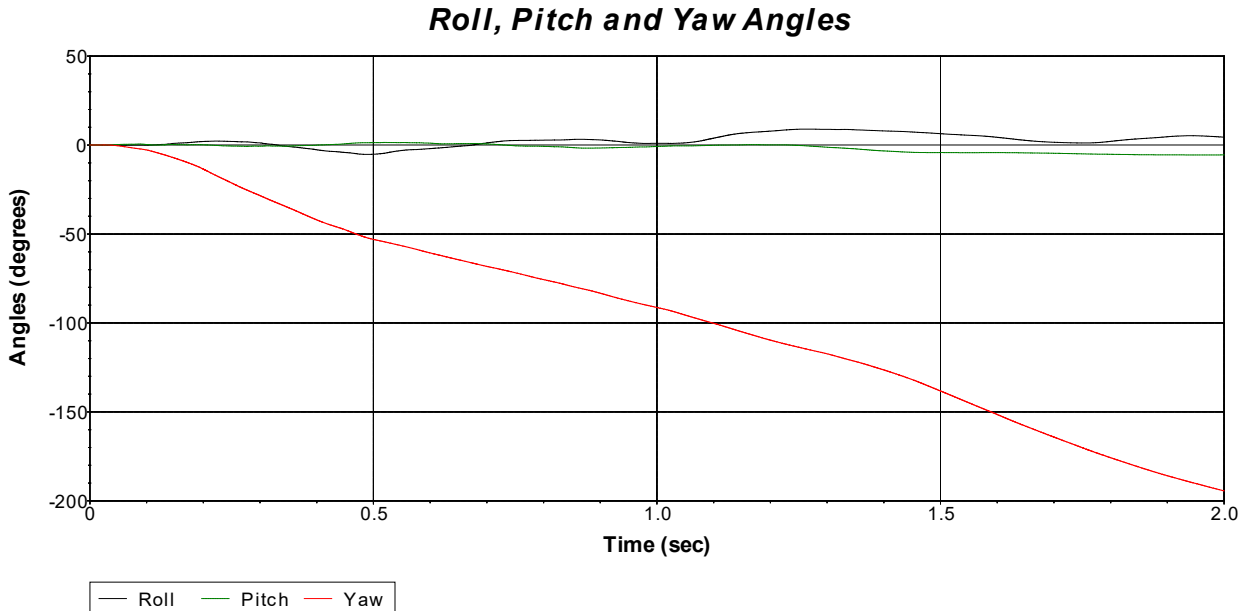


(g) 0.600 s

(h) 0.700 s

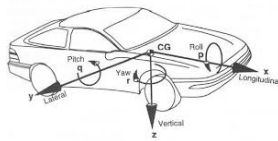
Figure E.5. Sequential Photographs for Test No. 609971-03-2 (Rear Views).

E.3. VEHICLE ANGULAR DISPLACEMENTS



Axes are vehicle-fixed.
Sequence for
determining orientation:

1. Yaw.
2. Pitch.
3. Roll.



Test Number: 609971-03-2
 Test Standard Test Number: *MASH* Test 3-11
 Test Article: MGS Guardrail with Flare
 Test Vehicle: 2014 RAM 1500
 Inertial Mass: 5019
 Gross Mass: 5019
 Impact Speed: 60.3
 Impact Angle: 24.5

Figure E.6. Vehicle Angular Displacements for Test No. 609971-03-2.

E.4. VEHICLE ACCELERATIONS

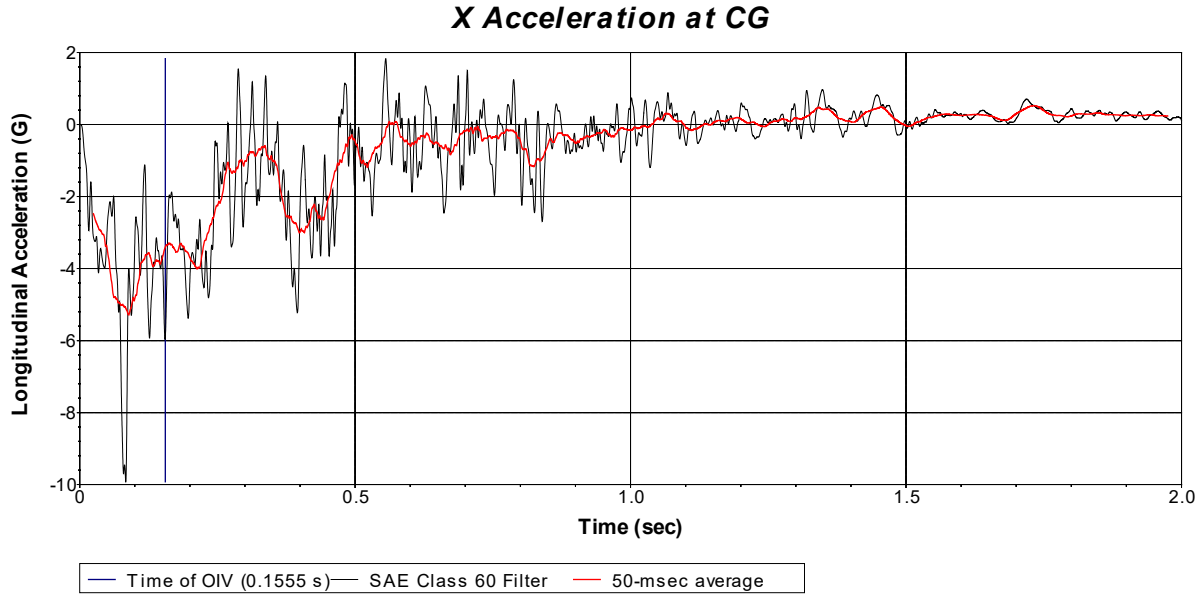


Figure E.7. Vehicle Longitudinal Accelerometer Trace for Test No. 609971-03-2 (Accelerometer Located at Center of Gravity).

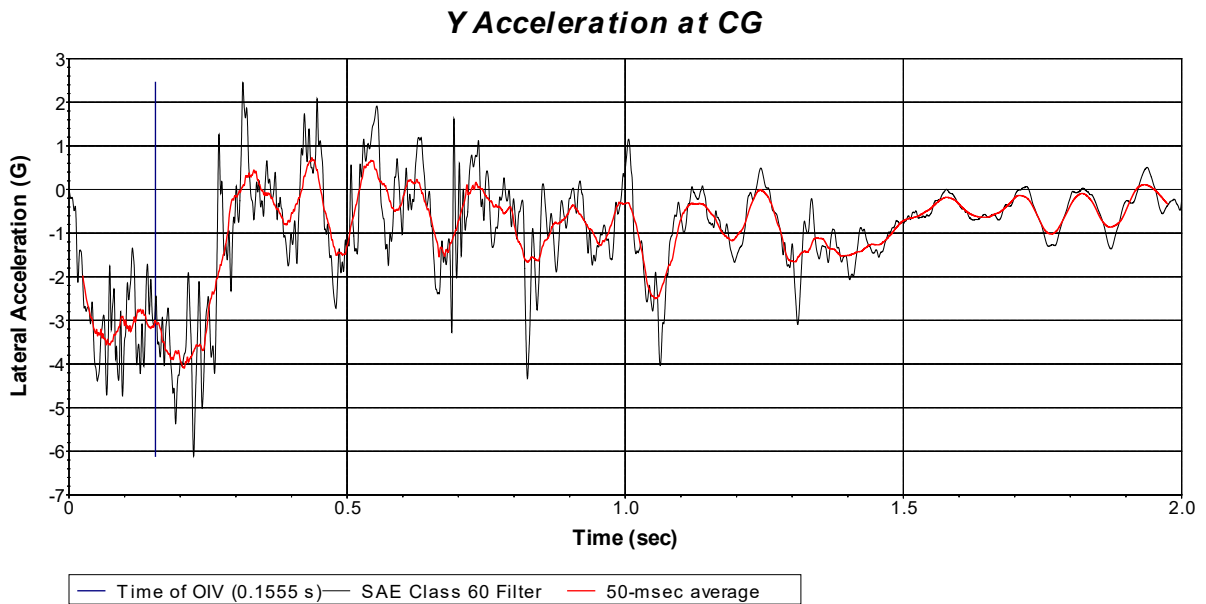
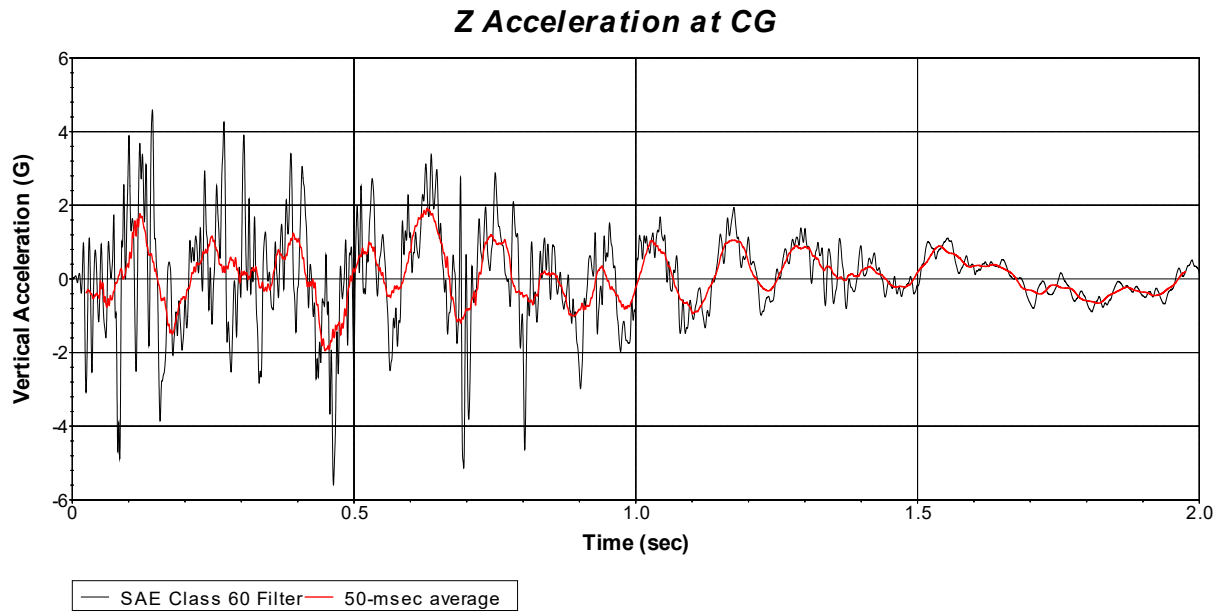


Figure E.8. Vehicle Lateral Accelerometer Trace for Test No. 609971-03-2 (Accelerometer Located at Center of Gravity).



**Figure E.9. Vehicle Vertical Accelerometer Trace for Test No. 609971-03-2
(Accelerometer Located at Center of Gravity).**